Hong Kong Journal of Radiology

Vol. 26 No. 2, 2023 Pages 81-164

Hong Kong Journal of Radiology

HKJR

香港放射科醫學雜誌

VOLUME 26 • NUMBER 2 • 2023

ISSN 2223-6619

Highlights of this issue:

- Transradial Access for Neurointervention: A Case Series from a Tertiary Centre in Hong Kong
- Treatment Outcomes of Stage II or III Gastric Cancer Treated with Adjuvant Chemotherapy with TS-1 or XELOX after Radical Surgery
- Accuracy and Interobserver Agreement of the Correlation Between Prostate Imaging Reporting and Data System Version 2.1 and International Society of Urological Pathology Scores

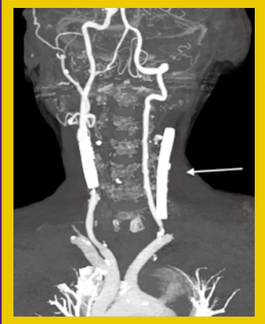

In the article "Transradial Access for Neurointervention: A Case Series from a Tertiary Centre in Hong Kong". Computed tomography angiogram of a patient with type III aortic arch and bilateral carotid stents. The left common carotid artery is occluded (arrow).

In the article "Transradial Diagnostic Cerebral Angiography: Local Experience, Technique, and Outcomes". Colour Doppler ultrasound shows partial radial artery occlusion (arrow) at the puncture site.

Official Publication of
Hong Kong College of Radiologists

HKAM PRESS

The Royal College of Radiologists

HONG KONG COLLEGE OF RADIOLOGISTS 香港放射科醫學院

RADIOLOGY HONG KONG 2023

10th Joint Scientific Meeting of RCR & HKCR
31st Annual Scientific Meeting of HKCR

18TH - 19TH NOVEMBER 2023
(SAT & SUN)

HONG KONG ACADEMY OF MEDICINE
JOCKEY CLUB BUILDING
HONG KONG SAR, CHINA

Multidisciplinary Symposium
Prostate Cancer

Subspecialty Focus
Urological Malignancies
Cardiovascular Radiology
Head & Neck Malignancies
Medico-legal Issues

君子莫急

If it be true the gentleman hadst known about modern diagnostic imaging and treatments of prostate cancer, the gent wouldst behold less worried

For details

HKJR

COVER IMAGES

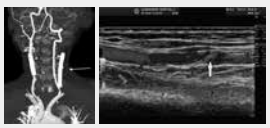

..... SEE PAGES 87 & 117

Hong Kong Journal of Radiology

Hong Kong Journal of Radiology is a continuation of the *Journal of the Hong Kong College of Radiologists*. This journal is dedicated to publish all aspects of clinical oncology, diagnostic radiology, and nuclear medicine.

VOLUME 26 • NUMBER 2 • JUNE 2023

Original Articles

Perspective

Case Reports

Pictorial Essays

ePub-only Articles

The following ePub-only articles can be found on the HKJR website <http://www.hkjr.org>.

When citing this journal, abbreviate as ***Hong Kong J Radiol***.

INFORMATION FOR SUBSCRIBERS

Hong Kong Journal of Radiology (**香港放射科醫學雜誌**) is the official peer-reviewed publication of the Hong Kong College of Radiologists and is published by the Hong Kong Academy of Medicine Press.

Frequency
Quarterly, 1 volume a year.

Correspondence concerning subscriptions should be addressed to:

Executive Assistant
Hong Kong Journal of Radiology
Room 909, 9/F, Hong Kong Academy of Medicine Jockey Club Building
99 Wong Chuk Hang Road, Aberdeen, Hong Kong
Tel: (852) 2871 8788; Fax: (852) 2554 0739
Email: hkjr@hkcr.org

Annual subscription rate

Hong Kong delivery:	HK$400 per volume.
Overseas delivery (by airmail):	US$100* per volume.
	* Bank charges shall be borne by the subscriber.

- Rates are the same for individuals and institutions.
- Renewals should be promptly received to avoid a break in journal delivery. The Hong Kong College of Radiologists does not guarantee to supply back issues on late renewals.

Change of address
The College must be notified 60 days in advance. Journals undeliverable because of an incorrect address will be destroyed. Send address changes to:

Hong Kong Journal of Radiology
Room 909, 9/F, Hong Kong Academy of Medicine Jockey Club Building
99 Wong Chuk Hang Road, Aberdeen, Hong Kong

Please return your Subscription Order Form to:

Hong Kong Journal of Radiology
Room 909, 9/F, Hong Kong Academy of Medicine Jockey Club Building
99 Wong Chuk Hang Road, Aberdeen, Hong Kong

I enclose payment (US$/HK$) _____
Please make bank draft, cheque, or cashier's order payable to **"Hong Kong College of Radiologists"**

Name (in English): _____

Address: _____

_____

Tel: _____ Fax: _____ Email: _____

Please (✓) accordingly
I would like to subscribe to the *Hong Kong Journal of Radiology*

❒ Hong Kong delivery: HK$400/volume
❒ Overseas delivery: US$100/volume*
(Postage charge included)
*Bank charges shall be borne by the subscriber.

❒ 3 volumes ❒ 2 volumes ❒ 1 volume

Subscription period: From Volume _____ to Volume _____

Hong Kong Journal of Radiology

Aims and Editorial Policy

Hong Kong Journal of Radiology **香港放射科醫學雜誌** is the official peer-reviewed academic journal of Hong Kong College of Radiologists, a founder College of the Hong Kong Academy of Medicine. The Journal is published quarterly and is indexed in EMBASE/*Excerpta Medica*, SCOPUS, Emerging Sources Citation Index, and Index Copernicus. Papers are published on all aspects of diagnostic imaging, clinical oncology, and nuclear medicine, including original research, editorials, review articles, and case reports. Papers on radiological protection, quality assurance, audit in radiology, and matters related to radiological training or education are included.

All papers submitted are subject to peer review, and the Editorial Board reserves the right to edit papers in preparation for publication in the Journal. Authors are asked to refer to the *Information for Authors* published in each issue of the Journal, regarding the style and presentation of their articles. Failure to do so may result in rejection of their papers by the Editorial Board.

Manuscripts should be submitted online via the HKAMedTrack <www.hkamedtrack.org/hkjr>. Correspondence should be sent to:

Managing Editor, HKJR Editorial Office
c/o Hong Kong Academy of Medicine Press
10/F, Hong Kong Academy of Medicine Jockey Club Building
99 Wong Chuk Hang Road, Aberdeen, Hong Kong
Tel: (852) 2871 8809; Fax: (852) 2515 9061
Email: hkjr@hkam.org.hk

Advertisements

Correspondence concerning advertisements should be addressed to:

Executive Assistant
Hong Kong College of Radiologists
Room 909, 9/F Hong Kong Academy of Medicine Jockey Club Building
99 Wong Chuk Hang Road, Aberdeen, Hong Kong.
Tel: (852) 2871 8788; Fax: (852) 2554 0739
Email: hkjr@hkcr.org

Reprints

Reprints of individual articles are available to authors only. Reprints in large quantities (non-authors), for commercial or academic use, may be purchased from the publisher. For information and prices, please send an email to: hkjr@hkam.org.hk.

Copyright

On acceptance of an article by the Journal, the corresponding author will be asked to transfer copyright of the article to the College. The Copyright Transfer Assignment Form will be sent to the author at the time of acceptance.

Disclaimer

Hong Kong Journal of Radiology and the publisher do not guarantee, directly or indirectly, the quality or efficacy of any product or service described in the advertisements or other material which is commercial in nature in this issue. All articles published, including editorials and letters, represent the opinions of the authors and do not reflect the official policy of the Journal, Hong Kong College of Radiologists, the publisher, or the institution with which the author is affiliated, unless this is clearly specified.

Hong Kong Journal of Radiology
ISSN 2223-6619 (Print)
ISSN 2307-4620 (Online)

Hong Kong J Radiol. 2023;26:84-90. Epub 9 Jun 2023 | https://doi.org/10.12809/hkjr2317508

ORIGINAL ARTICLE

Transradial Access for Neurointervention: A Case Series from a Tertiary Centre in Hong Kong

KH Fung[1], NR Mahboobani[1], JC Ng[1], KWS Ko[1], VWT Chan[1], KW Shek[1], NL Chan[2], JK Sham[2], CSK Chau[3], JWT Lo[3], TL Poon[2], KF Fok[2], WL Poon[1]

[1]Department of Radiology and Imaging, Queen Elizabeth Hospital, Hong Kong SAR, China
[2]Department of Neurosurgery, Queen Elizabeth Hospital, Hong Kong SAR, China
[3]Department of Medicine, Queen Elizabeth Hospital, Hong Kong SAR, China

ABSTRACT

Introduction: *Despite several retrospective studies showing the safety and efficacy of transradial access (TRA) for a variety of neurointerventions, the evidence in Asian populations is limited. The smaller size of the radial artery in Asians could cause technical difficulty in access as well as access site complications. This study aimed to assess the feasibility and safety of TRA for neurointervention in an Asian population.*

Methods: *We performed a retrospective review of neurointerventions performed with TRA in our hospital between January 2018 and June 2021. Technical success was defined as TRA with insertion of the sheath and completion of the intervention without crossover to conventional transfemoral access (TFA). The primary endpoint was the in-hospital stay plus the 30-day incidence of access site haematoma requiring surgical treatment or transfusion, symptomatic radial artery occlusion, hand ischaemia, arteriovenous fistula, pseudoaneurysm, and wound infection. The secondary endpoints were procedure-related complications including intra-operative vessel injury, cerebral thromboembolism, and haemorrhagic complications.*

Results: *A total of 45 patients underwent neurointerventions (transcatheter embolisation of aneurysms/arteriovenous malformations/tumours, and extracranial carotid stenting) via TRA. The technical success rate was 93.3%. There were no significant access site complications. The overall procedure-related complication rate was 11.1%.*

Conclusion: *In an Asian population, neurointervention via TRA is feasible, with a low crossover rate and low incidence of access site complications. In this case series, there was no increase in the procedure-related complication rate when compared with TFA.*

Key Words: *Aneurysm; Arteriovenous malformations; Carotid stenosis; Radial artery*

Correspondence: *Dr KH Fung, Department of Radiology and Imaging, Queen Elizabeth Hospital, Hong Kong SAR, China*
Email: fkh666@ha.org.hk

Submitted: 29 Nov 2021; Accepted: 13 May 2022.

Contributors: KHF, NRM and WLP designed the study. All authors acquired the data. KHF analysed the data and drafted the manuscript. NRM critically revised the manuscript for important intellectual content. All authors had full access to the data, contributed to the study, approved the final version for publication, and take responsibility for its accuracy and integrity.

Conflicts of Interest: All authors have disclosed no conflicts of interest.

Funding/Support: This research received no specific grant from any funding agency in the public, commercial, or not-for-profit sectors.

Data Availability: All data generated or analysed during the present research are included in this published article (and its supplementary information files).

Ethics Approval: This research was approved by the Research Ethics Committee (Kowloon Central/Kowloon East) of Hospital Authority, Hong Kong (Ref No.: KC/KE-21-0225/ER-1). Patient consent was waived by the Committee due to the retrospective nature of the research.

中文摘要

神經介入的橈動脈入路：來自香港一所三級醫療中心的病例系列

馮景謙、馬承志、吳昆倫、高偉琛、陳煒達、石家偉、陳諾麟、沈雋、鄒韶君、勞慧婷、潘德立、霍錦福、潘偉麟

引言：儘管多項回顧性研究表明經橈動脈入路用於各種神經介入的安全性和有效性，但亞洲人群的證據有限。亞洲人的橈動脈較小可能會導致導管插入困難以及插入部位併發症。本研究旨在評估經橈動脈入路在亞洲人群中進行神經介入的可行性和安全性。

方法：我們對2018年1月至2021年6月期間在本院使用經橈動脈入路進行的神經介入進行了回顧性分析。技術成功的定義為經橈動脈入路插入鞘管並完成介入而無需採用傳統經股動脈通路。主要終點是住院時間加上需要手術治療或輸血的穿刺部位血腫、有症狀的橈動脈閉塞、手部缺血、動靜脈瘺、假性動脈瘤和傷口感染的30天發生率。次要終點是手術相關併發症，包括術中血管損傷、腦血栓栓塞和出血併發症。

結果：共有45名患者通過經橈動脈入路接受了神經介入（動脈瘤／動靜脈畸形／腫瘤的經導管栓塞，以及顱外頸動脈支架置入術）。技術成功率為93.3%。沒有明顯的插入部位併發症。總體手術相關併發症發生率為11.1%。

結論：在亞洲人群中通過經橈動脈入路進行神經介入是可行的，需採用經橈動脈入路的手術率低，穿刺部位併發症發生率亦低。在本病例系列中，與經股動脈通路相比，手術相關併發症的發生率沒有增加。

INTRODUCTION

Transradial access (TRA) has evolved as the standard approach for cardiac interventions. Compared to conventional transfemoral access (TFA), TRA has a demonstrated lower rate of access site complications, improved postprocedural quality of life, and reduced hospital costs in large-scale randomised trials.[1-9] At first, TRA was not widely used in neurointervention due to technical challenges in puncturing and obtaining access for a large-bore sheath in the small radial artery. In recent years, TRA has been gaining popularity for neurointerventions due to two major advantages. First, the superficial location and compressibility of the radial artery can reduce access site bleeding and related complications, especially when large-bore vascular access is needed together with the need to administer dual antiplatelet treatment. Second, TRA has anatomical and technical advantage in patients with type III and bovine arch morphology.[10]

There are reports from Western countries demonstrating low rates of access site complications and crossover to TFA in TRA neurointerventions.[11-13] However, there are limited reports on TRA for neurointervention in Asian populations. There are differences in the size of the radial arteries between patients of various ethnicities. The mean internal diameter of the radial artery has been reported to be 3.64 ± 0.74 mm in the Western population[14] compared to 2.63 ± 0.35 mm in the Asian population.[15] The smaller radial artery diameter in Asians could potentially affect arterial accessibility of and also the rate of access site complications.

The aim of our study was to assess our experience with TRA in 45 neurointerventions in a tertiary neurointervention centre with a predominant Asian patient population.

METHODS

This was a retrospective study performed in a tertiary neurointervention centre in Hong Kong. Our patient population is primarily Asian and predominantly Chinese. We reviewed consecutive neurointerventional cases performed with TRA in Queen Elizabeth Hospital between January 2018 and June 2021. The neurointerventions performed include carotid stenting,

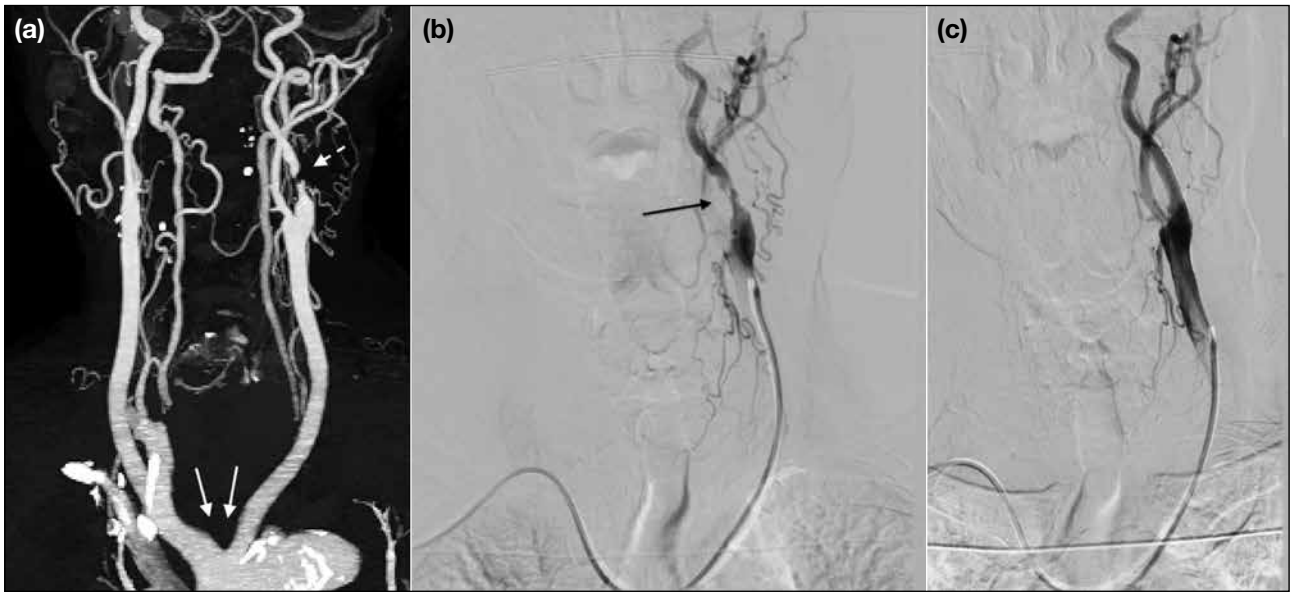

Figure 1. (a) Computed tomography angiogram of the neck showing severe left proximal internal carotid artery (ICA) stenosis (dashed arrow) in a patient with bovine arch (arrows). (b) Left ICA angiogram with transradial access (TRA) showing severe left proximal cervical ICA stenosis (arrow). (c) Left carotid stent performed with TRA. Post–carotid stent angiogram showed satisfactory angiographic result.

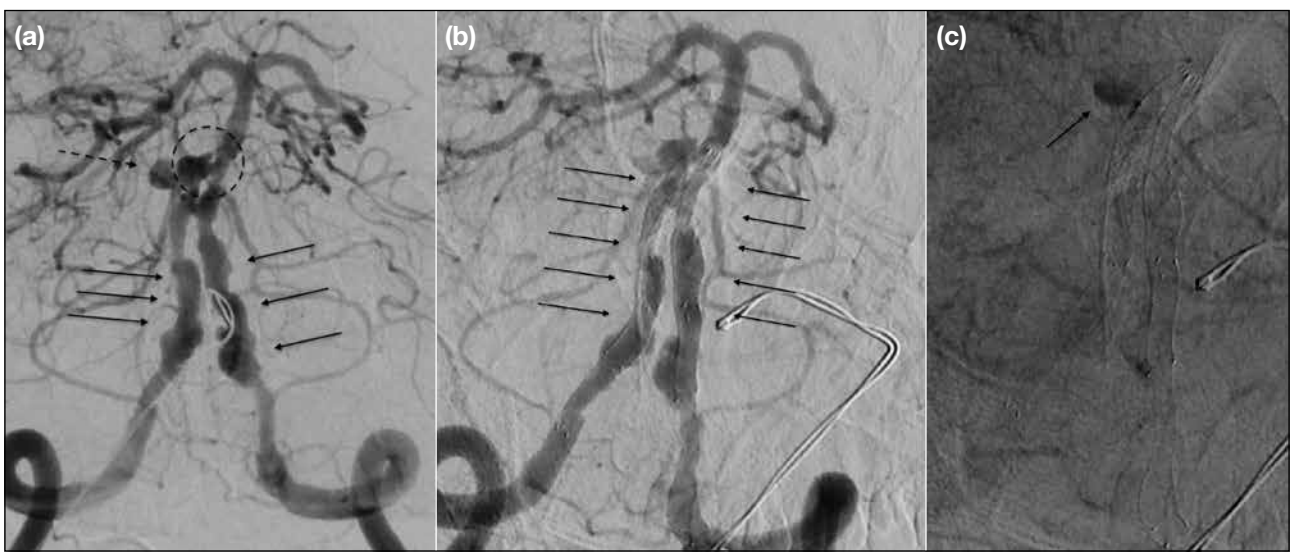

Figure 2. (a) Bilateral vertebral angiogram shows dissection along intradural segment of both vertebral arteries with alternating segments of stenoses and dilatations (arrows). Fenestration of right vertebrobasilar junction is shown (dashed circle). There is an aneurysm arising from the right vertebrobasilar junction (dashed arrow). (b) Two flow diverters were deployed from the right vertebrobasilar junction to the right vertebral artery proximal V4 segment, followed by deployment of two flow diverters from the left vertebrobasilar junction to left vertebral artery distal V3 segment. Bilateral flow diverters (arrows) were patent. (c) Post–flow diverter deployment angiogram showing contrast stasis in the right vertebrobasilar junction aneurysm (arrow).

transcatheter embolisation (TCE) of intracranial aneurysms, stenting of intracranial arteries, TCE of arteriovenous malformations, and tumour TCE.

The decision to perform neurointervention using TRA was made prior to the procedure in cases with factors reported to favour TRA, which include but are not limited to type II/III aortic arch, bovine arch (Figure 1), posterior circulation vascular lesions (Figure 2), high bleeding risk due to use of dual antiplatelet therapy, obesity, and failed

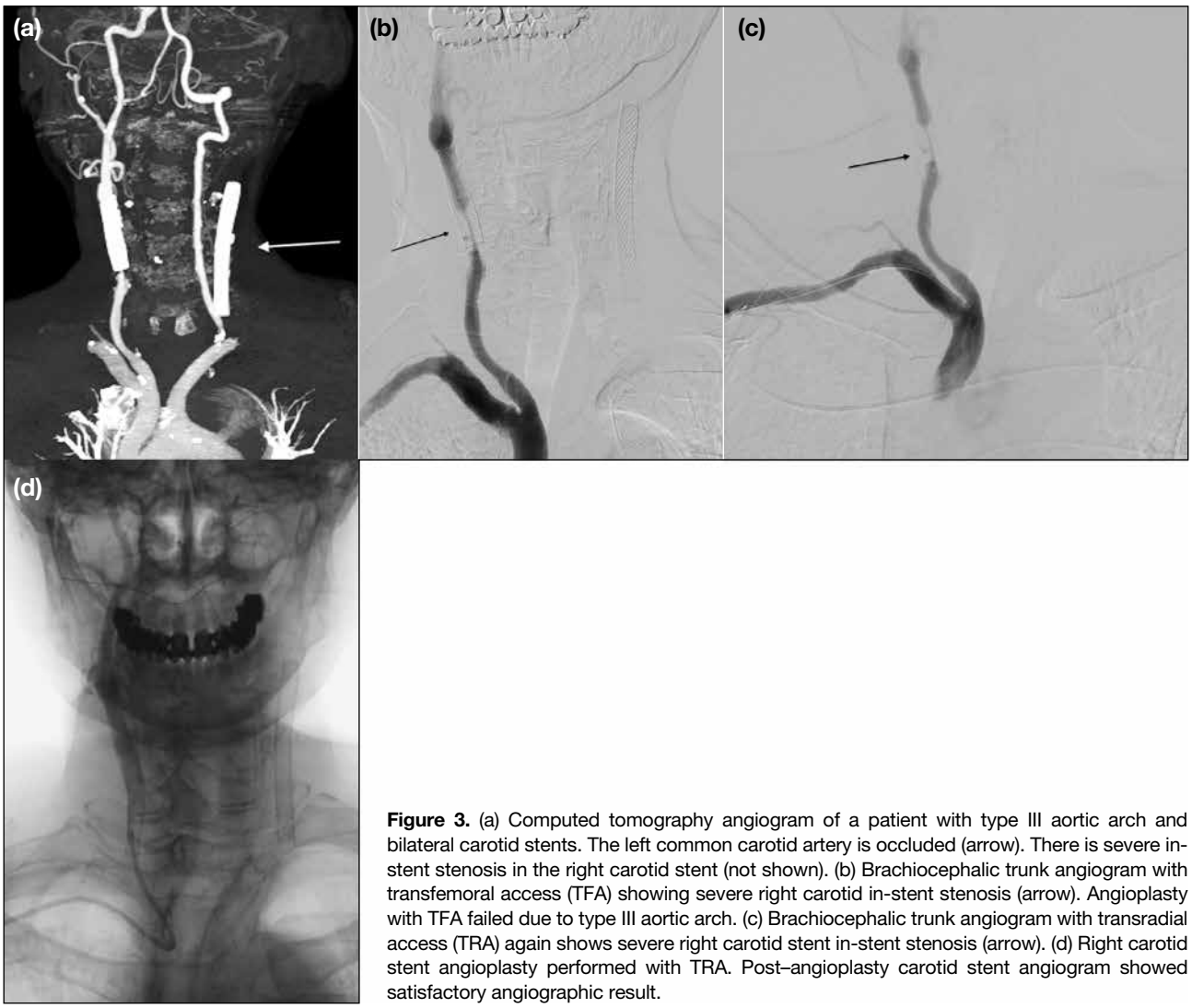

Figure 3. (a) Computed tomography angiogram of a patient with type III aortic arch and bilateral carotid stents. The left common carotid artery is occluded (arrow). There is severe in-stent stenosis in the right carotid stent (not shown). (b) Brachiocephalic trunk angiogram with transfemoral access (TFA) showing severe right carotid in-stent stenosis (arrow). Angioplasty with TFA failed due to type III aortic arch. (c) Brachiocephalic trunk angiogram with transradial access (TRA) again shows severe right carotid stent in-stent stenosis (arrow). (d) Right carotid stent angioplasty performed with TRA. Post–angioplasty carotid stent angiogram showed satisfactory angiographic result.

TFA (Figure 3). All cases meeting the inclusion criteria were included in this study except there was one case excluded as the patient was observed with Barbeau type D waveform. The list of factors was based on medical knowledge and neurointervention experience, and the decision was made by neurointervention operators.

Endovascular Procedure

Our standard approach was to perform the Barbeau test prior to radial artery puncture. For Barbeau types A, B and C, the neurointervention would proceed with TRA; for Barbeau type D, neurointervention would be performed with TFA.

The puncture site of the radial artery was either at the wrist (2 to 3 cm proximal to palmar wrist crease) or the distal radial artery (at the anatomical snuffbox). The choice of access site was based on the calibre of the radial artery measured with ultrasound at the respective sites and also operators' preference. The choice of right or left radial artery depended on the location of the target lesion. For example, for right vertebral artery or right internal carotid artery lesion, right transradial approach was used; for left vertebral artery lesion, left transradial approach was used.

TRA was achieved with a single-wall puncture under ultrasound guidance, followed by insertion of a 6-F sheath (Radifocus Introducer II Transradial Kit; Terumo, Tokyo, Japan). An antispasmodic cocktail (2.5 mg of verapamil and 200 μg of nitroglycerin) was administered via the radial sheath; this became our standard practice and was

administered in the last 38 cases in this series with close monitoring of blood pressure. Haemodilution (aspirating a substantial amount [a few mm] of blood into syringe) and slow injection of the antispasmodic cocktail were adopted to mitigate the burning sensation associated with the cocktail and to avoid a sudden drop in blood pressure. A bolus of heparin (50 units/kg) and heparin infusion (600 units/h) were administered intravenously.

The supra-aortic vessels were catheterised by advancing a guide catheter (Benchmark 071; Penumbra, Alameda [CA], US; Neuron 053, Penumbra, Alameda [CA], US; or Mach 1; Boston Scientific, Natick [MA], US), over a standard hydrophilic angled 0.035-inch guidewire (Terumo, Tokyo, Japan), with or without the aid of a 5-Fr diagnostic catheters such as a Simmons 2–shaped catheter (Terumo, Tokyo, Japan), Torcon NB Advantage Catheter (Cook Medical, Bloomington [IN], US) or JB2 catheter (Cordis, Miami [FL], US). The guide catheter could be preloaded with the diagnostic catheter or exchanged for a diagnostic catheter over a guidewire.

Upon completion of the procedure, the radial artery puncture site was closed with application of a haemostatic bandage (Stepty P; Nichiban, Tokyo, Japan) for 4 hours. Patients were then examined for access site haematoma and for distal perfusion. All patients were reviewed for access site complications during the hospital stay and underwent follow-up in the outpatient clinic.

Outcome

Technical success was defined as TRA with insertion of the sheath and completion of neurointervention without crossover to conventional TFA for intervention. The primary endpoint was the in-hospital stay plus 30-day incidence of significant access site complications including access site haematoma requiring surgical treatment or transfusion, symptomatic radial artery occlusion, hand ischaemia, arteriovenous fistula, pseudoaneurysm, or wound infection. The secondary endpoints were procedure-related complications including intraoperative vessel injury, and cerebral thromboembolic and haemorrhagic complications.

RESULTS

Between January 2018 and June 2021, 45 neurointerventions were performed with TRA in our institution. Patient demographics, neurointervention performed, target lesion, rationale for TRA, and location of radial artery puncture are listed in the online supplementary Table.

All 45 patients were Asian and 43 of them (95.6%) were Chinese. There were 17 cases (37.8%) of TCE of aneurysm(s) in the anterior circulation, 16 cases (35.6%) of TCE of aneurysm(s) in the posterior circulation (Figure 2), 10 cases (22.2%) of carotid stenting (Figures 1 and 3), one case (2.2%) of embolisation of a meningioma, and one case (2.2%) of TCE of an arteriovenous malformation in the posterior fossa.

We performed 46 radial artery punctures in the 45 neurointerventions. There were 34 punctures (73.9%) at wrist level and 12 punctures (26.1%) at the anatomical snuffbox.

The overall rate of technical success of TRA was 93.3%, with no instances of failure in obtaining radial access. There was no case of radial artery vasospasm nor radial loop requiring crossover to TFA. There were three cases with crossover (6.7%) to TFA due to severe acute angulation between the right subclavian artery and the right common carotid artery.

For the primary safety endpoints, there was no significant access site haematoma, symptomatic radial artery occlusion, hand ischaemia, arteriovenous fistula, pseudoaneurysm, or wound infection during in-hospital stay and 30 days thereafter.

For secondary endpoints, five patients (11.1%) had procedure-related complications. There were two cases of intra-operative aneurysm rupture, two cases of thromboembolism (one case resolved with intra-arterial eptifibatide injection with no clinical sequelae; the other case suffered a middle cerebral artery territory infarct noted on postoperative day 2), and one case of intra-operative in-stent stenosis.

DISCUSSION

There is increasing utilisation of TRA in diagnostic and interventional cerebral angiography, with good clinical outcomes. It is becoming the preferred choice of access by patients.[16,17] There are published case series demonstrating feasibility and safety of TRA in a variety of neurointerventions, such as aneurysm TCE,[11] flow diverting stent placement[12] and mechanical thrombectomy,[13] which were all performed in Western countries. There is no corresponding literature in Asian populations.

Our case series is the first which consists of Asian (100%) and predominantly Chinese patients (95.6%).

It demonstrates a high success rate in performing neurointerventions with TRA, which is similar to published case series with Caucasian patients, despite the smaller radial artery diameter in Asians when compared to Caucasians.[14,15] The crossover rate in our case series was similar compared to other published case series. In a systemic review of TRA in neurointerventions which consisted of 21 studies (n = 1342 patients),[10] the crossover rate was 4.77%. Radial artery spasm is one of the potential difficulties in performing neurointervention with TRA. It was only rarely encountered in this case series. The antispasmodic cocktail was very effective in preventing and treating radial artery spasm. The fact that we performed all neurointerventions apart from carotid stenting with general anaesthesia was a protective factor. Another potential difficulty in performing neurointervention with TRA was radial loops. Radial loops were only rarely encountered in this case series. The radial loop is a rare vascular anomaly with a reported frequency of 2.3% in one large multicentre case series.[18] In the few cases with radial loop which we encountered in this case series, the loop was reduced with advancement of the catheter with the aid of a guidewire.

TRA also demonstrated safety among our patient group with no significant access site complications observed in our case series. In a systematic review,[10] the major access site complication rate was reported to be 0.15%.

The overall procedure-related complication rate in our case series was 11.1% (5 out of 45 cases). All five complicated cases were TCE of intracranial aneurysms. In subgroup analysis, the complication rate of TCE of intracranial aneurysms with TRA was 15.2%, which is within the reported range in the literature.[19-22] The overall TRA procedure–related complication rate was similar to that with TFA in our centre (10%-20%).

Limitations

Our study has a few limitations. First, it was a single-centre study which limits its generalisability. However, the neurointerventions in this series were performed by 11 operators with variable lengths of experience in neurointervention from <1 year to >20 years. This could suggest that TRA can be performed by operators with different levels of experience.

Second, this study has a small sample size. Neurointervention with TRA was increasingly performed in our centre because operators were gaining experience and confidence in TRA. According to cardiac literature and studies regarding diagnostic cerebral angiography with TRA, there is a 30- to 50-case learning curve,[23,24] and we expect our crossover and procedure-related complication rate will improve with our increasing case volume of TRA.

CONCLUSION

This case series is believed to be the first one to demonstrate that TRA is feasible and safe to perform for a variety of neurointerventions in Asian patients, who have relatively smaller radial artery calibres when compared to Caucasian patients. The crossover rate was low and there was a high success rate of 93.3% with TRA. There were no significant access site complications in this case series. There was no increase in the procedure-related complication rate with TRA when compared with TFA in our centre.

REFERENCES

1. Jolly SS, Amlani S, Hamon M, Yusuf S, Mehta SR. Radial versus femoral access for coronary angiography or intervention and the impact on major bleeding and ischemic events: a systematic review and meta-analysis of randomized trials. Am Heart J. 2009;157:132-40.
2. Agostoni P, Biondi-Zoccai GG, de Benedictis ML, Rigattieri S, Turri M, Anselmi M, et al. Radial versus femoral approach for percutaneous coronary diagnostic and interventional procedures: systematic overview and meta-analysis of randomized trials. J Am Coll Cardiol. 2004;44:349-56.
3. Kiemeneij F, Laarman GJ, Odekerken D, Slagboom T, van der Wieken R. A randomized comparison of percutaneous transluminal coronary angioplasty by the radial, brachial and femoral approaches: the access study. J Am Coll Cardiol. 1997;29:1269-75.
4. Mamas MA, Tosh J, Hulme W, Hoskins N, Bungey G, Ludman P, et al. Health economic analysis of access site practice in England during changes in practice: insights from the British Cardiovascular Interventional Society. Circ Cardiovasc Qual Outcomes. 2018;11:e004482.
5. Mann JT 3rd, Cubeddu MG, Schneider JE, Arrowood M. Right radial access for PTCA: a prospective study demonstrates reduced complications and hospital charges. J Invasive Cardiol. 1996;8 Suppl D:40D-44D.
6. Valgimigli M, Frigoli E, Leonardi S, Vranckx P, Rothenbühler M, Tebaldi M, et al. Radial versus femoral access and bivalirudin versus unfractionated heparin in invasively managed patients with acute coronary syndrome (MATRIX): final 1-year results of a multicentre, randomised controlled trial. Lancet. 2018;392:835-48.
7. Sciahbasi A, Pristipino C, Ambrosio G, Sperduti I, Scabbia EV, Greco C, et al. Arterial access-site–related outcomes of patients undergoing invasive coronary procedures for acute coronary syndromes (from the ComPaRison of Early Invasive and Conservative Treatment in Patients With Non–ST-ElevatiOn Acute Coronary Syndromes [PRESTO-ACS] Vascular Substudy). Am J Cardiol. 2009;103:796-800.
8. Valgimigli M, Gagnor A, Calabró P, Frigoli E, Leonardi S, Zaro T, et al. Radial versus femoral access in patients with acute coronary

syndromes undergoing invasive management: a randomised multicentre trial. Lancet. 2015;385:2465-76.
9. Kok MM, Weernink MG, von Birgelen C, Fens A, van der Heijden LC, van Til JA. Patient preference for radial versus femoral vascular access for elective coronary procedures: the PREVAS study. Catheter Cardiovasc Interv. 2018;91:17-24.
10. Joshi KC, Beer-Furlan A, Crowley RW, Chen M, Munich SA. Transradial approach for neurointerventions: a systematic review of the literature. J Neurointerv Surg. 2020;12:886-92.
11. Chivot C, Bouzerar R, Yzet T. Transitioning to transradial access for cerebral aneurysm embolization. AJNR Am J Neuroradiol. 2019;40:1947-53.
12. Li Y, Chen SH, Spiotta AM, Jabbour P, Levitt MR, Kan P, et al. Lower complication rates associated with transradial versus transfemoral flow diverting stent placement. J Neurointerv Surg. 2021;13:91-5.
13. Phillips TJ, Crockett MT, Selkirk GD, Kabra R, Chiu AH, Singh T, et al. Transradial versus transfemoral access for anterior circulation mechanical thrombectomy: analysis of 375 consecutive cases. Stroke Vasc Neurol. 2021;6:207-13.
14. Bertrand B, Sene Y, Huygue O, Monségu J. Doppler ultrasound imaging of the radial artery after catheterization [in French]. Ann Cardiol Angeiol (Paris). 2003;52:135-8.
15. Yoo BS, Lee SH, Ko JY, Lee BK, Kim SN, Lee MO, et al. Procedural outcomes of repeated transradial coronary procedure. Catheter Cardiovasc Interv. 2003;58:301-4.
16. Snelling BM, Sur S, Shah SS, Khandelwal P, Caplan J, Haniff R, et al. Transradial cerebral angiography: techniques and outcomes. J Neurointerv Surg. 2018;10:874-81.
17. Stone JG, Zussman BM, Tonetti DA, Brown M, Desai SM, Gross BA, et al. Transradial versus transfemoral approaches for diagnostic cerebral angiography: a prospective, single-center, non-inferiority comparative effectiveness study. J Neurointerv Surg. 2020;12:993-8.
18. Lo TS, Nolan J, Fountzopoulos E, Behan M, Butler R, Hetherington SL, et al. Radial artery anomaly and its influence on transradial coronary procedural outcome. Heart. 2009;95:410-5.
19. Henkes H, Fischer S, Weber W, Miloslavski E, Felber S, Brew S, et al. Endovascular coil occlusion of 1811 intracranial aneurysms: early angiographic and clinical results. Neurosurgery. 2004;54:268-80.
20. Brilstra EH, Rinkel GJ, van der Graaf Y, van Rooij WJ, Algra A. Treatment of intracranial aneurysms by embolization with coils: a systematic review. Stroke. 1999;30:470-6.
21. Lozier AP, Connolly ES Jr, Lavine SD, Solomon RA. Guglielmi detachable coil embolization of posterior circulation aneurysms: a systematic review of the literature. Stroke. 2002;33:2509-18.
22. Murayama Y, Nien YL, Duckwiler G, Gobin YP, Jahan R, Frazee J, et al. Guglielmi detachable coil embolization of cerebral aneurysms: 11 years' experience. J Neurosurg. 2003;98:959-66.
23. Hess CN, Peterson ED, Neely ML, Dai D, Hillegass WB, Krucoff MW, et al. The learning curve for transradial percutaneous coronary intervention among operators in the United States: a study from the National Cardiovascular Data Registry. Circulation. 2014;129:2277-86.
24. Zussman BM, Tonetti DA, Stone J, Brown M, Desai SM, Gross BA, et al. Maturing institutional experience with the transradial approach for diagnostic cerebral arteriography: overcoming the learning curve. J Neurointerv Surg. 2019;11:1235-8.

Hong Kong J Radiol. 2023;26:91-99. Epub 8 Jun 2023 | https://doi.org/10.12809/hkjr2317576

ORIGINAL ARTICLE **CME**

Treatment Outcomes of Stage II or III Gastric Cancer Treated with Adjuvant Chemotherapy with TS-1 or XELOX after Radical Surgery

TCY So, KC Lee, ECY Wong

Department of Clinical Oncology, Pamela Youde Eastern Hospital, Hong Kong SAR, China

ABSTRACT

Introduction: *Capecitabine plus oxaliplatin (XELOX) and tegafur/gimeracil/oteracil (TS-1, also known as 'S-1') are two commonly used adjuvant chemotherapy regimens for gastric cancer in Hong Kong. This study aimed to review the outcomes of patients receiving these two regimens, to investigate important clinical factors that may impact on the risk of disease recurrence, and to explore the roles of neutrophil-to-lymphocyte ratio and platelet-to-lymphocyte ratio (PLR) in prognostication after radical surgery.*

Methods: *Patients who received adjuvant treatment (either XELOX or TS-1) for gastric cancer following radical surgical resection from January 2016 to December 2020 at our hospital were included. Patient demographics, overall survival (OS), and disease-free survival (DFS) were analysed.*

Results: *A total of 65 patients were included (XELOX: n = 40; TS-1: n = 25). XELOX appeared to have more favourable OS and DFS, although the result was confounded by older and frailer patients in the TS-1 group. An elevated PLR was associated with inferior OS after surgery (p = 0.036). Cox regression analysis showed that Eastern Cooperative Oncology Group (ECOG) performance status score of 2 and nodal stage of N2 to N3 were two independent factors associated with inferior OS. ECOG performance status score of 2, nodal stage of N2 to N3, and chemotherapy dose intensity <70% were significantly associated with a higher risk of relapse.*

Conclusion: *Poorer ECOG performance status and more advanced nodal stage are independent factors associated with inferior OS and DFS, and lower chemotherapy dose intensity (<70%) resulted in a higher risk of disease relapse. NLR and PLR is a simple clinical marker that may be further explored as a prognostic marker for gastric cancer after radical surgery.*

Key Words: *Blood platelets; Lymphocytes; Neutrophils; Prognosis; Stomach neoplasms*

Correspondence: *Dr TCY So, Department of Clinical Oncology, Pamela Youde Eastern Hospital, Hong Kong SAR, China*
Email: scy027@ha.org.hk

Submitted: 6 May 2022; Accepted: 2 Dec 2022.

Contributors: TCYS and ECYW designed the study. TCYS acquired, analysed the data and drafted the manuscript. KCL and ECYW critically revised the manuscript for important intellectual content. All authors had full access to the data, contributed to the study, approved the final version for publication, and take responsibility for its accuracy and integrity.

Conflicts of Interest: All authors have disclosed no conflicts of interest.

Funding/Support: This research received no specific grant from any funding agency in the public, commercial, or not-for-profit sectors.

Data Availability: All data generated or analysed during the present research are available from the corresponding author on reasonable request.

Ethics Approval: This research has been approved by the Hong Kong East Cluster Research Ethics Committee of Hospital Authority, Hong Kong (Ref. No.: HKECREC-2022-021) and was conducted in compliance with the Declaration of Helsinki. The requirement for patient consent was waived by the Committee due to the retrospective nature of the study.

中文摘要

根治性手術後使用TS-1或XELOX輔助化療治療II期或III期胃癌的治療結果

蘇駿寅、李建忠、王晉彥

簡介：卡培他濱聯合奧沙利鉑（XELOX）及替加氟／吉美嘧啶／氧嗪酸（TS-1，又稱S-1）是香港兩種常用於胃癌的輔助化療方案。本研究旨在回顧接受這兩種方案的病人的結果，調查可能影響疾病復發風險的重要臨床因素，以及研究在根治性手術後嗜中性白血球與淋巴細胞比例（NLR）及血小板與淋巴細胞比例（PLR）在預測方面的角色。

方法：本研究包括於2016年1月至2020年12月期間在本院進行根治性手術切除後接受輔助治療（XELOX或TS-1）的胃癌病人，並分析了有關患者的人口特徵、整體存活及無疾病存活。

結果：本研究共包括65名患者（XELOX：n = 40；TS-1：n = 25）。雖然XELOX的整體存活及無疾病存活似乎較好，但這些結果受TS-1組別中年紀較大及較虛弱的患者影響。血小板與淋巴細胞比例上升與較差的術後整體存活相關（p = 0.036）。Cox迴歸分析顯示美國東岸癌症臨床研究合作組織（ECOG）身體功能狀態評分為2分及癌症分期為N2至N3，是與較差的整體存活相關的兩個獨立因素。ECOG身體功能狀態評分為2分、癌症分期為N2至N3及化療劑量強度<70%與較高復發風險顯著相關。

結論：較差的ECOG身體功能狀態及較晚期的癌症分期是與較差的整體存活及無疾病存活相關的獨立因素，而較低的化療劑量強度<70%造成較高的疾病復發風險。NLR和PLR是簡單的臨床標記，可成為日後的研究方向，以此比例作為根治性手術後胃癌的預後標記。

INTRODUCTION

Gastric cancer was the sixth commonest cancer in Hong Kong, accounting for 3.7% of all new cancer cases in 2019.[1] Although the incidence has been gradually declining, compatible with global trends due to efficacious *Helicobacter pylori* eradication therapy,[2] gastric cancer remains more prevalent in Asian countries than in the West.

Clear surgical resection with D2 lymphadenectomy and chemotherapy is considered the standard of care for resectable locoregionally advanced gastric cancer nowadays,[3] and this has been advocated in several international guidelines.[4,5] Adjuvant chemoradiotherapy (45 Gy over 25 fractions concurrent with 5-fluorouracil and leucovorin) had once been widely adopted, but was later criticised for the inclusion of a high proportion of patients with D1 lymphadenectomy in the study recommending it.[6]

The choice of chemotherapy regimen significantly differs among different parts of the world. In European countries, perioperative chemotherapy, such as the combination of epirubicin, cisplatin, and 5-fluorouracil[7] or 5-fluorouracil, leucovorin, oxaliplatin, and docetaxel,[8] is frequently used, whereas in Hong Kong, clinicians tend to use adjuvant chemotherapy as in most Asian countries. The two most commonly used regimens of adjuvant chemotherapy after radical surgery are capecitabine plus oxaliplatin (XELOX) and tegafur/gimeracil/oteracil (TS-1, also known as 'S-1'). They both demonstrated significant benefits when compared with surgery alone in randomised clinical trials[9,10] conducted in Asian countries. Despite the two regimens having been widely used, there are no prospective randomised clinical trials directly comparing their efficacy.

Regarding the prognostic stratification of patients with resected gastric cancer, several clinical and pathological parameters have long been adopted to predict the recurrence of gastric cancer including age, comorbidities, tumour size, differentiation status, and presence of lymphovascular or perineural invasion.[11-14] In recent years, the clinical utility of the peripheral neutrophil-

to-lymphocyte ratio (NLR) and platelet-to-lymphocyte ratio (PLR) as systemic inflammatory markers has been addressed. In relation to cancer prognosis, several meta-analyses showed that elevated NLR and PLR correlated with tumour progression and poor survival in a number of gastrointestinal cancers.[15,16] However, what the same observation connotes in the adjuvant setting remains uncertain.

This retrospective study was conducted with three aims: to compare the efficacy of adjuvant XELOX with TS-1 chemotherapy for patients with stage II or III gastric cancer who received radical surgery in our locality; to investigate important clinical factors that may impact on the risk of disease recurrence; and to explore the prognostic value of NLR and PLR as potentially useful and easily available clinical parameters.

METHODS

Patients and Data Collection

Patients who received adjuvant treatment (XELOX: n = 40; TS-1: n = 25) for gastric cancer following radical surgical resection from January 2016 to December 2020 at the Department of Clinical Oncology, Pamela Youde Eastern Hospital, Hong Kong were included in the study. Patients with metastatic disease at presentation (including small-volume peritoneal metastasis) or double primary cancers were excluded. Patients who received adjuvant radiotherapy were also excluded. Relevant clinical and pathological parameters were captured from clinical notes and the Clinical Management System of Hospital Authority.

Treatment

XELOX consists of oral capecitabine (1000 mg/m^2 twice daily on days 1-14 of each cycle) plus intravenous oxaliplatin (130 mg/m^2 on day 1 of each cycle) up to 8 cycles. TS-1 is oral chemotherapy (daily dose according to body surface area [BSA]: patients with BSA <1.25 m^2 received 80 mg daily, those BSA ranging from ≤1.25 m^2 to 1.50 m^2 received 100 mg daily, and those with BSA ≥1.50 m^2 received 120 mg daily) given for 4 weeks followed by 2 weeks of rest for a total of 9 cycles.

In practice, patients of an advanced age, borderline Eastern Cooperative Oncology Group (ECOG) performance status and pre-existing neuropathy would be more likely to be given TS-1, as it is a non–self-financed item under the institution.

Doses and schedule modifications were conducted based on patients' ECOG performance status, organ functions, and toxicities by clinicians' decisions. Dose reduction of chemotherapy was conducted in a stepwise manner (75%-85% of the initial dose for 1st dose reduction, then 60%-70% for the 2nd dose reduction). The relative total dose intensity (RTDI) is the ratio of the delivered actual dose intensity (ATDI) to the standard planned dose intensity (PTDI) for a chemotherapy regimen, which is calculated as follows:

$$\text{RTDI (\%)} = \frac{\text{ATDI}}{\text{PTDI}} \times 100$$

$$\text{PTDI (mg/week)} = \frac{\text{Planned total dose (mg)}}{\text{Planned duration of therapy (weeks)}}$$

$$\text{ATDI (mg/week)} = \frac{\text{Actual total dose (mg)}}{\text{Duration of therapy (weeks)}}$$

Follow-up and Assessment

Patients were seen by doctors prior to each cycle of chemotherapy, when tolerance of chemotherapy and results of blood tests would be recorded in the Clinical Management System. Patients who had completed the adjuvant chemotherapy would be followed up at an interval of 3 to 6 months. Computed tomography was performed if there was clinical suspicion of disease relapse. Disease relapse was defined as any radiological and/or histological confirmation of recurrence. Elevated tumour markers alone were not considered as relapse without proof of recurrent disease.

Statistical Analysis

Statistical analysis was performed using SPSS (Windows version 22; IBM Corp, Armonk [NY], United States). Clinical and pathological data were retrospectively reviewed and analysed by descriptive statistics. Pearson's Chi squared test was used for testing any significant correlations and differences between groups.

Treatment outcomes, including disease-free survival (DFS, the time from surgery to disease relapse) and overall survival (OS, the time from diagnosis of disease to death from any cause) were analysed by the Kaplan-Meier method and the difference between groups were tested with the log-rank test. Different clinical parameters were tested for their impact on DFS and OS by Cox regression analysis.

In order to have an accurate assessment of the baseline NLR and PLR of our patients, the complete blood counts right before the administration of first cycle

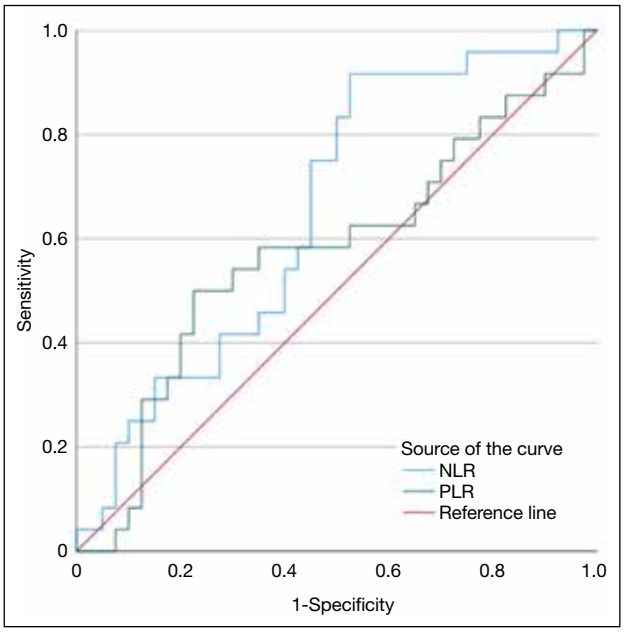

Figure 1. Receiver operating curve (ROC) analysis for optimal cut-off values of neutrophil-to-lymphocyte ratio (NLR) and platelet-to-lymphocyte ratio (PLR).

of chemotherapy were recorded. This is to minimise the effect due to postoperative inflammation and chemotherapy on peripheral blood counts.

Using all-cause mortality as an endpoint for NLR and PLR, the optimal cut-off values were determined by receiver operating curve analysis as shown in Figure 1. The area under the curve of NLR and PLR was 0.653 and 0.575, respectively. The optimal cut-off values determined by the Youden's index for NLR and PLR were 1.9 and 169, respectively.

RESULTS

Patient Characteristics

Sixty-five patients were identified and included in the analysis. Forty patients received XELOX and 25 received TS-1. The median follow-up time for this study was 33.7 months (range, 6.5-78.9).

Patient baseline characteristics are summarised in Table 1. The median age of the entire cohort was 66.0 years. The mean and median age in the XELOX group were 57.7 and 59.0 years respectively, compared to 69.4 and 71.0 years in the TS-1 group. Patients who received TS-1 were significantly older, with 72.0% of them ≥66 years compared to 37.5% in XELOX group (p = 0.007).

Table 1. Patient baseline characteristics of XELOX and TS-1 groups.*

	XELOX group (n = 40)	TS-1 group (n = 25)	p Value (Pearson's Chi squared)
Sex			
Male	25 (62.5%)	15 (60.0%)	0.840
Female	15 (37.5%)	10 (40.0%)	0.840
Age, y			
<66	25 (62.5%)	7 (28.0%)	0.007
≥66	15 (37.5%)	18 (72.0%)	0.007
Mean (median)	57.7 (59.0)	69.4 (71.0)	
ECOG performance status score			
0-1	39 (97.5%)	15 (60.0%)	< 0.001
2	1 (2.5%)	10 (40.0%)	< 0.001
Pretreatment PET			
No	25 (62.5%)	16 (64.0%)	0.903
Yes	15 (37.5%)	9 (36.0%)	0.903
Histology			
Well or moderately differentiated	12 (30.0%)	12 (48.0%)	0.165
Poorly differentiated	27 (67.5%)	13 (52.0%)	0.165
Others	1 (2.5%)	0	0.165
Tumour stage			
T1	2 (5.0%)	0	0.809
T2	6 (15.0%)	2 (8.0%)	0.809
T3	17 (42.5%)	12 (48.0%)	0.809
T4	15 (37.5%)	11 (44.0%)	0.809
Nodal stage			
N0	7 (17.5%)	2 (8.0%)	0.198
N1	6 (15.0%)	9 (36.0%)	0.198
N2	7 (17.5%)	5 (20.0%)	0.198
N3	20 (50.0%)	9 (36.0%)	0.198
Overall stage (AJCC 8th edition)			
IIA	8 (20.0%)	2 (8.0%)	0.380
IIB	6 (15.0%)	8 (32.0%)	0.380
IIIA	7 (17.5%)	5 (20.0%)	0.380
IIIB	12 (30.0%)	5 (20.0%)	0.380
IIIC	7 (17.5%)	5 (20.0%)	0.380
Lymphovascular invasion			
Present	28 (70.0%)	17 (68.0%)	0.822
Absent	9 (22.5%)	5 (20.0%)	0.822
Unknown	3 (7.5%)	3 (12.0%)	0.822
Perineural invasion			
Present	21 (52.5%)	15 (60.0%)	0.571
Absent	16 (40.0%)	7 (28.0%)	0.571
Unknown	3 (7.5%)	3 (12.0%)	0.571
Extent of nodal dissection			
D1	2 (5.0%)	3 (12.0%)	0.240
D1 plus	3 (7.5%)	0	0.240
D2	35 (87.5%)	22 (88.0%)	0.240
Pattern of relapse			
No. of cases	27	22	
Local relapse	1 (2.5%)	2 (8.0%)	0.271
Nodal relapse	9 (22.5%)	6 (24.0%)	0.220
Distant relapse	10 (25.0%)	7 (28.0%)	0.222
Peritoneal relapse	7 (17.5%)	7 (28.0%)	0.339

Abbreviations: AJCC = American Joint Committee on Cancer; ECOG = Eastern Cooperative Oncology Group; PET = positron emission tomography; TS-1 = tegafur/gimeracil/oteracil; XELOX = capecitabine plus oxaliplatin.
* Data are shown as No. (%), unless otherwise specified.

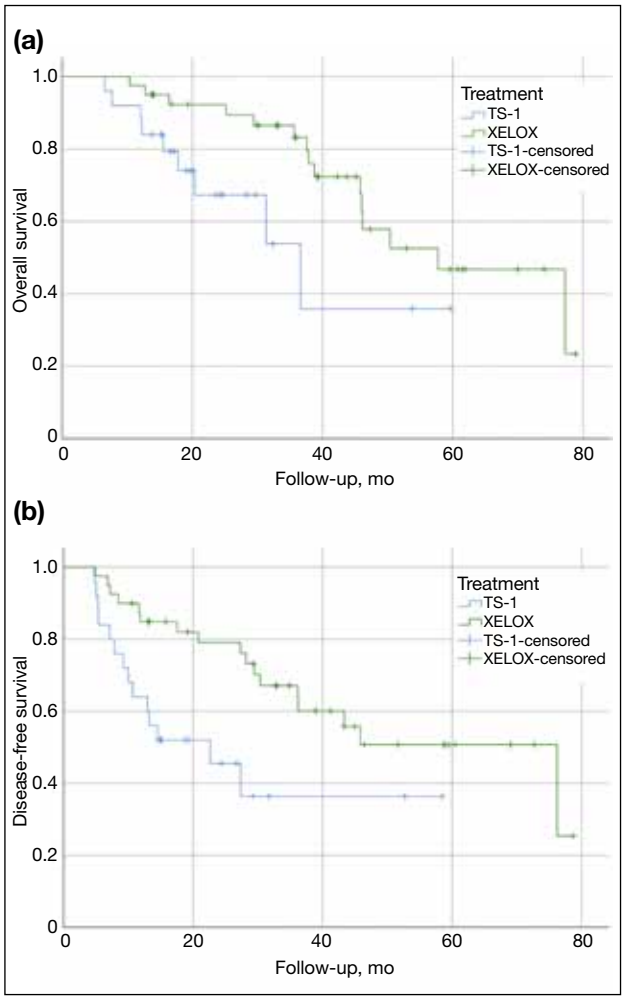

Figure 2. Kaplan-Meier analysis of (a) overall survival (p = 0.037, log-rank test) and (b) disease-free survival (p = 0.012, log-rank test) in all patients with respect to treatment with TS-1 (tegafur/gimeracil/oteracil) or XELOX (capecitabine plus oxaliplatin).

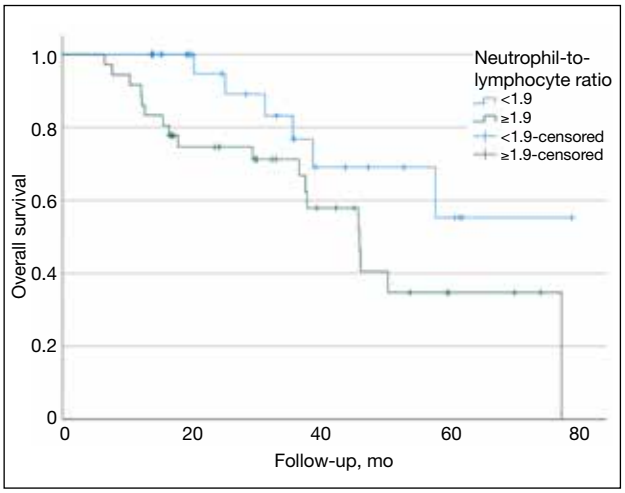

Figure 3. High neutrophil-to-lymphocyte ratio (≥1.9) versus low neutrophil-to lymphocyte-ratio (<1.9) on overall survival (p = 0.051).

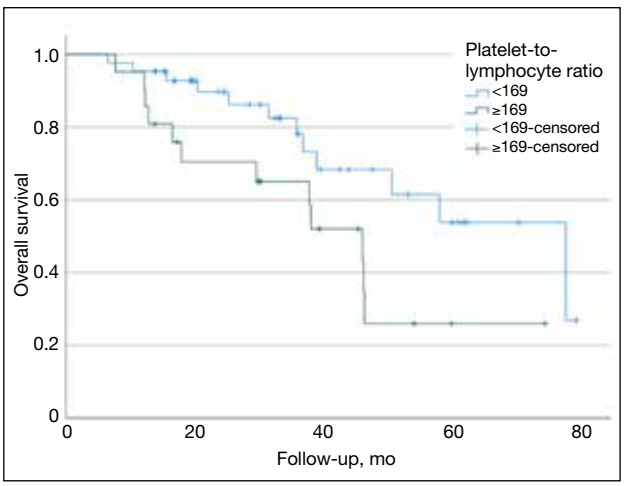

Figure 4. High platelet-to-lymphocyte ratio (≥169) versus low platelet-to-lymphocyte ratio (<169) on overall survival (p = 0.036).

All included patients had an ECOG performance status score of ≤2. There were significantly more patients with ECOG performance status score ≤1 in the XELOX group (97.5%) than in TS-1 group (60.0%) [p < 0.001].

Overall and Disease-Free Survival

The median OS was 38.9 months for the XELOX group and 22.9 months for TS-1 group. The observed OS and DFS in the XELOX group were significantly longer than those in the TS-1 group (Figure 2) [p = 0.037 and 0.012, respectively]. However, it should be interpreted carefully as the baseline patients' characteristics suggested a bias towards prescribing TS-1 in the older age-group and less fit patients. These factors likely confound the survival analysis.

Neutrophil-to-Lymphocyte Ratio and Platelet-to-Lymphocyte Ratio

Overall survival analysis showed that patients with high NLR (≥1.9) before adjuvant chemotherapy had shorter OS than those with low NLR (<1.9), although the difference was marginally significant (p = 0.051; Figure 3). The same analysis also demonstrated that patients with high PLR (≥169) before adjuvant chemotherapy had significantly shorter OS than those with low PLR (<169) [p = 0.036; Figure 4].

In relation to clinical characteristics, patients with elevated NLR correlated with female gender (borderline

Table 2. Clinical characteristics of patients with high and low neutrophil-to-lymphocyte ratio.*

	High NLR (n = 36)	Low NLR (n = 29)	p Value (Pearson's Chi squared
Sex			
Male	26 (72.2%)	14 (48.3%)	0.049
Female	10 (27.8%)	15 (51.7%)	0.049
Age, y			
<66	18 (50.0%)	14 (48.3%)	0.890
≥66	18 (50.0%)	15 (51.7%)	0.890
ECOG performance status score			
0-1	30 (83.3%)	24 (82.8%)	0.951
2	6 (16.7%)	5 (17.2%)	0.951
Histology			
Well or moderately differentiated	11 (30.6%)	13 (44.8%)	0.229
Poorly differentiated	25 (69.4%)	15 (51.7%)	0.229
Others	0	1 (3.5%)	0.229
Overall stage (AJCC 8th edition)			
II	12 (33.3%)	12 (41.4%)	0.303
III	24 (66.7%)	17 (58.6%)	0.303
Lymphovascular invasion			
Present	28 (77.8%)	17 (58.6%)	0.232
Absent	6 (16.7%)	8 (27.6%)	0.232
Unknown	2 (5.6%)	4 (13.8%)	0.232
Perineural invasion			
Present	23 (63.9%)	13 (44.8%)	0.251
Absent	11 (30.6%)	12 (41.4%)	0.251
Unknown	2 (5.6%)	4 (13.8%)	0.251
Treatment received			
XELOX	21 (58.3%)	19 (65.5%)	0.554
TS-1	15 (41.7%)	10 (34.5%)	0.554

Abbreviations: AJCC = American Joint Committee on Cancer; ECOG = Eastern Cooperative Oncology Group; NLR = neutrophil-to-lymphocyte ratio; TS-1 = tegafur/gimeracil/oteracil; XELOX = capecitabine plus oxaliplatin.
* Data are shown as No. (%), unless otherwise specified.

Table 3. Clinical characteristics of patients with high and low platelet-to-lymphocyte ratio.*†

	High PLR (n = 21)	Low PLR (n = 43)	p Value (Pearson's Chi squared)
Sex			
Male	15 (71.4%)	24 (55.8%)	0.229
Female	6 (28.6%)	19 (44.2%)	0.229
Age, y			
<66	12 (57.1%)	19 (44.2%)	0.330
≥66	9 (42.9%)	24 (55.8%)	0.330
ECOG performance status score			
0-1	17 (81.0%)	36 (83.7%)	0.783
2	4 (19.0%)	7 (16.3%)	0.783
Histology			
Well or moderately differentiated	6 (28.6%)	17 (39.5%)	0.507
Poorly differentiated	15 (71.4%)	25 (58.1%)	0.507
Others	0	1 (2.3%)	0.507
Overall stage (AJCC 8th edition)			
II	3 (14.3%)	20 (46.5%)	0.012
III	18 (85.7%)	23 (53.5%)	0.012
Lymphovascular invasion			
Present	17 (81.0%)	28 (65.1%)	0.412
Absent	3 (14.3%)	10 (23.3%)	0.412
Unknown	1 (4.8%)	5 (11.6%)	0.412
Perineural invasion			
Present	13 (61.9%)	22 (51.2%)	0.587
Absent	7 (33.3%)	16 (37.2%)	0.587
Unknown	1 (4.8%)	5 (11.6%)	0.587
Treatment received			
XELOX	14 (66.7%)	25 (58.1%)	0.512
TS-1	7 (33.3%)	18 (41.9%)	0.512

Abbreviations: AJCC = American Joint Committee on Cancer; ECOG = Eastern Cooperative Oncology Group; PLR = platelet-to-lymphocyte ratio; TS-1 = tegafur/gimeracil/oteracil; XELOX = capecitabine plus oxaliplatin.
* Data are shown as No. (%), unless otherwise specified.
† Missing data = 1 (one patient has platelet clumped).

p value of 0.049) and elevated PLR was associated with more advanced disease (p = 0.012) [Tables 2 and 3].

Clinical and Pathological Parameters on Overall Survival and Disease-Free Survival

As shown in Table 4, univariate Cox regression analysis showed that ECOG performance status score of 2, nodal stage of N2 to N3, and elevated PLR (≥169) were adverse prognostic factors for OS, while ECOG performance status score of 2, nodal stage of N2 to N3, and RTDI of chemotherapy <70% were adverse factors associated with disease relapse.

Multivariable Cox regression analysis demonstrated that ECOG performance status score of 2 and nodal stage of N2 to N3 were the two independent adverse prognostic factors for OS (Table 4). For DFS, ECOG performance status score of 2, nodal stage of N2 to N3, and RTDI of chemotherapy <70% were the three independent factors associated with disease relapse (Table 5).

DISCUSSION

Our study revealed that the XELOX group had more favourable oncological outcomes (both DFS and OS) than the TS-1 group. However, it should be noted that patients included in the TS-1 group in out centre were older (p = 0.007) and of worse ECOG performance status (p < 0.001). This is largely due to the fact that the institutional guideline recommends TS-1 as the treatment of choice for older patients with anticipated

Table 4. Cox regression analysis on multiple clinical and pathological parameters on overall survival.

Variable	Univariate		Multivariable	
	HR (95% CI)	p Value	HR (95% CI)	p Value
Age, y (<66, ≥66)	1.166 (0.520-2.612)	0.71		
Sex (male, female)	0.886 (0.375-2.092)	0.783		
ECOG performance status score (0-1, 2)	3.218 (1.143-9.061)	0.027	4.817 (1.509-15.38)	0.008
Histology (differentiated, poorly differentiated)	2.261 (0.836-6.115)	0.108		
Lymphovascular invasion (No, Yes)	0.442 (0.130-1.506)	0.192		
Perineural invasion (No, Yes)	0.676 (0.275-1.661)	0.393		
Tumour stage (T1-T2 vs T3-T4)	1.062 (0.353-3.197)	0.915		
Nodal stage (N0-N1 vs N2-N3)	8.337 (1.952-35.60)	0.004	9.473 (2.114-42.45)	0.003
NLR (<1.9, ≥1.9)	2.437 (0.966-6.147)	0.059		
PLR (<169, ≥169)	2.348 (1.031-5.346)	0.042	1.738 (0.759-3.979)	0.191
Relative total dose intensity (≤70% vs <70%)	1.873 (0.838-4.188)	0.126		

Abbreviations: CI = confidence interval; ECOG = Eastern Cooperative Oncology Group; HR = hazard ratio; NLR = neutrophil-to-lymphocyte ratio; PLR = platelet-to-lymphocyte ratio.

Table 5. Cox regression analysis on multiple clinical and pathological parameters on disease-free survival.

Variable	Univariate		Multivariable	
	HR (95% CI)	p Value	HR (95% CI)	p Value
Age, y (<66, ≥66)	1.416 (0.693-2.894)	0.34		
Sex (male, female)	0.607 (0.278-1.325)	0.21		
ECOG performance status score (0-1, 2)	2.780 (1.157-6.676)	0.022	3.288 (1.297-8.337)	0.012
Histology (differentiated, poorly differentiated)	1.985 (0.850-4.633)	0.113		
Lymphovascular invasion (No, Yes)	0.529 (0.200-1.397)	0.198		
Perineural invasion (No, Yes)	0.531 (0.234-1.206)	0.131		
Tumour stage (T1-T2 vs T3-T4)	1.445 (0.496-4.209)	0.500		
Nodal stage (N0-N1 vs N2-N3)	3.798 (1.454-9.925)	0.006	3.136 (1.180-8.330)	0.022
NLR (<1.9, ≥1.9)	2.129 (0.980-4.627)	0.056		
PLR (<169, ≥169)	1.962 (0.957-4.024)	0.066		
Relative total dose intensity (≤70% vs <70%)	3.383 (1.650-6.935)	0.001	2.936 (1.405-6.138)	0.004

Abbreviations: CI = confidence interval; ECOG = Eastern Cooperative Oncology Group; HR = hazard ratio; NLR = neutrophil-to-lymphocyte ratio; PLR = platelet-to-lymphocyte ratio.

poor tolerance to XELOX and that under such circumstances, only the drug costs of TS-1 would be covered by the institution. There has not been any randomised controlled trial comparing the efficacy of the two regimens. Retrospective studies[17-20] did not demonstrate statistically significant differences in DFS between adjuvant TS-1 and XELOX (Table 6). In the subgroup analysis, one study[17] demonstrated the use of XELOX in stage II disease was associated with better OS while another study[18] suggested the same but in stage IIIB/C disease only. Apart from XELOX, combination chemotherapy with more than three agents has shown superior treatment outcomes in recent years. Combination of TS-1 with oxaliplatin[21] or docetaxel[22] is considered a preferred option for high-risk patients and is increasingly recognised as a new standard of care.

In our cohort, elevated PLR is associated with inferior OS after curative surgery and there was a similar trend for NLR despite not reaching statistical significance (p = 0.051). NLR and PLR are important parameters indicating systemic inflammation. It is observed that a chronic inflammatory state confers unfavourable oncological outcomes.[23] Several meta-analyses revealed that elevated NLR and PLR were associated with tumour progression and poor survival in gastrointestinal cancers.[15,16] Microscopically, various inflammatory cytokines and growth factors in the tumour microenvironment are known to dampen hosts' anti-tumour immune response. In tumour models, inflammatory cytokines such as interleukin 6 (IL-6), IL-8 and IL-11 are associated with chemotherapy resistance in gastric cancer through mechanisms such as inhibition of apoptosis pathways, increasing efflux of chemotherapeutic agents, and evasion of DNA damage.[24-26] We therefore postulated that in an adjuvant setting, the persistent inflammatory state after curative surgery possibly led to tumour evasion from immunosurveillance and enhanced chemoresistance

Table 6. Summary of selected retrospective studies comparing XELOX and TS-1 regimens.

	Inclusion criteria	No. of eligible patients	Place of study	Outcomes
Oh et al[17]	• Stage II/III gastric cancer • R0 resection • D2 dissection	1461 (TS-1: n = 825; XELOX: n = 636)	Korea	OS/DFS: No statistically significant difference in DFS OS differs for stages IIA (p = 0.024) and IIB (p = 0.015) Prognostic factor(s): XELOX vs TS-1: HR = 0.47; 95% CI = 0.25-0.89; p = 0.021 in stage II only
Kim et al[18]	• Stage II/III gastric cancer • R0 resection • D2 dissection	1088 (TS-1: n = 846; XELOX: n = 242)	Korea	OS/DFS: No difference in DFS Inferior OS for TS-1 for stages IIIB (65.8% vs 68.6%; p = 0.019) and IIIC (48.4% vs 66.7%; p = 0.002) compared to XELOX
Cho et al[19]	• Stage III gastric cancer • R0 resection • D2 dissection	206 (TS-1: n = 92; XELOX: n = 114)	Korea	OS/DFS: No statistically significant difference in OS and DFS Prognostic factor(s): Nodal stage (HR = 5.639; 95% CI = 1.297-24.522; p = 0.021) and cycle completion (HR = 5.734; 95% CI = 3.007-10.936; p < 0.001) are independent predictors of OS
Lee et al[20]	• Stage II/III gastric cancer • R0 resection • D2 dissection	584 (TS-1: n = 429; XELOX: n = 155)*	Korea	OS/DFS: No statistically significant difference in DFS Prognostic factor(s): Tumour stage (T4 vs T1: HR = 11.667; 95% CI = 1.595-85.351; p = 0.016), nodal stage (N0 vs N3: HR = 2.788; 95% CI = 1.502-5.174; p = 0.001), and completion of chemotherapy (HR = 2.213; 95% CI = 1.618-3.028; p < 0.001) are independent prognostic factors of DFS

Abbreviations: CI = confidence interval; DFS = disease-free survival; HR = hazard ratio; OS = overall survival; TS-1 = tegafur/gimeracil/oteracil; XELOX = capecitabine plus oxaliplatin.
* Propensity score–matched.

of micrometastases.[27] NLR and PLR are two readily accessible clinical parameters and may serve as simple prognostic tools in addition to performance status, stage, and age.

Our study revealed that the RTDI is an independent prognostic factor for disease recurrence. Inadequate chemotherapy dose intensity is either attributed to excessive dose reduction or failure to complete scheduled cycles within the planned time interval. It is noteworthy that severe adverse events of chemotherapy (≥ Grade 3) have been shown to be quite uncommon (≤6%) with TS-1 in a large-scale clinical trial,[28] although these patients were generally frailer and older. For elderly patients who may be more vulnerable to chemotherapy toxicity, proper geriatric assessments (such as comorbidity and frailty indices) are needed, as biological age is not a reliable indicator for chemotherapy dose adjustment, and an adaptive dose optimisation approach is recommended based on patients' tolerance of each cycle.

This study has several limitations. First, it is only a single-centre retrospective study in which the small sample size limits its statistical power. Second, there is imbalance between the baseline characteristics of the two groups of patients. Similar to the Korean studies,[17-20] patients in the TS-1 group were generally older and had a worse ECOG performance status. There is a tendency for clinicians to prescribe a more conservative chemotherapy dosage in this group of patients, which may explain the lower dose intensity of TS-1 than XELOX. Propensity score matching should be performed in a larger cohort to reduce the bias due to these confounding variables. Third, a much large sample size is needed to further evaluate the prognostic power of NLR and PLR on OS and DFS in the adjuvant setting. In our cohort, high PLR appeared to correlate with patients with more advanced disease (stage III), which is an important confounding factor.

CONCLUSION

In conclusion, we compared the OS and DFS between adjuvant XELOX and TS-1 in our local gastric cancer patients. Clinical outcomes were statistically better with XELOX- than TS-1–treated patients. However, the results should be viewed with caution because of the limited sample size and obvious imbalance in baseline characteristics. ECOG performance status score of 2

and advanced nodal stage of N2 to N3 are independent adverse prognostic factors associated with poor OS and a higher rate of disease recurrence. NLR and PLR are readily available markers that may be further explored as prognostic markers for gastric cancer after radical surgery. We also speculated that the RTDI of chemotherapy of <70% might affect the risk of disease relapse.

REFERENCES

1. Centre for Health Protection, Department of Health, Hong Kong SAR Government. Stomach cancer. Available from: https://www.chp.gov.hk/en/healthtopics/content/25/55.html. Accessed 2 May 2022.
2. Rawla P, Barsouk A. Epidemiology of gastric cancer: global trends, risk factors and prevention. Prz Gastroenterol. 2019;14:26-38.
3. Randle RW, Swords DS, Levine EA, Fino NF, Squires MH, Poultsides G, et al. Optimal extent of lymphadenectomy for gastric adenocarcinoma: a 7-institution study of the US gastric cancer collaborative. J Surg Oncol. 2016;113:750-5.
4. Smyth EC, Verheij M, Allum W, Cunningham D, Cervantes A, Arnold D, et al. Gastric cancer: ESMO Clinical Practice Guidelines for diagnosis, treatment and follow-up. Ann Oncol. 2016;27(suppl 5):v38-49.
5. Hakkenbrak, NA, Jansma EP, van der Wielen N, van der Peet DL, Straatman J. Laparoscopic versus open distal gastrectomy for gastric cancer: a systematic review and meta-analysis. Surgery. 2022;171:1552-61.
6. Macdonald JS, Smalley SR, Benedetti J, Hundahl SA, Estes NC, Stemmermann GN, et al. Chemoradiotherapy after surgery compared with surgery alone for adenocarcinoma of the stomach or gastroesophageal junction. N Engl J Med. 2001;345:725-30.
7. Cunningham D, Allum WH, Stenning SP, Weeden S. Perioperative chemotherapy in operable gastric and lower oesophageal cancer: final results of a randomised, controlled trial (the MAGIC trial, ISRCTN 93793971). J Clin Oncol. 2005;23(16 suppl):4001.
8. Al-Batran SE, Homann N, Schmalenberg H, Kopp HG, Haag GM, Luley KB, et al. Perioperative chemotherapy with docetaxel, oxaliplatin, and fluorouracil/leucovorin (FLOT) versus epirubicin, cisplatin, and fluorouracil or capecitabine (ECF/ECX) for resectable gastric or gastroesophageal junction (GEJ) adenocarcinoma (FLOT4-AIO): a multicenter, randomized phase 3 trial. J Clin Oncol. 2017;35(15 suppl):4004.
9. Bang YJ, Kim YW, Yang HK, Chung HC, Park YK, Lee KH, et al. Adjuvant capecitabine and oxaliplatin for gastric cancer after D2 gastrectomy (CLASSIC): a phase 3 open-label, randomised controlled trial. Lancet. 2012;379:315-21.
10. Sasako M, Sakuramoto S, Katai H, Kinoshita T, Furukawa H, Yamaguchi T, et al. Five-year outcomes of a randomized phase III trial comparing adjuvant chemotherapy with S-1 versus surgery alone in stage II or III gastric cancer. J Clin Oncol. 2011;29:4387-93.
11. Liang YX, Deng JY, Guo HH, Ding XW, Wang XN, Wang BG, et al. Characteristics and prognosis of gastric cancer in patients aged ≥70 years. World J Gastroenterol. 2013;19:6568-78.
12. Stiekema J, Cats A, Kuijpers A, van Coevorden F, Boot H, Jansen EP, et al. Surgical treatment results of intestinal and diffuse type gastric cancer. Implications for a differentiated therapeutic approach? Eur J Surg Oncol. 2013;39:686-93.
13. Feng F, Liu J, Wang F, Zheng G, Wang Q, Liu S, et al. Prognostic value of differentiation status in gastric cancer. BMC Cancer. 2018;18:865.
14. Asplund J, Gottlieb-Vedi E, Leijonmarck W, Mattsson F, Lagergren J. Prognosis after surgery for gastric adenocarcinoma in the Swedish Gastric Cancer Surgery Study (SWEGASS). Acta Oncol. 2021;60:513-20.
15. Yodying H, Matsuda A, Miyashita M, Matsumoto S, Sakurazawa N, Yamada M, et al. Prognostic significance of neutrophil-to-lymphocyte ratio and platelet-to-lymphocyte ratio in oncologic outcomes of esophageal cancer: a systematic review and meta-analysis. Ann Surg Oncol. 2016;23:646-54.
16. Zhang J, Zhang HY, Li J, Shao XY, Zhang CX. The elevated NLR, PLR and PLT may predict the prognosis of patients with colorectal cancer: a systematic review and meta-analysis. Oncotarget. 2017;8:68837-46.
17. Oh SE, An JY, Choi MG, Lee JH, Sohn TS, Bae JM. Comparison of long-term efficacy in S-1 and capecitabine with oxaliplatin as adjuvant chemotherapy for patients with gastric cancer after curative surgery: a retrospective, single-center observational study. Technol Cancer Res Treat. 2021;20:15330338211039679.
18. Kim IH, Park SS, Lee CM, Kim MC, Kwon IK, Min JS, et al. Efficacy of adjuvant S-1 versus XELOX chemotherapy for patients with gastric cancer after D2 lymph node dissection: a retrospective, multi-center observational study. Ann Surg Oncol. 2018;25:1176-83.
19. Cho JH, Lim JY, Cho JY. Comparison of capecitabine and oxaliplatin with S-1 as adjuvant chemotherapy in stage III gastric cancer after D2 gastrectomy. PLoS One. 2017;12:e0186362.
20. Lee CM, Yoo MW, Son YG, Oh SJ, Kim JH, Kim HI, et al. Long-term efficacy of S-1 monotherapy or capecitabine plus oxaliplatin as adjuvant chemotherapy for patients with stage II or III gastric cancer after curative gastrectomy: a propensity score-matched multicenter cohort study. J Gastric Cancer. 2020;20:152-64.
21. Park SH, Lim DH, Sohn TS, Lee J, Zang DY, Kim ST, et al. A randomized phase III trial comparing adjuvant single-agent S1, S-1 with oxaliplatin, and postoperative chemoradiation with S-1 and oxaliplatin in patients with node-positive gastric cancer after D2 resection: the ARTIST 2 trial. Ann Oncol. 2021;32:368-74.
22. Kodera Y, Yoshida K, Kochi M, Ichikawa W, Kakeji Y, Sano T, et al. A randomized phase III study comparing S-1 plus docetaxel with S-1 alone as a postoperative adjuvant chemotherapy for curatively resected stage III gastric cancer (JACCRO GC-07 trial). J Clin Oncol. 2018;36(15 suppl):4007.
23. Baniyash M, Sade-Feldman M, Kanterman J. Chronic inflammation and cancer: suppressing the suppressors. Cancer Immunol Immunother. 2014;63:11-20.
24. Ham IH, Oh HJ, Jin H, Bae A, Jeon SM, Choi KS, et al. Targeting interleukin-6 as a strategy to overcome stroma-induced resistance to chemotherapy in gastric cancer. Mol Cancer. 2019;18:68.
25. Kuai WX, Wang Q, Yang XZ, Zhao Y, Yu R, Tang XJ. Interleukin-8 associates with adhesion, migration, invasion and chemosensitivity of human gastric cancer cells. World J Gastroenterol. 2012;18:979-85.
26. Ma J, Song X, Xu X, Mou Y. Cancer-associated fibroblasts promote the chemo-resistance in gastric cancer through secreting IL-11 targeting JAK/STAT3/Bcl2 pathway. Cancer Res Treat. 2019;51:194-210.
27. Olive KP. Fanning the flames of cancer chemoresistance: inflammation and anticancer therapy. J Oncol Pract. 2017;13:181-3.
28. Sakuramoto S, Sasako M, Yamaguchi T, Kinoshita T, Fujii M, Nashimoto A, et al. Adjuvant chemotherapy for gastric cancer with S-1, an oral fluoropyrimidine. N Engl J Med. 2007;357:1810-20.

Hong Kong J Radiol. 2023;26:100-10. Epub 7 Jun 2023 | https://doi.org/10.12809/hkjr2317452

ORIGINAL ARTICLE **CME**

Accuracy and Interobserver Agreement of the Correlation Between Prostate Imaging Reporting and Data System Version 2.1 and International Society of Urological Pathology Scores

Gulsen Yucel Oguzdogan[1], Zehra Hilal Adibelli[1], Ertugrul Sefik[2], Hulya Mollamehmetoglu[1], Ibrahim Halil Bozkurt[2], Enver Vardar[3], Bulent Gunlusoy[2], Hulya Cetin Tuncez[1]

[1]Department of Radiology, University of Health Sciences, Izmir Faculty of Medicine, Izmir Bozyaka Training and Research Hospital, Izmir, Turkey
[2]Department of Urology, University of Health Sciences, Izmir Faculty of Medicine, Izmir Bozyaka Training and Research Hospital, Izmir, Turkey
[3]Department of Pathology, University of Health Sciences, Izmir Faculty of Medicine, Izmir Bozyaka Training and Research Hospital, Izmir, Turkey

ABSTRACT

Introduction: *This research aims to evaluate accuracy and interobserver agreement on the correlation between the Prostate Imaging Reporting and Data System version 2.1 (PI-RADS v2.1) and the International Society of Urological Pathology (ISUP) scores.*

Methods: *We examined patients who underwent prostate multiparametric magnetic resonance imaging (MpMRI) prior to transrectal ultrasound–guided cognitive fusion biopsy between April and December 2019. MpMRI examinations were evaluated by two radiologists according to PI-RADS v2.1. Interobserver agreement was recorded and the final PI-RADS category was decided by consensus. The correlation of cognitive fusion biopsy results with PI-RADS v2.1 score was evaluated. Lesions with Gleason score ≥7 were considered to be clinically significant prostate cancer.*

Results: *A total of 84 patients with 106 lesions were included in the study. The rates of prostate cancer in the PI-RADS groups 1, 2, 3, 4, and 5 were 0%, 0%, 22.2%, 56%, and 94.45%, respectively. There was a positive correlation with an area under the curve value of 0.814 between the PI-RADS v2.1 and the ISUP score. Using PI-RADS ≥3 as the cut-off value in the peripheral zone (PZ) and the whole gland, the negative predictive value for malignancy was 100%. For PI-RADS ≥4, it was 76.47% for PZ and 80.65% for the whole gland. Without applying cut-off values, the interobserver agreement for PI-RADS score was* $\varkappa = 0.562$.

Conclusion: *Our data support the notion that PI-RADS v2.1 facilitates the evaluation of MpMRI and improves interobserver agreement.*

Key Words: *Biopsy; Histology; Magnetic resonance imaging; Neoplasm grading; Prostatic neoplasms*

Correspondence: *Dr Gulsen Yucel Oguzdogan, Department of Radiology, University of Health Sciences, Izmir Faculty of Medicine, Izmir Bozyaka Training and Research Hospital, Izmir, Turkey*
Email: gulsenyuceloguzdogan@gmail.com

Submitted: 8 Aug 2021; Accepted: 15 Nov 2021.

Contributors: GYO, ZHA and ES designed the study. GYO and HM acquired the data. GYO, HM and HCT analysed the data. GYO drafted the manuscript. GYO and ZHA critically revised the manuscript for important intellectual content. All authors had full access to the data, contributed to the study, approved the final version for publication, and take responsibility for its accuracy and integrity.

Conflicts of Interest: All authors have disclosed no conflicts of interest.

Funding/Support: This research received no specific grant from any funding agency in the public, commercial, or not-for-profit sectors.

Ethics Approval: Ethical approval for the research was obtained from the ethics review committee of University of Health Sciences, Izmir Faculty of Medicine, Izmir Bozyaka Training and Research Hospital, Turkey (Ref No.: 01). Oral and written consent for treatment/procedures and publication were obtained from all patients.

中文摘要

前列腺影像報告和數據系統第2.1版與國際泌尿病理學會評分之間相關性的準確性和觀察者間的一致性

Gulsen Yucel Oguzdogan、Zehra Hilal Adibelli、Ertugrul Sefik、Hulya Mollamehmetoglu、Ibrahim Halil Bozkurt、Enver Vardar、Bulent Gunlusoy、Hulya Cetin Tuncez

簡介：本研究旨在評估前列腺影像報告和數據系統第2.1版（PI-RADS v2.1）與國際泌尿病理學會（ISUP）評分之間相關性的準確性和觀察者間的一致性。

方法：我們檢視2019年4月至12月期間經直腸超聲引導融合活檢之前接受前列腺多參數磁共振成像（MpMRI）的患者。MpMRI檢查由兩名放射科醫生根據PI-RADS v2.1進行評估。研究記錄了觀察者間的一致性，最終的PI-RADS類別由協商決定，並評估融合活檢結果與PI-RADS v2.1評分的相關性。Gleason評分≥7的病變認為是有臨床意義的前列腺癌。

結果：本研究共納入84例患者106個病灶。PI-RADS 1、2、3、4及5組前列腺癌發生率分別為0%、0%、22.2%、56%及94.45%。PI-RADS v2.1與ISUP評分呈正相關，曲線下面積為0.814。以周邊區和整個腺體的PI-RADS≥3為界值，惡性腫瘤的陰性預測值為100%。PI-RADS≥4時，周邊區陰性預測值為76.47%，全腺體陰性預測值則為80.65%。在不應用閾值的情況下，PI-RADS評分的觀察者間一致性為 $\kappa = 0.562$。

結論：我們的研究數據證明PI-RADS v2.1有助促進MpMRI的評估並增加觀察者間的一致性。

INTRODUCTION

Prostate cancer (PCa) is the most commonly observed cancer in men in the world and the second most common cause of cancer-related deaths.[1] A study of 1,056 men who died from causes other than PCa found that 68% to 77% of men aged 60 to 79 years had occult PCa identified at autopsy, indicating a high prevalence of the disease.[2,3] Advanced-stage PCa poses a high risk of morbidity and mortality. Recent studies have focused on distinguishing between lesions expressed as 'silent disease' with almost no malignant potential, such as tumours with a Gleason score (GS) of 6 and high-grade cancers.[4] Due to limited sensitivity and specificity of serum prostate-specific antigen (PSA) screening, digital prostate examination, and transrectal ultrasound (TRUS)–guided biopsy, advanced imaging methods are needed to perform target-specific biopsies and to reduce the negative biopsy rate.[5] Advanced methodology is needed to direct patients to treatment or active surveillance. To ensure standardisation and reduce differences emerging in the selection of parameters and interpretation of images in prostate magnetic resonance imaging (MRI), the European Society of Urogenital Radiology issued relevant guidelines in 2012.[5,6] Rapid developments in this field and limitations encountered during the use of the Prostate Imaging Reporting and Data System version 1 (PI-RADS v1) led to an update of the PI-RADS, and PI-RADS v2 was subsequently published in 2015.[7] In 2019, PI-RADS v2.1, including changes ensuring more accurate and reproducible interpretations, was published.[8,9]

This study aimed to investigate the correlation of the PI-RADS v2.1 score with the histopathological result and the International Society of Urological Pathology (ISUP) score in patients with suspected PCa undergoing multiparametric MRI (MpMRI) examinations scored with PI-RADS v2.1 and diagnosed with TRUS-guided cognitive fusion biopsy and to assess the compatibility between different experience levels of the radiologists.

METHODS

In this single-centre study, 166 consecutive patients who underwent MpMRI for PCa between April and

December 2019 were evaluated. Ethical approval was obtained from our institution, and oral and written consents were obtained from all patients. Twelve patients with unsuitable image quality for evaluation, 26 patients with a previous biopsy and with PCa treatment before testing, and 44 patients with no tissue diagnosis due to PI-RADS 1 or who declined biopsy were excluded from the study. A total of 106 lesions in 84 patients diagnosed with TRUS-guided cognitive fusion biopsy in our hospital were included in the final study group. Patients' age, serum PSA value, PSA density (PSAd), and prostate volume were recorded. The prostate MpMRI was performed with a 1.5T scanner (Siemens MAGNETOM Aera; Siemens Inc, Erlangen, Germany) with an 18-channel pelvic coil according to the protocols shown in Table 1. All sequences were assessed on a syngo.via workstation (Siemens, Erlangen, Germany).

Assessment of Images and Histopathological Correlation

MpMRI images were evaluated before biopsy according to the PI-RADS v2.1 guidelines by two radiologists with 25 years of experience (reader 1) and 2 years of experience (reader 2) in abdominal MRI. The appearance, location, and dimensions of lesions were first independently assessed by the two radiologists. Lesion location was defined according to the sector map in the PI-RADS v2.1 guidelines. Lesions including both the peripheral zone (PZ) and transitional zone (TZ) or lesions with extraprostatic extension were defined as diffuse cancer. Lesions were scored according to PI-RADS v2.1 criteria on T2-weighted imaging (T2WI) and diffusion-weighted imaging (DWI). Dynamic contrast-enhanced (DCE) imaging–MRI was defined as 'negative' or 'positive' and each lesion was given a PI-RADS v2.1 (category 1-5) score for later evaluation of interobserver agreement. Differences in PI-RADS scores between the readers were settled by consensus in 28 lesions (Table 2). Interobserver agreement on these variables and histopathological correlation with PI-RADS v2.1 score were evaluated. Negative MpMRI findings were scored as PI-RADS 1.

The biopsy decision was based on MpMRI findings and clinical suspicion of PCa. MpMRI TRUS-guided cognitive fusion biopsy was performed with an 18-gauge automatic biopsy needle (Tru-Cut; Merit Medical, South Jordan [UT], United States). MpMRI TRUS-guided cognitive fusion biopsy is done by determining suspicious areas through MpMRI, approximately defining this area with TRUS and then carrying out the biopsy procedure. The hypoechogenic-hyperechogenic foci of ultrasound images during MpMRI TRUS-guided cognitive fusion biopsy were considered, where two

Table 1. Multiparametric magnetic resonance imaging (MpMRI) protocols (1.5T Siemens MAGNETOM Aera).

	Sequence	Slice thickness, mm	No. of slices	Voxel size, mm^3	Field of view, mm	TE, ms	TR, ms	Gap, mm	b Value, s/mm^{2*}	Flip angle
T2W coronal	HASTE	5	30	1.4 × 1.4 × 5	360 × 360	92	1400	1		180°
T2W axial	HASTE	6	30	1.5 × 1.5 × 6	380 × 380	91	1400	1.2		180°
T2W sagittal	HASTE	5	30	1.2 × 1.2 × 5	300 × 300	92	1400	0		180°
T2W coronal	TSE	3	20	0.7 × 0.7 × 3	224 × 224	96	5490	0		160°
T2W axial	TSE	3	24	0.6 × 0.6 × 3	200 × 200	101	6620	0		160°
DWI		3	20	0.8 × 0.8 × 3	200 × 200	80	5000	0	50, 800, 1200, 1800, 2000†	-
T1W axial (for evaluating lymph nodes)	TSE	4	26	0.9 × 0.9 × 4	300 × 300	20	552	0.8		167°
T1 map axial	VIBE	3, 5	20	1.4 × 1.4 × 3.5	260 × 260	1, 9	4, 11	0		2°, 15°
T1W DCE-MRI‡	VIBE	3, 5	20	1.4 × 1.4 × 3.5	260 × 260	1, 58	4, 46	0		12°
Post-contrast T1W axial	TSE	4	34	0.6 × 0.6 × 4	360 × 360	11	606	0.8		180°

Abbreviations: DCE = dynamic contrast-enhanced; DWI = diffusion-weighted imaging; HASTE = half-Fourier acquisition single-shot turbo spin echo; T1W = T1-weighted; T2W = T2-weighted; TE = time of echo; TR = time of repetition; TSE = turbo spin echo; VIBE = volumetric interpolated breath-hold examination.

* There is no widely accepted optimal 'high b value' beyond the requirement for a DWI set with a b value ≥1400 s/mm^2.[9]

† Calculated b value.

‡ In DCE imaging, a gadolinium-based contrast agent with an automatic injector at 0.1-0.2 mmol/kg concentration and 2-4 mL/s injection rate via intravenous were used and T1 axial sections were obtained over 240-300 s once every 7 s before, during, and after administration covering the entire prostate.

Table 2. Distribution of Prostate Imaging Reporting and Data System (PI-RADS) scores assigned to lesions by two readers before consensus.

Variable	PI-RADS score of the 1st reader					Total
PI-RADS score of the 2nd reader	1	2	3	4	5	
1	**5**	0	0	0	0	5
2	0	**2**	14	1	0	17
3	0	2	**37**	5	1	45
4	0	0	2	**17**	2	21
5	0	0	1	2	**15**	18
Final PI-RADS score	5	4	54	25	18	106

samples were taken from each lesion by correlating them with the foci defined in MpMRI and marked on the sector map.[7] In addition to cognitive fusion biopsy, 12-core systematic biopsy was performed for the safety of the patients. To improve the accuracy of biopsy localisation, one of three experienced urologists (with 15, 18 and 22 years of experience) performed the TRUS-biopsy procedure with assistance from both radiologists to pinpoint the lesion location. Biopsy specimens were evaluated by a urogenital pathologist. Lesions with GS ≥7 was considered as clinically significant PCa (csPCa). Lesions were grouped according to the ISUP scoring method (ISUP 1, GS 3+3; ISUP 2, GS 3+4; ISUP 3, GS 4+3; ISUP 4, GS 4+4; ISUP 5, GS ≥ 9).[10] On MpMRI, lesions with a PI-RADS v2.1 score ≥3 were recorded as positive, while lesions scoring <3 were recorded as negative.

Statistical Methods

In descriptive analyses, continuous variables are presented as mean ± standard deviation or median (interquartile range) and categorical variables as a percentage (%). The compliance of the data to normal distribution was evaluated using the Shapiro–Wilk test. If the data had a normal distribution, a *t* test was used to compare two groups; under non-parametric conditions, the Mann–Whitney *U* test was used. Comparison of continuous variables between three and more categories was made using the one-way analysis of variance or the non-parametric equivalent of the Kruskal–Wallis test. The strength of the correlation between two continuous variables was assessed using the Spearman's rank correlation coefficient. Accordingly, correlation coefficient (r) values <0.2 show very weak or no correlation, values from 0.2 to 0.4 show weak correlation, values from 0.4 to 0.6 show moderate correlation, values from 0.6 to 0.8 show a high correlation, and values >0.8 are interpreted as very high correlation. Interobserver agreement was evaluated using kappa coefficients ($\varkappa$) and was assessed as follows: 0.01-0.20, slight agreement; 0.21-0.40, fair agreement; 0.41-0.60, moderate agreement; 0.61-0.80, substantial agreement; and 0.81-0.99, almost perfect agreement. To evaluate the success of the obtained variables, to diagnose PCa, and to determine cut-off points, the area under the curve (AUC) of a receiver operating characteristic, sensitivity, specificity, positive predictive value (PPV), and negative predictive value (NPV) were computed. SPSS (Windows version 22.0; IBM Corp, Armonk [NY], United States) and MedCalc (MedCalc Software Ltd, Mariakerke, Belgium) were used for statistical analyses. A p value of < 0.05 was accepted as statistically significant.

RESULTS

The mean age, PSA level, prostate volume, and mean PSAd values for the 84 cases included in the study were 63.5 ± 7.5 years, 11.68 ± 17.34 ng/mL, 62.4 ± 38.08 cm^3, and 0.23 ± 0.39 ng/mL^2, respectively. There were no statistically significant differences between malignant and benign diseases for age and PSA values. Prostate volume in the malignant group was found to be significantly lower while PSAd was higher than that in the benign group (both $p < 0.001$) [Table 3].

Of the 106 lesions examined in this study from the 84 patients, 26 (24.5%) were benign prostatic tissue, 36 (34.0%) were prostatitis, 43 (40.6%) were malignant lesions, and one (0.9%) was high-grade prostatic intraepithelial neoplasia. Among malignant lesions, 65.1% were localised in the PZ, 14% in the TZ, and 20.9% were diffuse cancers.

These 106 lesions were identified as PI-RADS category 1 (n = 5), 2 (n = 4), 3 (n = 54), 4 (n = 25), and 5 (n = 18). No malignancy was detected in PI-RADS 1 or 2 lesions. Systematic biopsy was performed on these patients with the decision of the clinician due to the increase in PSA level, rectal examination findings, and the age of the

Table 3. Descriptive statistics of patients included in the current study.

	Histopathological diagnosis				
	Malignant (n = 43)		Benign (n = 63)		p Value
	Mean ± standard deviation	Median (interquartile range)	Mean ± standard deviation	Median (interquartile range)	
Age, y	65.24 ± 7.90	65.0 (59.75-70.0)	62.07 ± 6.90	62.50 (57.0-66.0)	0.053
PSA level, ng/mL	15.24 ± 24.12	7.56 (5.28-11.19)	8.75 ± 7.52	6.94 (4.00-9.71)	0.259
Prostate volume, cm^3	46.11 ± 29.21	39.37 (30.74-50.53)	75.94 ± 39.51	72.50 (44.87-100.75)	<0.001
Lesion volume, cm^3	0.71 ± 0.94	NA	0.34 ± 0.34	NA	0.031
PSAd value, ng/mL^2	0.37 ± 0.55	0.20 (0.11-0.33)	0.13 ± 0.121	0.11 (0.07-0.147)	<0.001

Abbreviations: NA = not applicable; PSA = prostate-specific antigen; PSAd = prostate-specific antigen density.

Table 4. Statistical parameters for cancer detection in peripheral zone (PZ) and transitional zone (TZ).

Zone	Sequence	Cut-off value	Sensitivity	Specificity	PPV	NPV	Accuracy
PZ							
	T2WI	PI-RADS ≥3 +ve	100%	27.78%	51.85%	100%	59.38%
		PI-RADS ≥4 +ve	32.14%	97.22%	90%	64.81%	68.75%
	DWI	PI-RADS ≥3 +ve	92.86%	13.89%	45.61%	71.43%	48.44%
		PI-RADS ≥4 +ve	46.43%	91.67%	81.25%	68.75%	71.88%
	MpMRI (T2WI, DWI and DCEI)	PI-RADS ≥3 +ve	100%	11.11%	46.67%	100%	52.98%
		PI-RADS ≥4 +ve	71.43%	72.22%	66.67%	76.47%	71.87%
TZ							
	T2WI	PI-RADS ≥4 +ve	33.33%	90.91%	50%	83.33%	78.57%
	DWI	PI-RADS ≥4 +ve	33.33%	59.09%	18.18%	76.47%	53.57%
	MpMRI (T2WI, DWI and DCEI)	PI-RADS ≥4 +ve	33.33%	90.91%	50%	83.33%	78.57%

Abbreviations: +ve = positive; DCEI = dynamic contrast-enhanced imaging; DWI = diffusion-weighted imaging; MpMRI = multiparametric magnetic resonance imaging; NPV = negative predictive value; PI-RADS = Prostate Imaging Reporting and Data System; PPV = positive predictive value; T2WI = T2-weighted imaging.

patient. Of the PI-RADS 3, 4, and 5 lesions, the PCa incidence was 22.2%, 56%, and 94.45%, respectively.

Table 4 shows the statistical parameters in PZ and TZ when the cut-off value was PI-RADS ≥3 positive and PI-RADS ≥4 positive for cancer detection on T2WI, DWI, and T2WI, DWI and DCE imaging combination (MpMRI). In TZ, there was no patient with PI-RADS <3, hence the diagnostic parameters for this variable were not calculated.

Expressed as median (interquartile range), the success of the PI-RADS score to predict cancer was found to have an AUC value of 0.764 (0.646-0.882) for PZ and 0.629 (0.347-0.910) for TZ. Evaluation by excluding the zonal anatomy found successful cancer predictions had AUC values of 0.773 (0.683-0.864), 0.722 (0.621-0.824), 0.740 (0.641-0.838), 0.619 (0.514-0.724), and 0.764 (0.646-0.882) for T2WI, DWI, DCE imaging, combination of T2WI and DWI (biparametric), and combination of T2WI, DWI and DCE imaging (MpMRI), respectively.

The sensitivity, specificity, NPV, and PPV values for PCa detection according to PI-RADS v2.1 and regardless of the zone, for T2WI and DWI independently, for biparametric and MpMRI assessment when PI-RADS ≥3 and ≥4 positive, are summarised in Table 5. The results for the cut-off values ≥3 and ≥4 are shown in Tables 4 and 5. The differences observed between sensitivity, specificity, PPV, and NPV values with each cut-off value were separately evaluated. Accordingly, when the PI-RADS score cut-off value ≥4 was taken as positive, the sensitivity and NPV decreased moderately, while specificity and PPV increased.

A total of 43 lesions (40.56%) were categorised into PI-RADS 4 and 5. Among these, 27 lesions (25.47%) had ISUP score >1. When PI-RADS 3 lesions were evaluated, 22.2% of these lesions were diagnosed as PCa, whereas no lesions had ISUP score >1. There was

Table 5. Statistical parameters for prostate cancer detection in the whole gland.*

	Cut-off value	Sensitivity	Specificity	PPV	NPV	Accuracy
T2WI	PI-RADS ≥3 +ve	100%	22.58%	47.25%	100%	53.77%
	PI-RADS ≥4 +ve	46.51%	93.75%	45.26%	94.04%	71.43%
DWI	PI-RADS ≥3 +ve	95.35%	14.52%	43.62%	81.82%	47.62%
	PI-RADS ≥4 +ve	54.55%	80.65%	23.84%	94.10%	69.81%
DCEI	PI-RADS ≥3 +ve	79.07%	68.85%	64.15%	82.35%	80.21%
T2WI-DWI (biparametric)	PI-RADS ≥3 +ve	100%	23.81%	47.25%	100%	54.85%
MpMRI (T2WI, DWI and DCEI)	PI-RADS ≥3 +ve	100%	12.90%	44.33%	100%	49.06%
	PI-RADS ≥4 +ve	72.09%	80.65%	72.09%	80.65%	77.36%

Abbreviations: +ve = positive; DCEI = dynamic contrast-enhanced imaging; DWI = diffusion-weighted imaging; MpMRI= multiparametric magnetic resonance imaging; NPV = negative predictive value; PI-RADS = Prostate Imaging Reporting and Data System; PPV = positive predictive value; T2WI = T2-weighted imaging.

* Sensitivity, specificity, NPVs, and PPVs for prostate cancer detection are shown for T2WI and DWI independently and MpMRI (T2WI, DWI and DCEI), when PI-RADS ≥3 and ≥4 scores are taken as positive according to PI-RADS version 2.1.

Table 6. Assessment of lesions' International Society of Urological Pathology (ISUP) scores according to their Prostate Imaging Reporting and Data System (PI-RADS) version 2.1 score ($p < 0.001$).

	Benign (n=63)	ISUP score 1 (n = 16)	ISUP score 2 (n = 6)	ISUP score 3 (n = 6)	ISUP score 4 (n = 6)	ISUP score 5 (n = 9)
PI-RADS 1	5	0	0	0	0	0
PI-RADS 2	4	0	0	0	0	0
PI-RADS 3	42	12	0	0	0	0
PI-RADS 4	11	4	4	3	2	1
PI-RADS 5	1	0	2	3	4	8
Total	63	16	6	6	6	9

Table 7. Correlation between International Society of Urological Pathology (ISUP) scores and diffusion-weighted imaging (DWI) scores of Prostate Imaging Reporting and Data System (PI-RADS) 4 lesions in the peripheral zone.

PI-RADS 4		ISUP score					
DWI score	DCE imaging status	1	2	3	4	5	Total
3	Upgraded to Group 4 with DCE positivity	4 (57.1%)	2 (28.6%)	0	0	1 (14.3%)	7
4	NA	0	2 (33.3%)	2 (33.3%)	2 (33.3%)	0	6
Total		4	4	2	2	1	13

Abbreviations: DCE = dynamic contrast-enhanced; NA = not applicable.

a positive correlation between PI-RADS v2.1 score with ISUP score and the correlation value was 0.814 ($p < 0.001$) [Table 6].

In PZ, for ISUP grades 1, 2, 3, 4, and 5, there were four (57.1%), two (28.6%), 0, 0, and one (14.3%) lesions upgraded to PI-RADS 4 with DWI score 3 and DCE positivity identified, respectively (Table 7). For lesions with DWI score 4 and PI-RADS 4, 0, two (33.3%), two (33.3%), two (33.3%), and 0 lesions were in ISUP grades 1, 2, 3, 4, and 5, respectively. We divided the PI-RADS 4 lesions into two groups according to the DWI score (DWI 3 and DWI 4). When we compared the lesions in these groups according to ISUP grades (ISUP 1 and >1 in Figures 1 and 2, respectively), we found that the DWI 4 group had higher ISUP grades ($p = 0.03$).

The interobserver agreement kappa value (κ) for the PI-RADS score without applying the cut-off value was 0.562, which represents moderate agreement. When stratified PI-RADS as <3 and ≥3, the κ for agreement between the two observers was 0.320, indicating a fair level of agreement. When stratified PI-RADS as <4 and ≥4, the κ was 0.770, which corresponds to a substantial agreement. When stratified PI-RADS as <3 and ≥3, the interobserver agreement for T2WI was moderate with

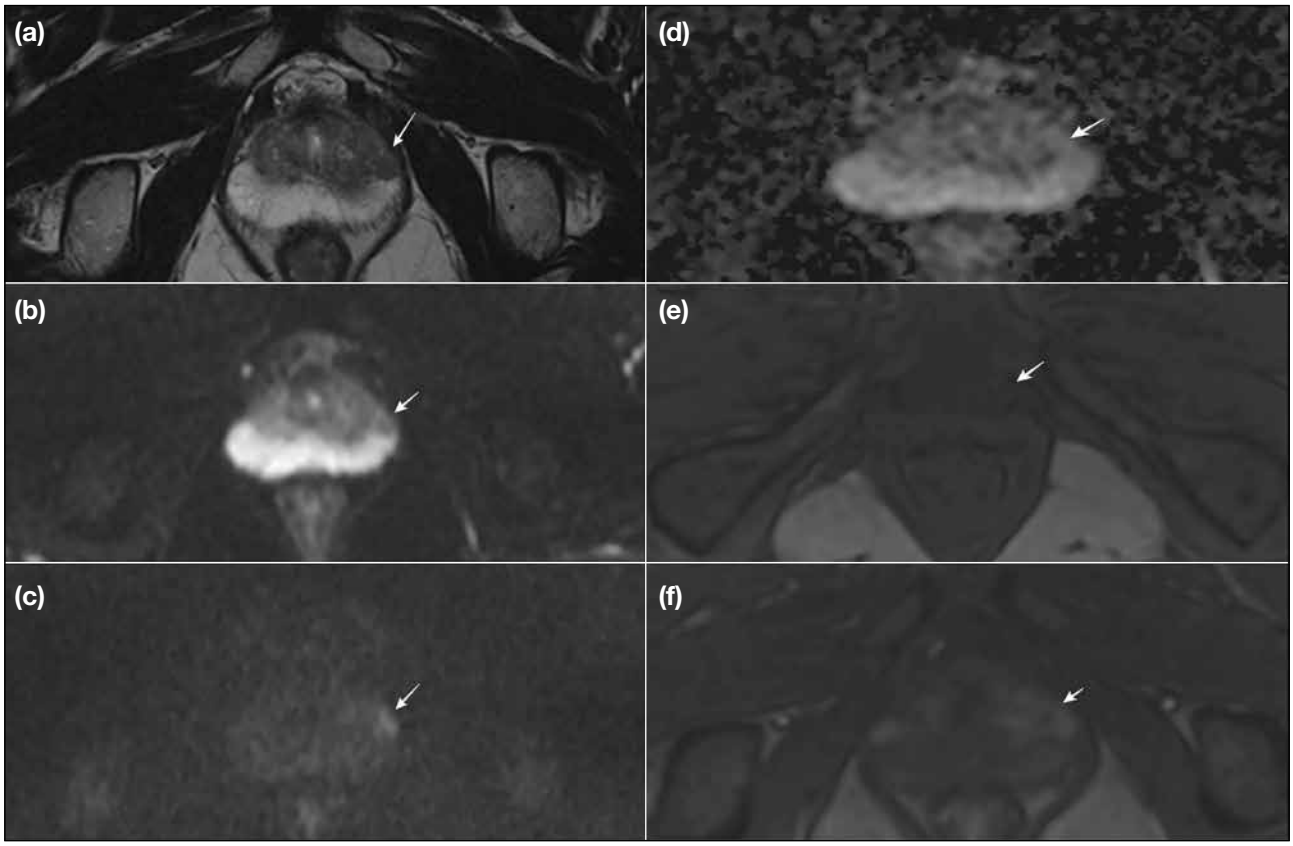

Figure 1. A 56-year-old man with prostate-specific antigen level of 5.6 ng/mL. Arrows indicated a Prostate Imaging Reporting and Data and System (PI-RADS) version 2.1 category 4 lesion visible in the peripheral zone. (a) Axial T2-weighted magnetic resonance (MR) image showing the lesion in the left-mid peripheral zone. The dimension of the lesion is 1.0 cm, which is consistent with a PI-RADS score of 3 on T2-weighted imaging. (b and c) show that the lesion is hypointense on diffusion-weighted imaging (DWI) [b = 50 s/mm^2] and hyperintense on DWI (b = 1800 s/mm^2). (d) Apparent diffusion coefficient map indicates that the lesion is mildly hypointense, giving it a PI-RADS score of 3 on DWI. (e) Pre-contrast T1-weighted and (f) dynamic contrast-enhanced MR images show early enhancement within the same location as the lesion in (a-d) with early enhancement for overall PI-RADS version 2.1 score of 4. Transrectal ultrasound–guided cognitive imaging fusion biopsy was defined as International Society of Urological Pathology score of 1.

$\varkappa$ = 0.575 and reached the substantial agreement with $\varkappa$ = 0.814 when PI-RADS was stratified as <4 and ≥4. Interobserver agreement for DWI was fair with $\varkappa$ = 0.321 when PI-RADS was stratified as <3 and ≥3 but reached the substantial level when PI-RADS was stratified as <4 and ≥4 ($\varkappa$ = 0.757). For DCE investigation with positive and negative scores evaluation, interobserver agreement was at substantial levels with $\varkappa$ = 0.721.

DISCUSSION

Our study revealed that serum PSA level did not correlate significantly with malignant or benign disease, and PSAd was significantly elevated in the malignant group. Jue et al[11] reported a sensitivity of 90% to 95% for PSAd and, considering the 0.15 ng/mL/cm^3 threshold value, they suggested that a high NPV may prevent unnecessary biopsy in patients with proportional PSA increase compared to prostate volume. There was a negative correlation found between prostate volume and malignancy diagnosis. This result is similar to the results of studies by Al-Khalil et al[12] and Tang et al,[13] suggesting that the aetiologies for increasing prostate volume may be interpreted as due to benign causes such as hyperplasia and prostatitis. The study of Haas et al[14] presented that patients with PCa were of advanced age. Droz et al[15] showed high mean age in the cancer group. In our study, the mean age in the cancer group was consistent with the literature and was higher compared to benign diseases of the prostate gland; however, the difference was not statistically significant (p = 0.053).

PI-RADS v2 is a scoring system widely used for

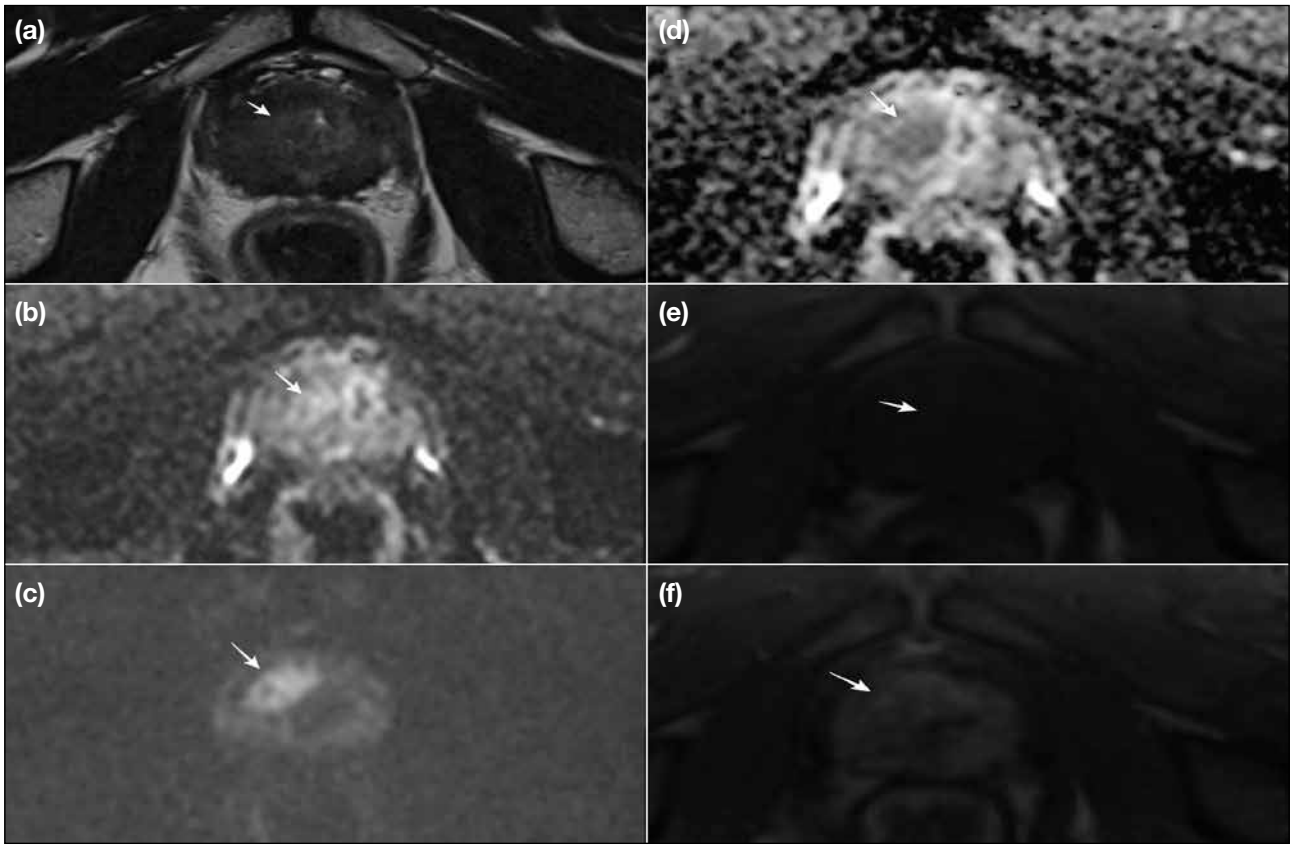

Figure 2. A 67-year-old man with prostate-specific antigen level of 8.31 ng/mL. Arrows indicate a Prostate Imaging Reporting and Data and System (PI-RADS) category 5 lesion visible in the peripheral zone. (a) Axial T2-weighted magnetic resonance (MR) image showing the lesion in the right apex/peripheral zone. The diameter of the lesion is 2.0 cm, which is consistent with a PI-RADS score of 5 on T2-weighted imaging. (b and c) show that the lesion is hypointense on diffusion-weighted imaging (DWI) [b = 50 s/mm^2] and hyperintense on DWI (b = 1800 s/mm^2). (d) Apparent diffusion coefficient map indicates that the lesion is significantly hypointense, giving it a PI-RADS score of 5 on DWI. (e) Pre-contrast T1-weighted and (f) dynamic contrast-enhanced MR images show early enhancement within the same location as the lesion in (a-d) with early enhancement for overall PI-RADS version 2.1 score of 5. Transrectal ultrasound–guided cognitive imaging fusion biopsy detected prostate cancer with International Society of Urological Pathology score of 5.

the detection of PCa and its reliability has been demonstrated by numerous studies.[16-24] When we examined these studies in the literature, the cut-off value for detection of csPCa on MpMRI of PI-RADS 3 or 4 ranged from 85.7% to 94.5% for sensitivity, 23% to 71% for specificity, 34% to 97% for PPV, and 50% to 92% for NPV.[16-21] Venderink et al[22] determined the csPCa rates (GS ≥ 3+4) for PI-RADS 3, 4, and 5 lesions were 17%, 34%, and 67%, respectively. Mathur et al[23] found the detection rates for csPCa were 6.1%, 33.3%, and 64.4% for PI-RADS 3, 4, and 5, respectively, and increased in proportion to the score. A study assessing 737 lesions with MpMRI-targeted TRUS-biopsy found the PCa rates for PI-RADS 1, 2, 3, 4 and 5 lesions were 0%, 10%, 12%, 22% and 72%, respectively.[24] In our study, the rates of PCa in PI-RADS 3, 4, and 5 groups were 22.2%, 56%, and 94.45%, respectively. None of the malignant lesions in the PI-RADS 3 group had ISUP score >1 pathology results (Table 6). As in all PI-RADS versions, disease management after scoring is not specified for patients in PI-RADS v2.1, in which it is stated that 'Category 3 lesions are of intermediate status with an equivocal risk of presenting csPCa'. There are limited studies in the literature regarding the selection of cases for follow-up biopsy.[9,25] Therefore, all PI-RADS 3 lesions were biopsied according to the clinician's preference.

There was a positive correlation between the PI-RADS v2.1 score and the ISUP score ($p < 0.001$) [Table 6]. A study by Walker et al[26] found a positive correlation between PI-RADS v2.1 scores and ISUP scores with a

correlation value of 0.5 and with increase in malignancies found with increasing PI-RADS score. Additionally, consistent with the study findings by Walker et al,[26] we also found that in the PZ when lesions with DWI score 3 were upgraded to the PI-RADS 4 group with DCE positivity and PI-RADS 4 lesions with DWI score 4 are compared, the PI-RADS 4 lesions with DWI score 4 were observed to have higher ISUP scores. These results clearly show that as the PI-RADS v2.1 score increases, the csPCa detection rate increases and can be interpreted as the tumours having more aggressive histopathology. This indicates that PI-RADS v2.1 is a valid and reliable scoring system as PI-RADS v2 does. However, in our study, the histopathological evaluation showed that 25.47% of lesions had ISUP score >1, while 40.56% of lesions had PI-RADS scores of 4 or 5. Therefore, it is clear that PI-RADS v2.1 also needs improvements and more objective recommendations, and further research may contribute to achieving this aim.

In our study, when cut-off values for PZ and whole gland are accepted as PI-RADS ≥3, the NPV for malignancy on MpMRI was 100%. For cut-off value of PI-RADS ≥4 lesions, the values were 76.47% for PZ, 83.33% for TZ, and 80.65% for the whole gland, which were compatible with the literature.[27-29] The high NPV is very important in terms of excluding cancer for patients without performing a biopsy. The sensitivity, specificity, PPV, and NPV analysis in terms of PI-RADS v2.1 sequences and zones are summarised in Tables 4 and 5. However, no study in the literature separately evaluated the sequences in PI-RADS v2.1. When we compared with meta-analyses performed for PI-RADS v2 in general, the sensitivity, specificity, PPV, and NPV values for the sequences were compatible with a meta-analysis by Chen et al.[30] In a study comparing PI-RADS v2 and v2.1, the diagnostic sensitivity, specificity, PPV and NPV for PI-RADS v2.1 were 94.3%, 24.2%, 46.1% and 86.1% for PZ and 93.8%, 42.1%, 45% and 93% for TZ when PI-RADS ≥3 was positive for the detection of GS ≥7 tumours by site, respectively.[31] In our study, taking the PI-RADS score cut-off value as ≥3 positive for PZ, the sensitivity for PCa was 100%, specificity was 11.11%, PPV was 46.67%, and NPV was 100%, similar to levels in the literature for PZ.

Although the PI-RADS v2 is well standardised and expanded for MpMRI use, studies have reported that interobserver agreement can be highly variable.[32-34] A study with three observers by Popita et al[35] found the interobserver $\varkappa$ were 0.643, 0.664, and 0.568. A study in which two radiologists examined 170 patients determined that the interobserver agreement for PI-RADS ≥3 was substantial (all zones $\varkappa = 0.63$, PZ $\varkappa = 0.62$, TZ $\varkappa = 0.53$) and for PI-RADS ≥4 was almost perfect (all zones $\varkappa = 0.91$, PZ $\varkappa = 0.91$, TZ $\varkappa = 0.87$).[36] Smith et al[37] found the interobserver agreement was fair with $\varkappa = 0.24$. Experienced observers demonstrated a higher level of compatibility in detecting both the whole gland and PZ lesions than observers with moderate levels of experience. When the sequence-specific interobserver agreement is assessed, values were $\varkappa = 0.24$, 0.24, and 0.23 for T2WI, DWI, and DCE imaging, respectively.[37] When comparing two radiologists with different levels of experience, we observed moderate compatibility for the use of PI-RADS v2.1 without the cut-off value (all zones $\varkappa = 0.562$) and the cut-off value of PI-RADS ≥4 (all zones $\varkappa = 0.77$). Our data show that the use of PI-RADS v2.1 increases interobserver agreement with more specific definitions. Increasing observers' experience and future PI-RADS updates may increase the agreement between inexperienced observers or observers with similar experiences.

Limitations

There are two major limitations of this study. Firstly, since the study was prospectively designed, there was no equal number of lesions according to pathological diagnosis and zones. Increasing the number of patients in the study may provide better results and beneficial statistical data for the literature. Secondly, the TRUS-guided cognitive fusion biopsy is limited by the operator's experience and lack of standardisation, which can impact its success rate.[38]

CONCLUSION

Our study revealed that PI-RADS v2.1 was highly effective in detecting lesions, determining patient selection for biopsy, and identifying risk level for patients with suspected PCa. Our data support the notion that PI-RADS v2.1 has improved interobserver agreement within the framework of PI-RADS, despite the presence of weak points that need to be addressed. When the cut-off value for cancer detection is increased to PI-RADS ≥4 from PI-RADS ≥3, the significant increase in the specificity, PPV, and interobserver agreement suggests that the PI-RADS 3 criteria should be revised in new versions of the PI-RADS. When lesions with DCE positivity and DWI score 3 upgraded from PI-RADS 3 to 4 and PI-RADS 4 lesions with DWI score 4 are compared, we identified significant differences between ISUP scores. For this reason, we suggest there should be

differences in the scoring of these groups. We believe that, as more data are to be obtained with further studies, PI-RADS guidelines will be more accurate.

REFERENCES

1. Siegel RL, Miller KD, Fuchs HE, Jemal A. Cancer statistics, 2021. CA Cancer J Clin. 2021;71:7-33.
2. Johnson LM, Turkbey B, Figg WD, Choyke PL. Multiparametric MRI in prostate cancer management. Nat Rev Clin Oncol. 2014;11:346-53.
3. Drost FJ, Rannikko A, Valdagni R, Pickles T, Kakehi Y, Remmers S, et al. Can active surveillance really reduce the harms of overdiagnosing prostate cancer? A reflection of real life clinical practice in the PRIAS study. Transl Androl Urol. 2018;7:98-105.
4. Dinh AH, Melodelima C, Souchon R, Lehaire J, Bratan F, Mège-Lechevallier F, et al. Quantitative analysis of prostate multiparametric MR images for detection of aggressive prostate cancer in the peripheral zone: a multiple imager study. Radiology. 2016;280:117-27.
5. Barentsz JO, Richenberg J, Clements R, Choyke P, Verma S, Villeirs G, et al. ESUR prostate MR guidelines 2012. Eur Radiol. 2012 ;22 :746-57.
6. Mottet N, Bellmunt J, Bolla M, Briers E, Cumberbatch MG, De Santis M, et al. EAU-ESTRO-SIOG Guidelines on Prostate Cancer. Part 1: Screening, diagnosis, and local treatment with curative intent. Eur Urol. 2017;71:618-29.
7. American College of Radiology. PI-RADSTM Prostate Imaging–Reporting and Data System. 2015. Available from: https://www.acr.org/Clinical-Resources/Reporting-and-Data-Systems/PI-RADS. Accessed 8 May 2023.
8. Richenberg JL. PI-RADS: past, present and future. Clin Radiol. 2016;71:23-4.
9. American College of Radiology. PI-RADS. Prostate imaging–reporting and data system. 2019 version 2.1. Available from: https://www.acr.org/-/media/ACR/Files/RADS/Pi-RADS/PIRADS-v2-1.pdf. Accessed 8 May 2023.
10. Epstein JI, Zelefsky MJ, Sjoberg DD, Nelson JB, Egevad L, Magi-Galluzzi C, et al. A contemporary prostate cancer grading system: a validated alternative to the Gleason score. Eur Urol. 2016;69:428-35.
11. Jue JS, Barboza MP, Prakash NS, Venkatramani V, Sinha VR, Pavan N, et al. Re-examining prostate-specific antigen (PSA) density: defining the optimal PSA range and patients for using PSA density to predict prostate cancer using extended template biopsy. Urology. 2017;105:123-8.
12. Al-Khalil S, Ibilibor C, Cammack JT, de Riese W. Association of prostate volume with incidence and aggressiveness of prostate cancer. Res Rep Urol. 2016;8:201-5.
13. Tang P, Jin XL, Uhlman M, Lin YR, Deng XR, Wang B, et al. Prostate volume as an independent predictor of prostate cancer in men with PSA of 10-50 ng ml(-1). Asian J Androl. 2013;15:409-12.
14. Haas GP, Delongchamps N, Brawley OW, Wang CY, de la Roza G. The worldwide epidemiology of prostate cancer: perspectives from autopsy studies. Can J Urol. 2008;15:3866-71.
15. Droz JP, Balducci L, Bolla M, Emberton M, Fitzpatrick JM, Joniau S, et al. Management of prostate cancer in older men: Recommendations of a working group of the International Society of Geriatric Oncology. BJU Int. 2010;106:462-9.
16. Ahmed HU, El-Shater Bosaily A, Brown LC, Gabe R, Kaplan R, Parmar MK, et al. Diagnostic accuracy of multi-parametric MRI and TRUS biopsy in prostate cancer (PROMIS): a paired validating confirmatory study. Lancet. 2017;389:815-22.
17. Grey AD, Chana MS, Popert R, Wolfe K, Liyanage SH, Acher PL. Diagnostic accuracy of magnetic resonance imaging (MRI) prostate imaging reporting and data system (PI-RADS) scoring in a transperineal prostate biopsy setting. BJU Int. 2015;115:728-35.
18. Abd-Alazeez M, Kirkham A, Ahmed HU, Arya M, Anastasiadis E, Charman SC, et al. Performance of multiparametric MRI in men at risk of prostate cancer before the first biopsy: a paired validating cohort study using template prostate mapping biopsies as the reference standard. Prostate Cancer Prostatic Dis. 2014;17:40-6.
19. Thompson JE, Moses D, Shnier R, Brenner P, Delprado W, Ponsky L, et al. Multiparametric magnetic resonance imaging guided diagnostic biopsy detects significant prostate cancer and could reduce unnecessary biopsies and over detection: a prospective study. J Urol. 2014;192:67-74.
20. Zhang L, Tang M, Chen S, Lei X, Zhang X, Huan Y. A meta-analysis of use of Prostate Imaging Reporting and Data System Version 2 (PI-RADS V2) with multiparametric MR imaging for the detection of prostate cancer. Eur Radiol. 2017;27:5204-14.
21. Woo S, Suh CH, Kim SY, Cho JY, Kim SH. Diagnostic performance of prostate imaging reporting and data system version 2 for detection of prostate cancer: a systematic review and diagnostic meta-analysis. Eur Urol. 2017;72:177-88.
22. Venderink W, van Luijtelaar A, Bomers JG, van der Leest M, Hulsbergen-van de Kaa C, Barentsz JO, et al. Results of targeted biopsy in men with magnetic resonance imaging lesions classified equivocal, likely or highly likely to be clinically significant prostate cancer. Eur Urol. 2018;73:353-60.
23. Mathur S, O'Malley ME, Ghai S, Jhaveri K, Sreeharsha B, Margolis M, et al. Correlation of 3T multiparametric prostate MRI using prostate imaging reporting and data system (PIRADS) version 2 with biopsy as reference standard. Abdom Radiol (NY). 2019;44:252-8.
24. Mehralivand S, Bednarova S, Shih JH, Mertan FV, Gaur S, Merino MJ, et al. Prospective evaluation of PI-RADSTM version 2 using the International Society of Urological Pathology prostate cancer grade group system. J Urol. 2017;198:583-90.
25. Yang S, Zhao W, Tan S, Zhang Y, Wei C, Chen T, et al. Combining clinical and MRI data to manage PI-RADS 3 lesions and reduce excessive biopsy. Transl Androl Urol. 2020;9:1252-61.
26. Walker SM, Mehralivand S, Harmon SA, Sanford T, Merino MJ, Wood BJ, et al. Prospective evaluation of PI-RADS version 2.1 for prostate cancer detection. AJR Am J Roentgenol. 2020;215:1098-103.
27. Wysock JS, Mendhiratta N, Zattoni F, Meng X, Bjurlin M, Huang WC, et al. Predictive value of negative 3T multiparametric magnetic resonance imaging of the prostate on 12-core biopsy results. BJU Int. 2016;118:515-20.
28. Pokorny MR, de Rooij M, Duncan E, Schröder FH, Parkinson R, Barentsz JO, et al. Prospective study of diagnostic accuracy comparing prostate cancer detection by transrectal ultrasound-guided biopsy versus magnetic resonance (MR) imaging with subsequent MR-guided biopsy in men without previous prostate biopsies. Eur Urol. 2014;66:22-9.
29. Itatani R, Namimoto T, Atsuji S, Katahira K, Morishita S, Kitani K, et al. Negative predictive value of multiparametric MRI for prostate cancer detection: outcome of 5-year follow-up in men with negative findings on initial MRI studies. Eur J Radiol. 2014;83:1740-5.
30. Chen Z, Zheng Y, Ji G, Liu X, Li P, Cai L, et al. Accuracy of dynamic contrast-enhanced magnetic resonance imaging in the diagnosis of prostate cancer: systematic review and meta-analysis. Oncotarget. 2017;8:77975-89.
31. Rudolph MM, Baur AD, Cash H, Haas M, Mahjoub S,

Hartenstein A, et al. Diagnostic performance of PI-RADS version 2.1 compared to version 2.0 for detection of peripheral and transition zone prostate cancer. Sci Rep. 2020;10:15982.
32. Benndorf M, Hahn F, Krönig M, Jilg CA, Krauss T, Langer M, et al. Diagnostic performance and reproducibility of T2w based and diffusion weighted imaging (DWI) based PI-RADSv2 lexicon descriptors for prostate MRI. Eur J Radiol. 2017;93:9-15.
33. Greer MD, Shih JH, Barrett T, Bednarova S, Kabakus I, Law YM, et al. All over the map: an interobserver agreement study of tumor location based on the PI-RADSv2 sector map. J Magn Reson Imaging. 2018;48:482-90.
34. Sonn GA, Fan RE, Ghanouni P, Wang NN, Brooks JD, Loening AM, et al. Prostate magnetic resonance imaging interpretation varies substantially across radiologists. Eur Urol Focus. 2019;5:592-9.
35. Popita C, Popita AR, Andrei A, Rusu A, Fetica B, Petrut B, et al. Interobserver agreement in prostate cancer detection using multiparametric MRI. J BUON. 2018;23:1061-9.
36. Purysko AS, Bittencourt LK, Bullen JA, Mostardeiro TR, Herts BR, Klein EA. Accuracy and interobserver agreement for Prostate Imaging Reporting and Data System, version 2, for the characterization of lesions identified on multiparametric MRI of the prostate. AJR Am J Roentgenol. 2017;209:339-49.
37. Smith CP, Harmon SA, Barrett T, Bittencourt LK, Law YM, Shebel H, et al. Intra- and interreader reproducibility of PI-RADSv2: a multireader study. J Magn Reson Imaging. 2019;49:1694-703.
38. Brown AM, Elbuluk O, Mertan F, Sankineni S, Margolis DJ, Wood BJ, et al. Recent advances in image-guided targeted prostate biopsy. Abdom Imaging. 2015;40:1788-99.

Hong Kong J Radiol. 2023;26:111-9. Epub 12 Jun 2023 | https://doi.org/10.12809/hkjr2317492

ORIGINAL ARTICLE

Transradial Diagnostic Cerebral Angiography: Local Experience, Technique, and Outcomes

HT Lau, YLE Chu, R Lee, WP Cheng, KW Ho

Department of Radiology, Queen Mary Hospital, Hong Kong SAR, China

ABSTRACT

Introduction: *Transradial approach (TRA) has become a popular alternative to traditional transfemoral approach for catheter cerebral angiography, as it offers advantages such as improved patient comfort, safety profile, and cost-effectiveness. This study aimed to evaluate the efficacy and safety of 'radial-first' approach in diagnostic neuroangiography in our locality.*

Methods: *We retrospectively analysed our database of consecutive catheter cerebral angiographies performed via TRA between September 2020 and July 2021. Patient demographics, procedural and radiographic metrics, radial access site–related complications, and total procedural time were recorded.*

Results: *A total of 52 TRA diagnostic cerebral angiographies were performed. Radial artery access was successfully obtained in all patients (n = 52). The rate of successful navigation through the brachial artery was 98.1% (n = 51), with an overall femoral crossover rate of 1.9% (n = 1). Satisfactory diagnostic images were obtained in all TRA cases (n = 51). Complications related to radial artery access were recorded in two cases (3.8%), including a case of transient radial arterial spasm and a case of transient radial artery occlusion. No access site–related permanent ischaemic symptoms were reported. Other severe access site complications such as pseudoaneurysm and arteriovenous fistula were not demonstrated.*

Conclusion: *TRA is a safe and feasible technique for diagnostic cerebral angiography in our locality, with a low complication rate.*

Key Words: *Angiography, digital subtraction; Cerebral angiography; Radial artery*

Correspondence: *Dr YLE Chu, Department of Radiology, Queen Mary Hospital, Hong Kong SAR, China*
Email: edchu.radiology@gmail.com

Submitted: 23 Oct 2021; Accepted: 4 Mar 2022.

Contributors: All authors designed the study, acquired and analysed the data. HTL and YLEC drafted the manuscript. All authors critically revised the manuscript for important intellectual content. All authors had full access to the data, contributed to the study, approved the final version for publication, and take responsibility for its accuracy and integrity.

Conflicts of Interest: All authors have disclosed no conflicts of interest.

Funding/Support: This research received no specific grant from any funding agency in the public, commercial, or not-for-profit sectors.

Data Availability: All data generated or analysed during the present research are available from the corresponding author on reasonable request.

Ethics Approval: This research was approved by the Hong Kong West Cluster Research Ethics Committee of Hospital Authority, Hong Kong (Ref No.: HKWC-2021-0649/ UW 21-617). The Ethics Committee waived the need for patient consent for this retrospective study.

中文摘要

經橈動脈診斷性腦血管造影：本地經驗、技術和結果

劉凱桃、朱賢麟、李雷釗、鄭永鵬、何家慧

引言：經橈動脈入路已成為傳統經股動脈導管腦血管造影術的流行替代方法，因其具有改善患者舒適度、安全性和成本效益等優勢。本研究旨在評估「優先採用經橈動脈入路」方法在我們本地診斷性神經血管造影術中的有效性和安全性。

方法：我們回顧性分析在2020年9月至2021年7月期間通過經橈動脈入路進行連續導管腦血管造影術的數據庫。我們記錄了患者的人口統計資料、手術和影像學指標、經橈動脈入路部位相關併發症和總手術時間。

結果：共進行了52次經橈動脈入路診斷性腦血管造影。所有患者（n = 52）經橈動脈入路插入均成功。通過肱動脈的成功導航率為98.1%（n = 51），一例後續採用了股動脈經路（1.9%）。所有經橈動脈入路病例（n = 51）都獲得了滿意的診斷圖像。兩例（3.8%）發生了與橈動脈通路相關的併發症，包括一例短暫性橈動脈痙攣和一例短暫性橈動脈閉塞。沒有與穿刺部位相關的永久性缺血症狀。未見其他通路部位嚴重併發症如假性動脈瘤和動靜脈等。

結論：經橈動脈入路是本地診斷性腦血管造影安全可行的技術，併發症發生率低。

INTRODUCTION

Catheter cerebral angiography is a common diagnostic method to examine cerebral vasculature. Traditionally, the procedures have been performed via the transfemoral route. However, the transfemoral approach (TFA) is not always feasible. For example, it will be problematic in patients with dissection of the thoracic aorta, iliofemoral occlusive disease, and inguinal infections. TFA angiography also requires patients to tolerate uncomfortable groin compression and bed rest after the procedures. Serious access site–related complications, including pseudoaneurysm, retroperitoneal haemorrhage, femoral artery dissection, and lower limb ischaemia are well recognised.[1-4]

There has been a notable trend of transition from TFA to the transradial approach (TRA) in cerebral angiography among the neuroangiography community. This transition was primarily fuelled by robust findings of TRA's lower access-related complications, lower mortality rates, decreased length of hospital stay, and increased patient satisfaction in the cardiology literature.[5,6] Both neuroangiography and interventional cardiology require arterial catheterisation supplying the vital organs which have narrow margin of error. Also, both of them first started as TFA. Given these similarities between the two fields, it was believed that the significant safety advantages of TRA for interventional cardiology might be transferrable to neuroangiography. This has been supported by recent data from the neuroangiographic literature, which have demonstrated favourable safety profiles, patient experiences, and cost-effectiveness of TRA over TFA.[3,7-11]

In light of the body of evidence demonstrating the clinical benefits of TRA, our centre has adopted a 'radial-first' approach in neuroangiography since September 2020. Here we present our initial experience in the transition from the traditional TFA to a 'radial-first' approach for diagnostic cerebral angiography, including the technical feasibility, safety, and complications of the TRA technique.

METHODS

Study Design

We retrospectively analysed our institutional database of consecutive catheter cerebral angiographies performed via TRA between September 2020 and July 2021. Patient demographics, procedural and radiographic metrics, radial access site–related complications, and total procedural time were recorded.

Patient Selection

All patients underwent preprocedural ultrasound

assessment in order to measure the diameter of the right radial artery and its patency. Patients with a radial artery diameter of <1.6 mm were excluded and the TFA was used instead. Patients requiring intervention in addition to diagnostic angiography were also excluded.

Operators

Transradial cerebral angiographies were performed by three operators during this time, including a neuroradiology trainee who had no prior endovascular experience and performed the procedure under the direct supervision of one of the two other Hong Kong College of Radiologists fellowship–qualified radiologists, who had performed a minimum of 500 TFA cerebral angiographies each.

Transradial Access Techniques

All TRAs used the right arm as the initial access site. The radial artery was accessed at a point 1 to 2 cm proximal to the wrist crease (standard TRA). The more distal radial artery was accessed at the anatomical snuffbox site (distal TRA) according to operator's preference. The patient was prepared and draped with the right arm placed at the patient's right side and the puncture location exposed. For a standard TRA, the patient's right distal forearm and hand were placed in a slightly supinated position of around 60°. Full supination of the hand can often result in discomfort and is not necessary. For distal TRA, the patient's arm was allowed to rest in a neutral position and hand supination was not required. A total of 1 to 2 mL of 1% lidocaine was infiltrated into the skin around the puncture site. Under ultrasound guidance, the radial artery was punctured using a 20-gauge needle via Seldinger or modified Seldinger technique according to the operator's preference. A 5-F vascular radial sheath introducer (Glidesheath Slender; Terumo, Tokyo, Japan or Prelude Radial Sheath; Merit Medical Systems, Inc, South Jordan [UT], US) was then placed over an 0.025-inch hydrophilic guidewire (Glidewire Hydrophilic Coated Guidewire; Terumo, Somerset [NJ], US). A cocktail containing 3000 units of heparin and 2.0 mg of verapamil diluted with 20 mL of blood prior to the infusion in order to avoid patient discomfort during injection was infused over 1 minute through the side-port of the sheath for antithrombotic and antispasmodic purposes, respectively. Heparin was withheld in cases where brain haemorrhage was a concern.

Catheter Navigation and Selection of the Great Vessels

After TRA was obtained, a 5-F Simmons 2 catheter (S2) (Radifocus Optitorque; Terumo, Somerset [NJ], US) was navigated over a 0.035-inch guidewire into the ipsilateral subclavian artery. The navigation of the forearm and brachium was performed under a monoplane setup with radial roadmap guidance (Artis zee biplane; Siemens Healthineers, Erlangen, Germany) in all of our cases, with the bed at a 10-degree clockwise rotation along patient's coronal plane. The radial roadmap is obtained in order to elucidate any radial artery anomalies and to avoid lodging the guidewire into small arterial branches during access to the subclavian. Loops that were difficult to pass with a 0.035-inch wire were navigated with a microcatheter system (Progreat Micro Catheter System; Terumo, Somerset [NJ], US) which would often straighten out the loop. Once the Simmons catheter was brought into the subclavian artery, the table was returned to its neutral position and the lateral plane was brought into position at 90° to the anteroposterior plane (Artis zee biplane).

In cases where imaging of the posterior fossa was of interest, we preferred to first catheterise the right vertebral artery, as this is often the great vessel encountered coming in from the right subclavian artery, and its catheterisation does not usually require reforming the S2 catheter. The catheter was then navigated to the arch to access the other great vessels. We preferred to reform the reverse curve of the Simmons catheter in the descending aorta first whenever possible. In cases where the aorta was too unfolded or too capacious to allow access to the descending aorta with the guidewire, we reformed it off the aortic valve.

Catheterisation and angiograms of the rest of the great vessels was then performed with a formed S2 catheter. In cases where it was difficult to select the left vertebral artery, depending on the operator's preference, catheterisation of the vessel with a S3 catheter was attempted. Alternatively, subclavian injection with a blood pressure cuff around the left arm was performed.

Haemostasis Technique

All arteriotomy closures were achieved with haemostatic compression bands. In standard TRA, a radial wristband (TR Band; Terumo, Somerset [NJ], US) was secured to the arteriotomy site and inflated. The sheath was then removed with the band inflated. The band was then slowly deflated until a small amount of bleeding occurred, after which we injected another 1 to 2 cc of air. By using the minimum amount of compression needed for haemostasis, we maximise the chances of preserved

Table 1. Departmental haemostasis protocol.

Release time of compression band (TR Band or PreludeSYNC DISTAL haemostasis device)	
Basic (5F vascular sheath, no risk factor): 1 hour	Risk factors (+30 min each): • 6F vascular sheath or above • Use of antiplatelet • Use of anticoagulant • Intraoperative heparin • Intraoperative integrilin • Platelet count <100 • Other bleeding tendency
Release 3-4 mL of air every 15 min: inflate 1-2 mL of air back if bleeding encountered and retry after 15 min	

radial artery patency. A similar approach is used in the closure of the distal TRA with a haemostasis device (PreludeSYNC DISTAL; Merit Medical Systems, Inc, South Jordan [UT], US).

We followed a departmental protocol for releasing the compression band in the postoperative unit (Table 1).

RESULTS

A total of 83 patients underwent diagnostic cerebral angiography in our institution from September 2020 to July 2021. TRA was used as the primary access technique in 52 patients (19 women and 33 men) with a median age of 53 years, ranging from 20 to 81 years. The results are summarised in Figure 1.

Radial artery access (including standard and distal TRA) was successfully obtained in all 52 patients. Radial artery anomalies, including a radial loop (Figure 2) and severe radial artery tortuosity (Figure 3) were demonstrated in two cases (3.8%). The rate of successful navigation through the radial and subsequent brachial artery via TRA was 98.1% (n = 51). A microcatheter-microwire system (Progreat Micro Catheter System) was used in one of the successful cases with severe radial tortuosity. In another case, a tight loop was encountered in the proximal radial artery (Figure 2) and the operator decided to crossover to a TFA.

Satisfactory diagnostic images were obtained in cases where catheters were successfully advanced past the brachial artery (n = 51). None of these cases required conversion to a TFA. The overall TFA crossover rate was 1.9% (n = 1) in our cohort.

The mean diameter of the radial artery and distal radial artery were 2.2 mm (range, 1.6-3.4) and 1.9 mm (range, 1-3), respectively. Distal TRA was attempted in 20 out of 52 cases. Access to the distal radial artery was unsuccessful in two cases requiring crossover to a standard TRA. Overall, standard TRA was performed in 34 cases (65.4%) and distal TRA were performed in 18 cases (34.6%). The mean diameter of the distal

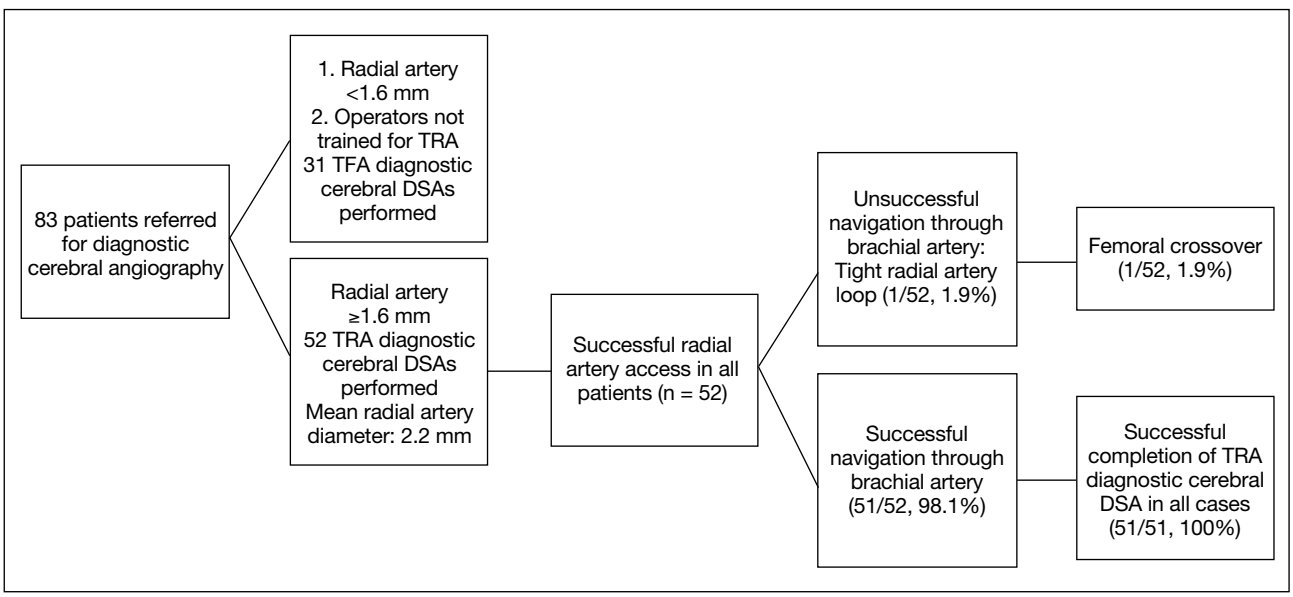

Figure 1. Flowchart showing subject recruitment and outcome.
Abbreviations: DSA = digital subtraction angiography; TFA = transfemoral approach; TRA = transradial approach.

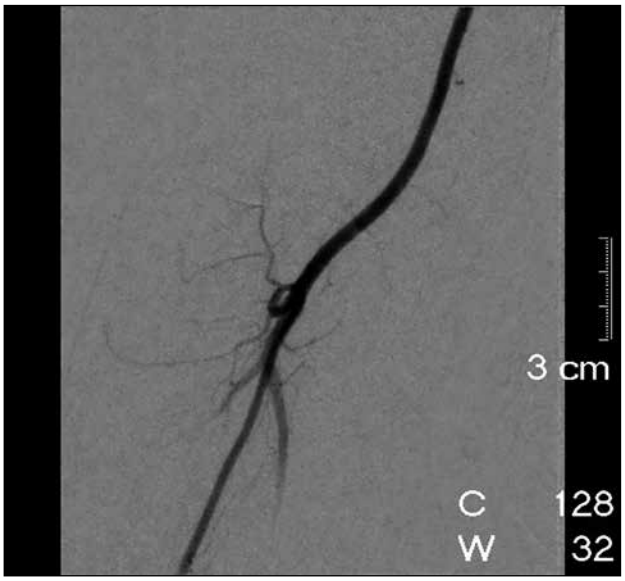

Figure 2. Proximal radial loop required femoral crossover.

Figure 3. Radial artery tortuosity required microcatheter-microwire system.

radial artery of successful distal TRAs was 2.2 mm, as compared to 1.7 mm in the two unsuccessful cases. The mean diameter of the radial artery in successful standard TRAs was 2.2 mm.

The mean total procedural time was 45 minutes (range, 7-98), while the mean number of supra-aortic vessel angiograms performed was 4.7. Choices of diagnostic catheters for successful angiograms of different vessels in our series are described in Table 2.

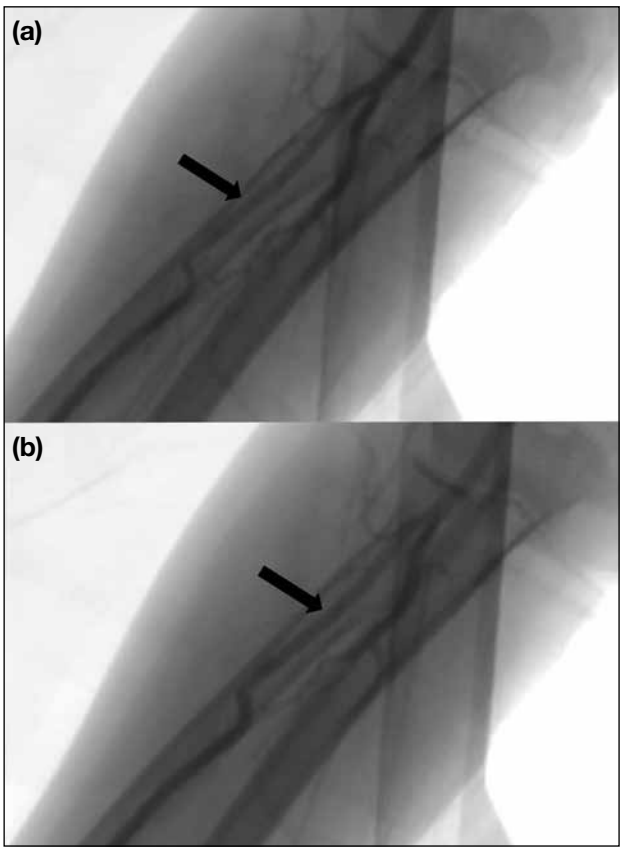

Figure 4. Transient radial artery spasm (arrow in [a]), resolved after administration of 2-mg intra-arterial verapamil (arrow in [b]).

Complications related to radial artery access were recorded in two cases (3.8%). This included a case of transient radial arterial spasm (Figure 4) which was managed with administration of 2-mg intra-arterial verapamil. The angiogram was successfully completed after the radial artery spasm was resolved. No complications were encountered and the patient was discharged on the day of the procedure. In the second case (distal TRA), the patient complained of reduced muscle strength of his right hand and fingers, which recovered spontaneously over a 2-week period. Sonographic assessment at initial presentation showed partial radial artery occlusion at the puncture site (Figure 5). This was spontaneously resolved together with the symptoms 2 weeks after the procedure. No access site–related permanent ischaemic symptoms were reported.

Other severe procedure-related vascular complications such as pseudoaneurysm, arteriovenous fistula, or functional disability of the hand described in the literature[4,7,8] were not demonstrated in our series.

Table 2. Choice of diagnostic catheter used in successful angiograms.*

Patient No.	Vessels catheterised with S2/Glidecath (in S2 tip)	Vessels catheterised with catheters other than S2/ Glidecath (in S2 tip)	Diagnostic catheter(s) used
1	Left CCA, Left VA	Nil	Nil
2	Left and right CCA, left and right ECA, left and right VA, left and right SCA	Nil	Nil
3	Left and right CCA, left and right ICA, right VA	Nil	Nil
4	Left and right CCA, left and right ICA	Nil	Nil
5	Left CCA, left ICA	Nil	Nil
6	Femoral crossover due to radial loop		
7	Left and right CCA	Right VA	Vert
8	Left and right CCA, left and right ICA, left and right ECA, left and left VA	Nil	Nil
9	Right VA	Nil	Nil
10	Right CCA, right ICA, right VA	Nil	Nil
11	Left CCA, left ICA	Nil	Nil
12	Left and right CCA, left ICA, left and right ECA, left and right VA	Nil	Nil
13	Left and right CCA, left and right ICA, left and right ECA, left and right VA	Nil	Nil
14	Left and right CCA, left and right ICA, left and right ECA, right VA	Left VA	S3
15	Left and right CCA, right ICA, right ECA, left and right VA	Nil	Nil
16	Right CCA, right ICA	Nil	Nil
17	Left and right CCA, left and right ICA, left and right ECA	Nil	Nil
18	Left and right CCA, left and right ICA, left and right ECA, left and right VA	Nil	Nil
19	Left and right CCA, left ICA, left and right ECA	Nil	Nil
20	Left and right CCA, right ICA, right VA	Nil	Nil
21	Left and right CCA, left ICA, left ECA, left and right VA	Nil	Nil
22	Left and right CCA, right VA	Nil	Nil
23	Right CCA, right ICA, right ECA	Left CCA, left and right VA	S1
24	Left and right CCA, left ICA, left ECA, right VA	Nil	Nil
25	Left CCA, left ICA, left ECA, left internal maxillary artery	Left facial artery	XT27
26	Right CCA, right ICA, right ECA	Left CCA, right VA	S3
27	Left CCA, left ICA	Nil	Nil
28	Left and right CCA, left and right VA	Nil	Nil
29	Left and right CCA, left and right ICA, left and right ECA, left and right VA	Nil	Nil
30	Left and right CCA, left and right ICA, left and right ECA, left VA	Nil	Nil
31	Left and right CCA, left ICA, left and right ECA, left VA	Nil	Nil
32	Left and right CCA, right VA	Nil	Nil
33	Left and right CCA, left and right ICA, right ECA, left VA	Left ECA	S3 and Renegade 27 microcatheter
34	Left and right CCA, left and right VA	Nil	Nil
35	Left and right CCA, left and right ICA, right VA	Nil	Nil
36	Right CCA, right ICA	Nil	Nil
37	Left and right CCA, left VA	Nil	Nil
38	Left and right CCA, left and right ICA, left and right ECA, left and right VA	Nil	Nil
39	Left and right CCA, left ICA, left ECA, right VA	Nil	Nil
40	Left and right CCA, left ICA, left ECA, right VA	Nil	Nil
41	Left and right CCA, left and right ICA	Nil	Nil
42	Left and right CCA, left and right ICA, left and right VA	Nil	Nil
43	Left CCA	Nil	Nil
44	Left and right CCA, left and right ICA, left and right VA	Nil	Nil
45	Left and right CCA, right ICA	Nil	Nil
46	Left and right CCA, left ICA, left ECA, left and right VA	Nil	Nil
47	Left and right CCA, left ICA, left ECA, right VA	Nil	Nil
48	Right VA	Nil	Nil
49	Left and right CCA, left and right ICA, left and right ECA, left and right VA	Nil	Nil
50	Right CCA, right ICA, right ECA	Nil	Nil
51	Left and right CCA, left VA, left and right SCA	Nil	Nil
52	Left CCA, left ICA	Nil	Nil

Abbreviations: CCA = common carotid artery; ECA = external carotid artery; ICA = internal carotid artery; SCA = superior cerebellar artery; VA = vertebral artery.

* Catheters: Glidecath = 5Fr Glidecath Hydrophilic Coated Catheter (Terumo, Somerset [NJ], US); Renegade 27 microcatheter = Renegade HI-FLO Microcatheter (Boston Scientific, Marlborough [MA], US); S1 = Simmons 1 catheter (Radifocus Optitorque; Terumo, Somerset [NJ], US); S2 = 5F Simmons 2 catheter (S2) (Radifocus Optitorque, Terumo, Somerset, [NJ], US); S3 = SIM3 (Torcon NB Advantage Catheter; Cook Medical, Bloomington [IN], US); Vert = Vertebral (Radifocus Optitorque; Terumo, Somerset [NJ], US); XT27 = Excelsior XT-27 Microcatheter (Stryker, Fermont [CA], US).

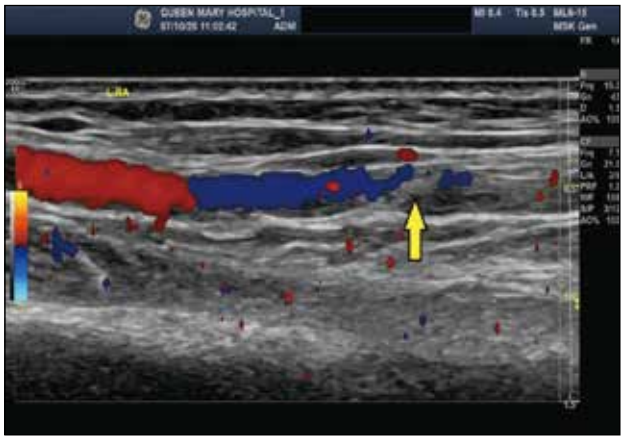

Figure 5. Colour Doppler ultrasound showed partial radial artery occlusion (arrow) at the puncture site.

In all, 38 patients underwent elective TRA diagnostic cerebral angiography and 13 cases were performed on an emergency basis. For elective cases, most of the patients were discharged on the same day as the procedure (n = 32, 84.2%), while five were discharged the following day according to different departmental practice. One patient, who underwent elective superficial temporal artery to middle cerebral artery bypass surgery for moyamoya disease on the same admission, was discharged 3 days after the TRA procedure.

Overall, a success rate of 98.1% (n = 51) for transradial cerebral angiography was achieved. In the case where the TRA was unsuccessful, the procedure was completed via TFA, for an overall crossover rate to femoral approach of 1.9%. Cerebral angiograms were successfully obtained in all cases when catheters were able to be advanced beyond the brachial artery. The radial access site–related complication rate was 3.8%.

DISCUSSION

Transradial Approach Benefits

All patients who underwent TRA cerebral angiography in an outpatient setting were ambulatory immediately after the procedure and most of them could be discharged on the same day.

It is well-established that observation time after TRA cerebral angiography is significantly shortened as compared to TFA; this in turn reduces nursing workload and hospital costs.[9] TRA is also associated with significantly fewer access site complications.[11] Uncomfortable groin compression and prolonged bed rest can be avoided for TRA procedures.

Preprocedural Collateral Circulation Assessment

We do not routinely perform preprocedural collateral testing such as Barbeau or Allen tests in accordance with recommendations from the American Heart Association, as they have been proven to be unreliable in predicting the incidence of hand ischaemia.[12-14]

Radial Cocktail

Nitroglycerin is one of the most common vasodilators applied prophylactically to prevent radial artery vasospasm.[3,7,10,15] However, its use in patients with potential neurovascular disease such as carotid stenosis may lead to complications such as transient ischaemic attack or even haemodynamic stroke due to an abrupt fall in blood pressure.[16,17] In our centre, we only included 2 mg of verapamil and 3000 units of heparin as a standard radial cocktail to reduce the risk of vasospasm during TRA. Overall, the rate of vasospasm, radial access site complications, and femoral crossover were all comparable to recent large-scale trials involving TRA cerebral angiograms with prophylactic nitroglycerin.[3,7,10]

Radial Artery Anomaly and Technical Challenges

Anomalous radial artery anatomy, including a radial loop, high-bifurcating radial origin, arterial tortuosity, atherosclerosis, and accessory branches, is relatively common. A recent study of 1540 patients reported the overall incidence of radial artery anomalies was 13.8%, and procedural failure was far more common in patients with anomalous anatomy than in patients with normal anatomy.[18]

A radial roadmap was essential in identifying difficult radial anatomy and therefore performed in all of our cases. We encountered three cases of difficult radial artery anatomy, including two cases of radial artery anomalies (radial loop and severe radial tortuosity) and a case of radial artery spasm despite pretreatment with verapamil and heparin.

For the patient with severe radial tortuosity, a microcatheter-microwire system (Progreat Micro Catheter System) was used to overcome the tortuous vessel. An additional 2-mg intra-arterial verapamil dose was used in the case with radial artery spasm. Successful TRA cerebral angiography was subsequently performed in both cases.

One patient failed TRA due to the presence of a tight

radial loop. In retrospect, it is possible that this could have been resolved with the use of a microcatheter or soft tip guidewire.

Choices of Diagnostic Catheter

The 5-F S2 catheter was our catheter of choice for diagnostic cerebral angiography, similar to many other centres worldwide.[7,8,19] First-pass success rate was 82.4% (n = 42) of the cases. With the aid of a 5-F Glidecath Hydrophilic Coated Catheter (Terumo, Somerset [NJ], US) in S2 tip shape, 88.2% (n = 45) of cases were completed. In our series, the right common carotid artery, both internal carotid arteries, the right external carotid artery, and both subclavian arteries were all successfully cannulated by either a S2 or Glidecath (in S2 tip shape) catheter.

The vertebral arteries are often different in diameter, with the left side more frequently being dominant.[20] The success rate of direct left vertebral artery catheterisation from a right radial approach is known to be lower compared to that of the rest of the great vessels.[19] Specifically, the passage of a diagnostic catheter from the aortic arch to the left vertebral artery through the left subclavian artery could be difficult, and the success rate depends on the angle of origin of the left vertebral artery.[21] Successful left vertebral artery catheterisation is less likely if the angle between the left vertebral artery and left subclavian artery is <90°.[21]

In our series, 91.3% (21 out of 23) of left vertebral artery angiograms were performed with a S2 or Glidecath (in S2 tip shape) catheter. The other two cases were performed with S1 (Radifocus Optitorque; Terumo, Somerset [NJ], US) and S3 (SIM3, Torcon NB Advantage Catheter; Cook Medical, Bloomington [IN], US) catheters, respectively. There was difficulty in forming the S2 curve in the descending arch in one patient, and the operator therefore switched to a S1 catheter to cannulate the left-sided supra-aortic vessels, including the left vertebral artery. In another case, a S3 catheter was used to perform a left vertebral artery angiogram as the S2 catheter failed to catheterise the vessel securely.

Haemostasis Protocol

All arteriotomy closures were achieved with a haemostatic compression band as mentioned (Table 1). None of our patients experienced severe bleeding complications at the radial artery access site, such as pseudoaneurysm or significant haematoma.

Limitations

Our study had some limitations, including its retrospective design and small sample size. Larger-scale studies are needed to validate our initial findings.

CONCLUSION

TRA is a safe and feasible way for diagnostic cerebral angiographies, with a low complication rate.

REFERENCES

1. Heiserman JE, Dean BL, Hodak JA, Flom RA, Bird CR, Drayer BP, et al. Neurologic complications of cerebral angiography. AJNR Am J Neuroradiol. 1994;15:1408-11.
2. Ricci MA, Trevisani GT, Pilcher DB. Vascular complications of cardiac catheterization. Am J Surg. 1994;167:375-8.
3. Wang Z, Xia J, Wang W, Xu G, Gu J, Wang Y, et al. Transradial versus transfemoral approach for cerebral angiography: a prospective comparison. J Interv Med. 2019;2:31-4.
4. Lee DH, Ahn JH, Jeong SS, Eo KS, Park MS. Routine transradial access for conventional cerebral angiography: a single operator's experience of its feasibility and safety. Br J Radiol. 2004;77:831-8.
5. Bertrand OF, Bélisle P, Joyal D, Costerousse O, Rao SV, Jolly SS, et al. Comparison of transradial and femoral approaches for percutaneous coronary interventions: a systematic review and hierarchical Bayesian meta-analysis. Am Heart J. 2012;163:632-48.
6. Bertrand OF, Patel T. Radial approach for primary percutaneous coronary intervention: ready for prime time? J Am Coll Cardiol. 2012;60:2500-3.
7. Jo KW, Park SM, Kim SD, Kim SR, Baik MW, Kim YW. Is transradial cerebral angiography feasible and safe? A single center's experience. J Korean Neurosurg Soc. 2010;47:332-7.
8. Matsumoto Y, Hongo K, Toriyama T, Nagashima H, Kobayashi S. Transradial approach for diagnostic selective cerebral angiography: results of a consecutive series of 166 cases. AJNR Am J Neuroradiol. 2001;22:704-8.
9. Romano DG, Frauenfelder G, Tartaglione S, Diana F, Saponiero R. Trans-radial approach: technical and clinical outcomes in neurovascular procedures. CVIR Endovasc. 2020;3:58.
10. Park JH, Kim DY, Kim JW, Park YS, Seung WB. Efficacy of transradial cerebral angiography in the elderly. J Korean Neurosurg Soc. 2013;53:213-7.
11. Tso MK, Rajah GB, Dossani RH, Meyer MJ, McPheeters MJ, Vakharia K, et al. Learning curves for transradial access versus transfemoral access in diagnostic cerebral angiography: a case series. J Neurointerv Surg. 2022;14:174-8.
12. Mason PJ, Shah B, Tamis-Holland JE, Bittl JA, Cohen MG, Safirstein J, et al. An update on radial artery access and best practices for transradial coronary angiography and intervention in acute coronary syndrome: a scientific statement from the American Heart Association. Circ Cardiovasc Interv. 2018;11:e000035.
13. Bertrand OF, Carey PC, Gilchrist IC. Allen or no Allen: that is the question! J Am Coll Cardiol. 2014;63:1842-4.
14. Valgimigli M, Campo G, Penzo C, Tebaldi M, Biscagllia S, Ferrari R, et al. Transradial coronary catheterization and intervention across the whole spectrum of Allen test results. J Am Coll Cardiol. 2014;63:1833-41.
15. da Silva RL, Luciano LS, Moreira DM, Fattah T, Trombetta AP, Panata L, et al. Randomised clinical trial comparing transradial catheterisation with or without prophylactic nitroglycerin. Br J Cardiol. 2017;24:100-4.

16. Ruff RL, Talman WT, Petito F. Transient ischemic attacks associated with hypotension in hypertensive patients with carotid artery stenosis. Stroke. 1981;12:353-5.
17. Belcaro G, Marchionno L. Hypotension as cause of TIAs (transient ischemic attacks) in patients with severe carotid stenosis and hypertension. Acta Chir Belg. 1983;83:436-8.
18. Lo TS, Nolan J, Fountzopoulos E, Behan M, Butler R, Hetherington SL, et al. Radial artery anomaly and its influence on transradial coronary procedural outcome. Heart. 2009;95:410-5.
19. Layton KF, Kallmes DF, Cloft HJ. The radial artery access site for interventional neuroradiology procedures. AJNR Am J Neuroradiol. 2006;27:1151-4.
20. Hong JM, Chung CS, Bang OY, Yong SW, Joo IS, Huh K. Vertebral artery dominance contributes to basilar artery curvature and peri-vertebrobasilar junctional infarcts. J Neurol Neurosurg Psychiatry. 2009;80:1087-92.
21. Luo N, Qi W, Tong W, Meng B, Feng W, Zhou X, et al. The effect of vascular morphology on selective left vertebral artery catheterization in right-sided radial artery cerebral angiography. Ann Vasc Surg. 2019;56:62-72.

Hong Kong J Radiol. 2023;26:120-6. Epub 17 May 2023 | https://doi.org/10.12809/hkjr2317347

ORIGINAL ARTICLE

Retrievable Inferior Vena Cava Filters: A 10-Year Retrospective Analysis

R Sum, KKP Lau

Department of Radiology, Monash Medical Centre, Melbourne, Australia

ABSTRACT

Introduction: *Inferior vena cava (IVC) filters are an effective form of venous thromboembolism prophylaxis when treatment with anticoagulation is contraindicated. In recent times, the retrievable IVC filter has gained favour in clinical practice as it circumvents the consequences of permanent filters, such as deep venous thrombosis. This study is a retrospective review of the retrievability of IVC filters since their introduction in our department.*

Methods: *Retrospective analysis was conducted on 118 consecutive adult patients (mean age 63.6 years) who underwent IVC filter insertion over a 10-year period. Patient data, including underlying medical condition, indication for filter insertion, number of retrievals, and filter complications, were recorded. Dwell time was calculated using Kaplan-Meier survival analysis.*

Results: *Among the 118 patients, the most common indication for filter insertion was bleeding due to anticoagulation therapy. Mean dwell time for IVC filters was 101.7 days. One patient died before retrieval. The overall successful retrieval rate was 89.0%. Among the 13 patients whose filters could not be retrieved, nine required lifelong anticoagulation and four were lost to follow-up. Three patients developed lower limb deep venous thrombosis due to delayed filter retrieval.*

Conclusion: *The majority of these filters can be retrieved successfully within the first year of insertion. Retrievable IVC filters are a feasible alternative to traditional permanent IVC filters. Complicating factors occur in a small percentage of these patients, which may prevent successful retrieval.*

Key Words: *Pulmonary embolism; Radiology, interventional; Vena cava filters; Venous thromboembolism; Venous thrombosis*

Correspondence: *Dr R Sum, Department of Radiology, Monash Medical Centre, Melbourne, Australia*
Email: r.rm.sum@gmail.com

Submitted: 23 Feb 2021; Accepted: 2 Jul 2021.

Contributors: KKPL designed the study. RS acquired and analysed the data, and drafted the manuscript. KKPL critically revised the manuscript for important intellectual content. Both authors had full access to the data, contributed to the study, approved the final version for publication, and take responsibility for its accuracy and integrity.

Conflicts of Interest: Both authors have disclosed no conflicts of interest.

Funding/Support: This research received no specific grant from any funding agency in the public, commercial, or not-for-profit sectors.

Data Availability: All data generated or analysed during the present study are available from the corresponding author on reasonable request.

Ethics Approval: This research was approved by the Human Research Ethics Committee of Monash Medical Centre, Melbourne, Australia (Ref No.: 76899). The patients were treated in accordance with the tenets of the Declaration of Helsinki and provided written informed consent for all treatments and procedures.

中文摘要

可回取下腔靜脈濾器的經驗：10 年回顧性分析

R Sum、KKP Lau

簡介：當有抗凝治療禁忌時，下腔靜脈濾器是預防靜脈血栓栓塞的一種有效方法。近年來，可回取下腔靜脈濾器在臨床實踐中獲得了青睞，因為它規避了永久性過濾器的後果，例如深靜脈血栓形成。本研究回顧本部門引入可回取下腔靜脈濾器的經驗。

方法：我們對10年間接受下腔靜脈濾器置入的118名連續成年患者（平均年齡63.6歲）進行回顧性分析。本研究記錄了患者數據，包括基礎疾病、濾器置入的指徵、濾器回取次數和濾器併發症，並使用Kaplan-Meier生存分析計算濾器置留時間。

結果：在該118名患者中，濾器置入最常見適應症為抗凝治療導致出血。下腔靜脈濾器平均置留時間為101.7天。一名患者在濾器回取前死亡。濾器回取整體成功率為89.0%。在濾器無法回取的13名患者中，9人需要終生抗凝，4人失訪。三名患者由於濾器回取延遲而出現下肢深靜脈血栓形成。

結論：大多數濾器可在置入第一年內成功回取。可回取下腔靜脈濾器是傳統永久性下腔靜脈濾器的可行替代方案。小部分患者出現併發因素，或會阻礙濾器成功回取。

INTRODUCTION

The use of inferior vena cava (IVC) filters to prevent venous thromboembolism (VTE) is a proven and effective treatment for patients with a contraindication to standard anticoagulation therapy or refractory VTE that has failed anticoagulation.[1] There have been significant developments in IVC filters over recent years. Permanent IVC filters were first introduced into clinical practice over 30 years ago — these remain inside the patient for life. However, evidence in the current literature demonstrates that the rate of complications increases with extended dwell times of IVC filters.[2,3] These complications can have significant detrimental clinical implications, including filter thrombosis and an increased risk of developing subsequent deep venous thrombosis (DVT) which may require lifelong anticoagulation.[3] For this reason, the retrievable filter was developed as an attractive alternative that avoids the long-term implications of permanent filters while still being able to provide protection against VTE in the relevant setting. However, retrievable filters are also subject to a series of complicating factors that can prevent their successful removal. Certain filter elements such as the hook, struts, and barbs are prone to endothelial overgrowth. Misalignment, migration, and fractures are also commonly encountered issues.[4] Retrievability can be delayed by emboli trapped by the filter.[5] According to the current literature, the incidence rates of these complications can vary significantly between institutions.[4]

Because the risk of VTE requires individual assessment and the intention of filtration is to prevent pulmonary embolism (PE), discontinuation is recommended as soon as the perceived risk of developing clinically significant PE is acceptably low.[2] There is no consensus on the recommended duration for filter dwell time. This study is a retrospective review of the retrievability of an IVC filter (Celect Platinum; Cook Medical, Bjaeverskov, Denmark) since its introduction in our department more than a decade ago.

METHODS

We reviewed 118 consecutive cases of adult patients who underwent IVC filter insertion and retrieval at a tertiary referral centre between 1 January 2008 and 1 August 2018. We excluded eight other patients as their IVC filters were inserted external to our institution. One patient died before any attempt at retrieval was feasible and this patient was excluded from data analysis. Patients' age, sex, underlying medical conditions, and indications for IVC filter insertion were recorded. Details of the insertion, including approach and dates, were noted. Details of subsequent retrieval attempts including the date, number of attempts, reasons for failure (if any), and complications were also recorded.

Filter insertion was undertaken either through a right jugular or right or left femoral venous puncture approach. The IVC filter was chosen for insertion through a 7-Fr introducer sheath. A cavagram was routinely performed after deployment to confirm its position.

As part of our department's filter retrieval procedure, an initial cavagram was performed through a right internal jugular venous puncture to exclude filter thrombus and other complicating factors. Filter retrieval was performed using a retrieval set (Günther Tulip; Cook Medical, Bjaeverskov, Denmark) through a right internal jugular venous approach. An 11-F introducer sheath was used for venous access. A 6.3-F retrieval loop system using the loop-snare technique was used to engage the filter hook. Kaplan-Meier analysis comparing successful and unsuccessful retrieval was performed with SPSS (Windows version 24.0; IBM Corp, Armonk [NY], United States). Statistical significance was calculated using Fisher's exact test. A p value of < 0.05 was considered to be statistically significant.

This study was prepared in accordance with STROBE (Strengthening the Reporting of Observational Studies in Epidemiology) reporting guidelines. Ethics approval in accordance with the National Health and Medical Research Council of Australia was obtained from the Human Research Ethics Committee of Monash Medical Centre, Melbourne, Australia.

Table 1. Patient demographics (n = 118).*

Sex	
Female	60 (50.8%)
Male	58 (49.2%)
Age, y (median [range])	63.6 (28-92)
Underlying medical conditions	
Malignancy	27 (22.9%)
Antiphospholipid syndrome	2 (1.7%)
Chronic lung/heart disease	4 (3.4%)
Intracranial haemorrhage†	16 (13.6%)
Liver disease	3 (2.5%)
Crohn's disease	2 (1.7%)
Sepsis	6 (5.1%)
Trauma	16 (13.6%)
Nil significance	42 (35.6%)

Abbreviation: CNS = central nervous system.
* Data are shown as No. (%), unless otherwise specified.
† Defined as any clinically significant intracranial bleeding during the current inpatient admission.

Table 2. Indications for filter insertion (n = 118).

	No. (%)
Bleeding	55 (46.6%)
Imminent surgery	35 (29.7%)
Thrombocytopaenia/coagulopathy	1 (0.8%)
Recent surgery	7 (5.9%)
Recurrent VTE despite anticoagulation therapy	4 (3.4%)
Inability to monitor anticoagulation	2 (1.7%)
Extensive proximal DVT	14 (11.9%)

Abbreviations: DVT = deep vein thrombosis; VTE = venous thromboembolism.

RESULTS

Patient Demographics

Most patients had had an underlying medical condition predisposing them to developing VTE (64.4%). The most common underlying condition was malignancy (22.9%), followed by intracranial haemorrhage (13.6%), trauma (13.6%), sepsis (5.1%), chronic heart and lung disease (3.4%), liver disease (2.5%), Crohn's disease (1.7%), and antiphospholipid syndrome (1.7%) [Table 1].

Indications for Inferior Vena Cava Filter Insertion

Consultation and approval by our institution's haematology unit was required prior to filter insertion. In all, 118 patients required IVC filters because anticoagulation was contraindicated. The most common reason for filter insertion was bleeding due to anticoagulation (46.6%), followed by imminent surgery (29.7%), extensive proximal DVT (11.9%), recent surgery (5.9%), recurrent VTE despite anticoagulation (3.4%), inability to monitor anticoagulation (1.7%), and thrombocytopaenia/coagulopathy (0.9%) [Table 2].

There were 79 filters inserted through a femoral approach and 39 inserted through a jugular approach. A total of 117 filters were successfully inserted without immediate complications. One filter demonstrated tilt immediately after being deployed but no attempts were made to reposition it thereafter (Figure 1).

In all successful retrievals, there were no immediate complications identified on routine post-retrieval cavagram. All retrievals were attempted through a right jugular approach.

Rates of Inferior Vena Cava Filter Retrieval

The indwelling time for filters was calculated using Kaplan-Meier product limit estimation (median = 88.0 days; range, 6.0-348.0). Out of the 117 retrieval attempts, 105 were successful (90.0%) with six of these 105

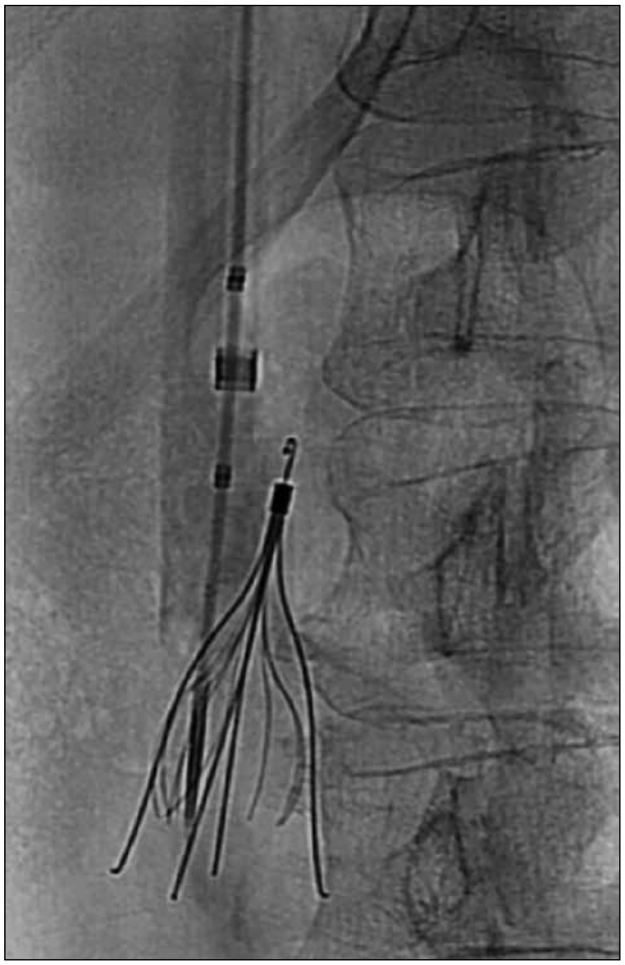

Figure 1. Cavagram in a 58-year-old male demonstrates significant medial tilt filter. The filter hook has embedded into the left lateral aspect of the caval wall. Multiple unsuccessful attempts were made at snaring at the hook and the decision was made to leave the filter in situ permanently.

Table 3. Retrieval outcomes (n = 117).*

Dwell time, days	
Mean	101.7
Median (range)	88.0 (6.0-348.0)
Retrieval outcome	
Not retrieved	12 (10.3%)
Retrieved	105 (89.7%)
Attempts	
1	106 (90.6%)
2	9 (7.7%)
3	2 (1.7%)
Patients undergoing their first attempt	
Successful	99 (84.6%)
Unsuccessful	18 (15.4%)
Aborted after unsuccessful first attempt (n = 7)	
Filter kept in situ permanently	5 (71.4%)
Lost to follow-up	2 (28.6%)
Patients undergoing a second attempt (n = 11)	
Successful	5 (45.5%)
Unsuccessful	6 (54.5%)
Aborted after unsuccessful second attempt (n = 4)	
Filter kept in situ permanently	3 (75.0%)
Lost to follow-up	1 (25.0%)
Patients who underwent their third attempt (n = 2)	
Successful	1 (50.0%)
Unsuccessful	1 (50.0%)

* Data are shown as No. (%), unless otherwise specified.

filters requiring more than one attempt (5.7%) [Table 3]. Twelve filters could not be retrieved (10.3%); their reasons are outlined below. A single retrieval attempt was conducted in 106 patients. Two attempts were performed in nine patients. Two patients underwent three retrieval attempts [Table 3].

During the first attempt, 99 filters were successfully retrieved (84.6%) while 18 filters could not be removed (15.4%). The barriers to retrieval in these 18 filters were endothelialisation of the filter hook in six patients (33.3%) [Figure 2], a large trapped thrombus in another six patients (33.3%) [Figure 3], thrombus formation around the filter hook in four patients (22.2%), and protrusion of the filter legs beyond the caval wall in two patients (11.1%) [Figure 3]. A second attempt was not performed in seven of these patients; in five, retrieval

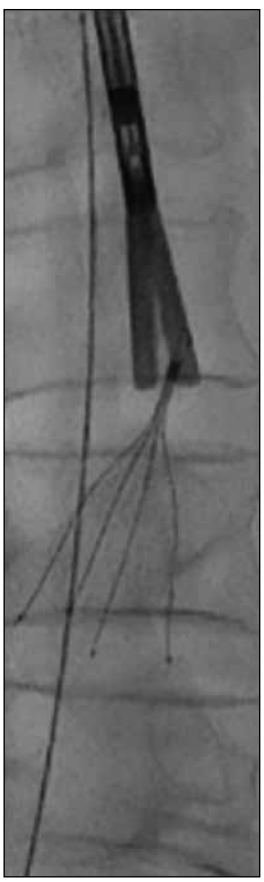

Figure 2. Cavagram in a 42-year-old female demonstrates filter tilt and endothelialisation of the filter into the caval wall. Endovascular forceps were used to carefully dissect the endothelial tissue incorporating the filter hook into the inferior vena cava. This allowed the hook to be freed and successfully snared.

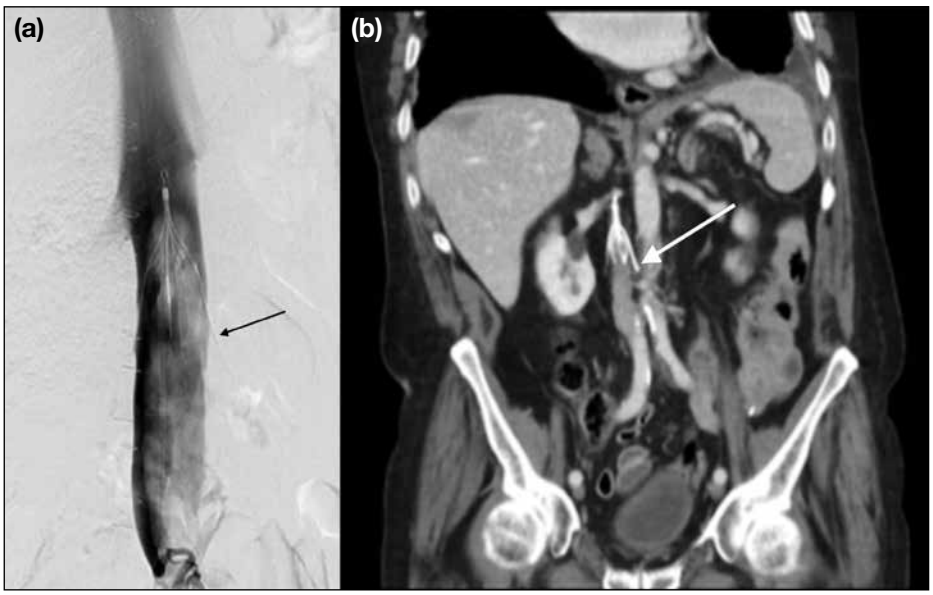

Figure 3. (a) Cavagram in a 70-year-old male demonstrates a large thrombus inside the filter (arrow). (b) There is penetration of the filter struts beyond the caval wall of the same patient on subsequent contrast-enhanced computed tomography (arrow). The filter could not be removed due to significant incorporation of the filter struts into the caval wall from all sides.

of the filter was deemed technically too difficult. The clinical haematology unit decided to keep them as permanent filters and these patients were started on long-term anticoagulation with warfarin. The remaining two patients were lost to follow-up (Table 3).

Of the 18 patients who failed first retrieval attempts, 11 underwent a second attempt while two of them had a third attempt. Among 11 patients who had the second retrieval attempt, five were successfully removed (45.5%) and six were not (54.5%). The reasons for a second failed retrieval were an inability to snare due to thrombus surrounding the filter hook (n = 3), filter thrombus (n = 2), and protrusion of the filter legs beyond the caval wall (n = 1). From these six unsuccessful second retrieval attempts, three filters were kept permanently and the patients were commenced on warfarin therapy. One patient was lost to follow-up (Table 3).

In the two remaining patients who failed the second retrieval attempt, a third retrieval attempt was performed. One was successfully retrieved after a period of anticoagulation for filter hook thrombus in addition to the use of a loop wire snare to engage the filter hook. The other retrieval was unsuccessful despite a third attempt and the decision was made by the clinical haematology unit to keep this as a permanent filter. The patient was subsequently commenced on long-term warfarin therapy (Table 3).

Rates of Follow-up

From the total cohort of 105 successful retrievals, 69 of these patients (65.7%) were reviewed by haematology while 36 patients (34.3%) were not. Among the 12 unsuccessful retrievals, nine patients were commenced on anticoagulation and were managed by a haematologist and three were lost to follow-up (Table 4).

Reasons for Failed Filter Retrieval

There were several factors complicating successful filter retrieval (Table 5). Eighteen patients had had complications with their filter at the time of attempted retrieval (15.3%) with some patients having more than one concurrent complication. Two of the most prevalent factors were trapped embolus within the filter (n = 8) and endothelialisation of the filter hook into the caval wall (n = 8). Filter tilt was seen in six patients. In four patients, the filter hook could not be snared despite multiple attempts at passing the retrieval wire, presumably due to the presence of thrombus surrounding the hook. There were two filters where elements other than the hook (such as the struts) were incorporated into the caval wall. In one patient, there was a combination of filter tilt and endothelialisation of the hook, which led to failure of retrieval (Figure 1). No subsequent attempts at retrieval were made for this patient.

In all cases where retrieval could not be performed due to a trapped embolus, a period of therapeutic low molecular

Table 4. Follow-up status (n = 117).*

	Not removed	Removed
Total	12 (10.3%)	105 (89.7%)
Reviewed by a haematologist after filter insertion	9 (75.0%)	69 (65.7%)
Not reviewed by a haematologist after filter insertion	3 (25.0%)	36 (34.3%)
Outcomes		
Lost to follow-up	3 (2.6%)	0
No referral was submitted to the haematology unit after filter insertion	0	36 (30.8%)
IVC filter left in situ	9 (7.7%)	0
Death before attempted retrieval	1 (0.9%)	0

Abbreviation: IVC = inferior vena cava.
* Data are shown as No. (%), unless otherwise specified.

Table 5. Reasons for failed inferior vena cava filter retrieval (n = 118).

	No. (%)
Total No. of patients with complications	18 (15.3%)
Tilt	6 (5.1%)
Endothelialisation	8 (6.8%)
Incorporation of other filter elements (struts and barbs) into the caval wall	2 (1.7%)
Trapped filter embolus	8 (6.8%)
Inability to snare due to filter hook thrombus	4 (3.4%)

weight heparin was commenced by the haematology unit for 3 months to reduce the thromboembolic load before further attempts at retrieval were considered. This occurred in four filters, three of which were thereafter successfully removed on the second attempt.

One patient had filter tilt and endothelialisation of the hook into the left side of the caval wall. After multiple attempts at manipulating the hook using a variety of snares and balloon insufflation to correct the tilt, the filter tip was eventually freed through blunt dissection of the hook from the caval wall using endovascular forceps and removed without immediate complications (Figure 2).

Three patients developed bilateral lower limb DVT as a result of prolonged dwell time of the IVC filter and multiple non-retrieval attempts, requiring a period of anticoagulation before successful retrieval.

DISCUSSION

This retrospective study provides insight into the management of retrievable IVC filters at our institution. Specifically, the data confirm a high retrieval performance in our department with 105 retrieved (89.0%) successfully from a total of 118 filters inserted over the 10-year study period.

A review of the current literature demonstrates that retrieval rates elsewhere are highly variable, ranging from 49.6% to as high as 96.6%.[6-9] Nearly 60.0% of our IVC filter retrievals occurred within the first 100 days of insertion with the final retrieval rate of 89.0% achieved by 350 days after insertion. Previous studies reveal that the retrieval of Celect filters is most likely to be successful within 3 to 4 months of placement which is also in keeping with our results.[10]

Currently, there is no well-documented consensus on a safe dwell time for retrievable filters. It is recommended that filters should be removed as soon as the risk of PE has resolved due to the risk of complications, although others have suggested that removal times be guided by manufacturers' guidelines.[11] Further, additional delays in retrieval can occur, especially if there are unforeseen changes in the patient's clinical trajectory during their admission or follow-up.

Prolonged dwell times can be problematic and result in a variety of complications as evidenced in our study. Analyses have shown retrievable IVC filters to have an overall complication rate ranging from 11.7% to 20.0%, which is also consistent with our findings (15.3%).[6,7] For instance, strut penetration is reported at a higher rate among conical filters such as the Celect filter.[12-15] While penetration is common among Celect filters, it is rarely associated with breakthrough PE, retrieval failure, or other local complications.[16] An example is seen in one patient where retrieval could not be performed on two attempts due to extensive trapped thrombus within the filter and strut penetration. The third attempt on the same patient was complicated by filter tilt and hook embedment into the posterior caval wall that prevented successful snaring (Figure 3).

The inherent morbidity implicated by long-term filter implantation should not be dismissed. In the PREPIC (Prevention of Recurrent Pulmonary Embolism by Vena Cava Interruption) trial, permanent IVC filters were associated with increased odds of developing recurrent DVT and a reliance on long-term anticoagulation.[3,17] This outcome was seen in seven patients who underwent failed retrieval attempts and were subsequently subjected

to lifelong warfarin. Short-term anticoagulation therapy was also required for three patients who experienced delays in filter retrieval and subsequently developed new lower limb DVT.

Currently, IVC filter insertion at our institution requires formal approval from the haematology unit prior to the procedure. However, there is no protocol for follow-up after their insertion. As a result, three patients were lost to follow-up and no clear anticoagulation plan or plan for filter removal was documented in their medical records. Delays in filter retrieval result in prolonged dwell times, which are detrimental from the increased risk of developing DVT and, in some cases, may subject patients to lifelong anticoagulation. A dedicated follow-up system is therefore required so that all patients undergoing IVC filter insertion are monitored by both interventional radiologists and haematologists to ensure appropriate filter retrieval timing and the optimal use of anticoagulation therapy.

Limitations

This study was from a single tertiary radiology centre, which was its major limitation. Another limitation was the lack of direct contact with those patients who were not followed up by the haematology unit.

CONCLUSION

Retrievable IVC filters are a feasible and safe alternative to permanent filters in VTE prevention. Our study demonstrates that a high retrieval rate can be achieved within 1 year of insertion. However, it is important to be aware that a small percentage of filters may be complicated by several factors that may warrant the use of advanced retrieval techniques. Prompt removal of the IVC filter when safe to do so is necessary due to the increased risk of developing DVT.

REFERENCES

1. Kaufman JA, Barnes GD, Chaer RA, Cuschieri J, Eberhardt RT, Johnson MS, et al. Society of Interventional Radiology clinical practice guideline for inferior vena cava filters in the treatment of patients with venous thromboembolic disease: developed in collaboration with the American College of Cardiology, American College of Chest Physicians, American College of Surgeons Committee on Trauma, American Heart Association, Society for Vascular Surgery, and Society for Vascular Medicine. J Vasc Interv Radiol. 2020;31:1529-44.
2. Kaufman JA, Kinney TB, Streiff MB, Sing RF, Proctor MC, Becker D, et al. Guidelines for the use of retrievable and convertible vena cava filters: report from the Society of Interventional Radiology Multidisciplinary Consensus Conference. J Vasc Interv Radiol. 2006;17:449-59.
3. Decousus H, Leizorovicz A, Parent F, Page Y, Tardy B, Girard P, et al. A clinical trial of vena caval filters in the prevention of pulmonary embolism in patients with proximal deep-vein thrombosis. Prévention du Risque d'Embolie Pulmonaire par Interruption Cave Study Group. N Engl J Med. 1998;338:409-15.
4. Deso SE, Idakoji I, Kuo WT. Evidence-based evaluation of inferior vena cava filter complications based on filter type. Semin Intervent Radiol. 2016;33:93-100.
5. Al-Hakim R, Kee ST, Olinger K, Lee EW, Moriarty JM, McWilliams JP. Inferior vena cava filter retrieval: effectiveness and complications of routine and advanced techniques. J Vasc Interv Radiol. 2014;25:933-9.
6. Doody O, Given MF, Kavnoudias H, Street M, Thomson KR, Lyon SM. Initial experience in 115 patients with the retrievable Cook Celect vena cava filter. J Med Imaging Radiat Oncol. 2009;53:64-8.
7. Lyon SM, Riojas GE, Uberoi R, Patel J, Lipp ME, Plant GR, et al. Short- and long-term retrievability of the Celect vena cava filter: results from a multi-institutional registry. J Vasc Interv Radiol. 2009;20:1441-8.
8. Tashbayev A, Belenky A, Litvin S, Knizhnik M, Bachar GN, Atar E. Retrievable inferior vena cava filters: indications, indwelling time, removal, success and complication rates. Isr Med Assoc J. 2016;18:104-7.
9. Lynch FC. A method for following patients with retrievable inferior vena cava filters: results and lessons learned from the first 1,100 patients. J Vasc Interv Radiol. 2011;22:1507-12.
10. Glocker RJ, Novak Z, Matthews TC, Patterson MA, Jordan WD, Pearce BJ, et al. Factors affecting Cook Günther Tulip and Cook Celect inferior vena cava filter retrieval success. J Vasc Surg Venous Lymphat Disord. 2014;2:21-5.
11. Sarosiek S, Crowther M, Sloan JM. Indications, complications, and management of inferior vena cava filters: the experience in 952 patients at an academic hospital with a level I trauma center. JAMA Inter Med. 2013;173:513-7.
12. Zhou D, Spain J, Moon E, Mclennan G, Sands MJ, Wang W. Retrospective review of 120 Celect inferior vena cava filter retrievals: experience at a single institution. J Vasc Interv Radiol. 2012;23:1557-63.
13. Andreoli JM, Lewandowski RJ, Vogelzang RL, Ryu RK. Comparison of complication rates associated with permanent and retrievable inferior vena cava filters: a review of the MAUDE database. J Vasc Interv Radiol. 2014;25:1181-5.
14. McLoney ED, Krishnasamy VP, Castle JC, Yang X, Guy G. Complications of Celect, Günther Tulip, and Greenfield inferior vena cava filters on CT follow-up: a single-institution experience. J Vasc Interv Radiol. 2013;24:1723-9.
15. Wang SL, Siddiqui A, Rosenthal E. Long-term complications of inferior vena cava filters. J Vasc Surg Venous Lymphat Disord. 2017;5:33-41.
16. Bos A, Van Ha T, van Beek D, Ginsburg M, Zangan S, Navuluri R, et al. Strut penetration: local complications, breakthrough pulmonary embolism, and retrieval failure in patients with celect vena cava filters. J Vasc Interv Radiol. 2015;26:101-6.
17. Bauer KA. Duration of anticoagulation: applying the guidelines and beyond. Haematology Am Soc Hematol Educ Program. 2010;2010:210-5.

Hong Kong J Radiol. 2023;26:127-32. Epub 20 Jun 2023 | https://doi.org/10.12809/hkjr2317543

PERSPECTVE

Entering the Era of Non-fasting Intravenous Contrast-Enhanced Computed Tomography

YS Chan[1], CCM Cho[1], CSL Tong[1], AWH Ng[2]

[1]Department of Imaging and Interventional Radiology, Prince of Wales Hospital, Hong Kong SAR, China
[2]AmMed Medical Diagnostic Center, Hong Kong SAR, China

ABSTRACT

An empirical fasting period of at least 4 hours prior to intravenous contrast administration for computed tomography scans has been an age-old practice. This is associated with patient discomfort, adverse effects on diabetic control, and limits the flexibility of scanning arrangements in urgent settings. The effect is further compounded by the rising number of urgent imaging requests with some patients requiring repeated fasting while waiting for scanning slots. International guidelines have been recently updated, stating that with the improved safety profile of contrast media, fasting is no longer routinely required. In this article, we discuss the current evidence and its implications for our local practice. We share our approach of a stepwise policy change with eventual full implementation of non-fasting policy to all eligible patients in our institution, and the safety data we compiled. Adoption of a non-fasting policy for contrast-enhanced computed tomography is a feasible and beneficial practice adhering to international standards.

Key Words: *Contrast media; Nausea; Pneumonia, aspiration; Vomiting*

中文摘要

進入無需禁食的靜脈顯影電腦斷層掃描的世代

陳奕璇、曹子文、唐倩儂、伍永鴻

電腦斷層掃描靜脈造影劑給藥前至少要求4小時的禁食期一直是一種經驗性做法。這可增加患者不適、不利糖尿病控制，並限制了緊急情況下掃描安排的靈活性。緊急掃描需求數量的增加進一步加劇了這些影響，一些患者在等待掃描時段時需要反覆禁食。最近更新的國際指引指出，隨着造影劑安全性提高，不再需要常規禁食。在本文中，我們討論了當前的證據及其對我們本地實踐的影響。我們分享了我們逐步改變政策的方法最終使我們機構中所有符合條件的患者無需禁食，以及我們收集的安全數據。採用對比顯影掃描的無需禁食政策符合國際標準，且可行有益。

Correspondence: *Dr YS Chan, Department of Imaging and Interventional Radiology, Prince of Wales Hospital, Hong Kong SAR, China*
Email: juliannayschan@cuhk.edu.hk

Submitted: 2 Mar 2022; Accepted: 17 May 2022.

Contributors: YSC and AWHN designed the study and acquired the data. YSC analysed the data and drafted the manuscript. All authors critically revised the manuscript for important intellectual content. All authors had full access to the data, contributed to the study, approved the final version for publication, and take responsibility for its accuracy and integrity.

Conflicts of Interest: All authors have disclosed no conflicts of interest.

Funding/Support: This study received no specific grant from any funding agency in the public, commercial, or not-for-profit sectors.

Data Availability: All data generated or analysed during the present study are available from the corresponding author on reasonable request.

INTRODUCTION

Computed tomography (CT) has been commercially available since the 1970s and is one of the most widely used imaging modalities.[1] Conventional intravenous iodinated contrast emerged in the 1970s to 1980s, allowing for its application in CT, and is now an almost indispensable part of daily practice.[2] From then till now, the contrast agents we use have undergone important changes.

The intravenous contrast used in CT is iodine-based and is classified based on osmolality. High-osmolar contrast media (HOCM) was the first generation of iodinated intravenous contrast and was associated with a high rate of adverse events (5%-8% acute adverse reactions, which essentially encompassed all contrast reactions, and 1%-2% moderate non–life-threatening adverse reactions, which included faintness, vomiting [severe], urticaria [profound], facial edema, laryngeal edema and bronchospasm [mild]).[3] The majority of the chemotoxic effects are mainly related to the hyperosmolality.[3] Nausea and vomiting are common adverse effects with reported incidences of 4.58% and 1.84%, respectively.[4] Subsequently, since the 1990s, iso-osmolar contrast media (IOCM) and low-osmolar contrast media (LOCM), which are associated with an overall much lower risk of adverse reactions, have replaced HOCM. A retrospective review by Hunt et al[5] reported an adverse reaction rate of 0.153% for LOCM based on 298,491 doses, the prevailing majority of which were mild reactions not requiring treatment. The incidences of nausea and vomiting with the use of non-ionic contrast media (including IOCM and LOCM) are also substantially lower than their high-osmolar counterparts, with a reported incidence of 0.05% to 1.99% for nausea, and 0% to 0.36% for vomiting.[6]

Historically, since the days of HOCM use, fasting has been practised prior to intravenous contrast administration due to the established emetic side-effects of HOCM, based on the hypothesis that there is higher risk of vomiting with a full stomach and to reduce the risk of aspiration pneumonia. This practice has not been changed for more than two decades despite the shift to IOCM and LOCM, until very recently. To date, it is still a common practice to adopt a period of fasting prior to contrast media administration before CT scan in Hong Kong and worldwide.[7,8]

There has been increasing recognition of the low risk of gastrointestinal side-effects resulting from IOCM and LOCM administration irrespective of fasting time, as well as trials abolishing the empirical implementation of fasting prior to contrast CT. Lee et al[8] reviewed existing literature and found no case of aspiration in 2001 patients who underwent contrast CT with prior fluid intake. A prospective observational study involving 110,836 cases found no significant difference in the incidence of nausea and vomiting between solid food non-fasting and fasting groups.[9] Prospective randomised controlled trials, each involving more than 2000 patients, were carried out in both hospitalised patients and outpatients, and found no significant difference in incidence of nausea and vomiting between patients fasted for at least 4 hours and patients without fasting, and no case of aspiration pneumonitis was identified.[10,11] There has been an additional report of a statistically significant reduction in the incidence of nausea after changing to a non-fasting policy in an institution in Japan.[12]

Latest Guidelines on Preparatory Fasting

In 2018, the European Society of Urogenital Radiology (ESUR) published their Guideline on Contrast Agents (v10.0), which stated that 'fasting is not recommended before administration of low- or iso-osmolar non-ionic iodine-based contrast media or of gadolinium-based agents'.[13] Later and most recently in 2021, the American College of Radiology (ACR) published their latest Manual on Contrast Media, stating that 'given the potential for negative consequences due to fasting and a lack of evidence that supports the need for fasting, fasting is not required prior to routine intravascular contrast material administration', with additional special consideration required for patients undergoing conscious sedation.[14]

Local Practice

Currently in Prince of Wales Hospital, the contrast agents used include iohexol 300 and 350 (LOCM), and iodixanol (IOCM), all of which have a well-established safety profile and are known to have a low risk of nausea and vomiting. As per department protocol of the Department of Imaging and Interventional Radiology at Prince of Wales Hospital, patients attending the department for contrast-enhanced CT were previously required to fast for at least 4 hours prior to study, unless in emergencies or other limited special considerations. The fasting status of hospitalised patients would be confirmed by the ward, and outpatients would receive written instruction to fast before the appointment.

A PRACTICAL APPROACH TO POLICY CHANGE: LOCAL EXPERIENCE

With the significant discrepancy between the fasting policy between Prince of Wales Hospital and international standards, we saw a pressing need to change our clinical practice. In view of the potential impact of policy change in terms of logistics, and potential doubts or confusion from clinical departments in initial implementation, we adopted a stepwise approach to policy change, combined with ongoing data collection to consolidate the local safety profile of contrast media use under the new policy. The policy change was implemented in four phases (Figure 1).

Phase 1: Preparatory Phase

We reviewed the potential practical issues to the policy change. While a generic implementation of the non-fasting policy would be convenient, we saw that there would be circumstances and specific indications where fasting would still be required. As there was no clear consensus statement or guideline detailing exclusion criteria to non-fasting policy, we decided on a list of exclusion criteria based on consensus opinion of specialists from our local institutes (Table 1).

We gathered data on the fasting time and any occurrence of vomiting after contrast scanning for the patients coming to the radiology department at Prince of Wales Hospital for 25 working days through a questionnaire filled in by attending radiographers and nurses. The electronic patient record of the patients who experienced vomiting and their available subsequent chest radiographs were reviewed to identify any aspiration pneumonia complications. This served to establish a baseline of our performance and compile a local safety profile of contrast media use for CT. After confirming a comparable incidence of vomiting and aspiration pneumonia to international published data, we proceeded with our pilot scheme, continuing to collect data through all four phases.

Table 1. Local exclusion criteria for non-fasting policy in Prince of Wales Hospital.

1.	Ongoing, planned, or requirement for sedation/anaesthesia
2.	Other indications for fasting not due to contrast use, e.g., preparation for potential intervention/surgery
3.	Patients with increased risk of aspiration
4.	Paediatric patient <6 years old
5.	The examination is to assess for subtle gallbladder pathology
6.	Patients undergoing computed tomography colonography and enterography

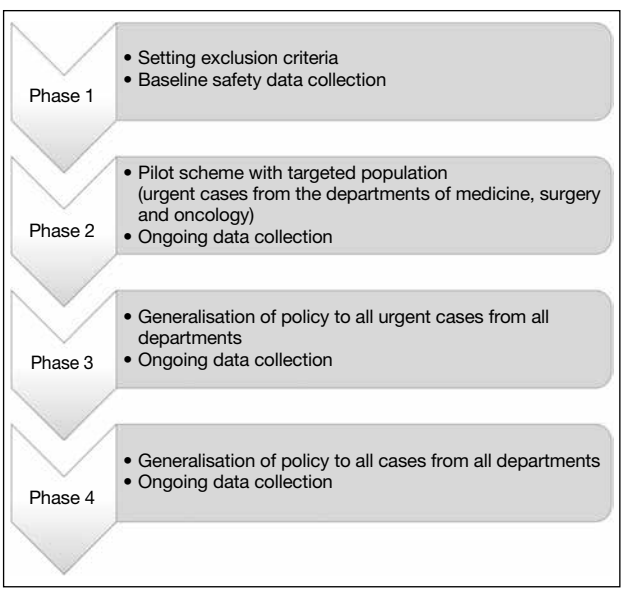

Figure 1. Action plan of policy change towards abolishment of preparatory fasting for contrast-enhanced computed tomography in Prince of Wales Hospital.

Phase 2: Pilot Scheme

We identified the departments of medicine, surgery and oncology at Prince of Wales Hospital as the three main sources of referrals to the radiology department for contrast-enhanced CT. A pilot scheme was then implemented with these three departments, during which the referred eligible patients (i.e., those not under the pre-set exclusion criteria) undergoing urgent contrast-enhanced CT were not required to fast prior to examination.

Phase 3: Generalisation of Non-fasting Policy to Urgent Cases

Subsequent to the pilot scheme, which was well-received with smooth operation, we proceeded with Phase 3, which was generalisation of the non-fasting policy to all urgent cases from all departments. The eligible patients referred from all departments undergoing urgent contrast-enhanced CT were not required to fast prior to examination.

Phase 4: Generalisation of Non-fasting Policy to All Cases

After allowing for a period of familiarisation of all departments with the new policy, we entered Phase 4,

extending the non-fasting policy to all cases, irrespective of urgent or elective setting. Previously, all patients booked for elective contrast-enhanced CT would receive fasting instructions. After the new policy was enforced, newly booked patients would no longer receive fasting instructions unless they fell into the exclusion criteria. No specific instructions were given to previously booked patients who had an appointment date after the new policy launch in order to avoid unnecessary confusion. For previously booked patients who arrived for contrast-enhanced CT without adequate fasting but who were not required to fast under the new policy, the scans were performed without delay.

Establishing a Local Safety Profile for Intravenous Contrast for Computed Tomography

The same duration (25 working days) and methods of data collection (questionnaire, electronic patient record, and chest radiograph review) were applied to Phases 2 through 4.

A total of 4357 attendances were recorded during our data collection through the four phases. There was a steady increase in the proportion of non-fasted attendances (Figure 2). The incidence of vomiting remained low. There was a total of six patients who vomited (0.13%), all of whom had fasted and did not have documented clinical or radiological evidence of aspiration pneumonia. A total of 594 patients were non-fasted and no vomiting occurred (Table 2).

DISCUSSION

Internationally, there is a shifting paradigm towards abolishment of routine preparatory fasting before intravenous contrast administration for CT scans. The recent updates in the ESUR guidelines and the ACR contrast manual provide a clear new international standard. There is also abundant evidence and international data confirming the safety profile of use of IOCM and LOCM, which are the agents used locally. Our experience with converting to a non-fasting preparation for contrast-enhanced CT is concordant with the findings

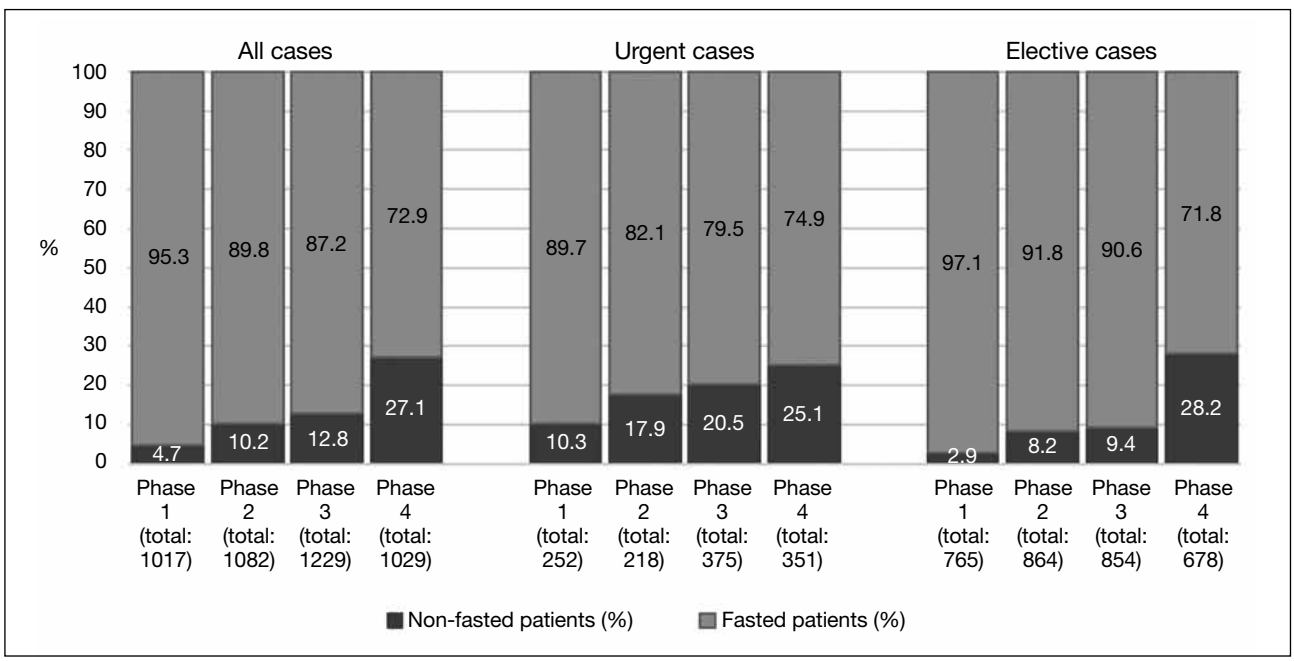

Figure 2. Distribution of fasting preparation among patients through the four phases.

Table 2. Number of cases with vomiting by fasting status in each data collection phase.

	Phase 1	Phase 2	Phase 3	Phase 4	Cumulative
Fasting cases with vomiting	3	2	1	0	6
Non-fasted cases with vomiting	0	0	0	0	0
Total cases with vomiting	3	2	1	0	6

Table 3. Potential disadvantages of universal preparatory fasting.

1.	Causes patient discomfort, with potential higher risk of nausea and vomiting, and may cause irritability and uncooperativeness
2.	Impacts glucose level and medication titration of diabetic patients
3.	Induces catabolic state in vulnerable patients
4.	Causes dehydration, which increases risk of contrast nephropathy and exacerbates the negative consequence of vomiting
5.	Decreases the flexibility of scan arrangement in urgent settings
6.	Delayed scans may prolong hospitalisation, bed occupancy and delay necessary treatment

of published studies, with a low incidence of vomiting and no occurrence of aspiration pneumonia. From a very early study by Oowaki et al[15] to a recent study by Tsushima et al,[12] longer fasting times were found to be associated with an increase in the adverse effect of nausea.[15] There are a number of potential disadvantages of universal preparatory fasting, which are summarised in Table 3. Fasting creates patient discomfort, disturbs nutritional balance in the weak, especially older adult and oncology patients, and potentially causes negative impact on diabetic control and medication titration. Fasting may also create dehydration, which is contradictory to the need of adequate hydration for prevention of contrast nephropathy, and further exacerbates the negative fluid balance should vomiting occur. For inpatients, dehydration can be avoided by administration of intravenous fluid. For outpatients, however, intravenous fluid is not a reasonable option. At an administrative level, the need for consideration of fasting duration also reduces flexibility in appointment arrangement. Empirical adherence to preparatory fasting can lead to unnecessary delays in management, as well as prolonged hospitalisation and bed occupancy. With the compelling evidence, a change in local practice is imperative.

Practically, the implementation of the non-fasting policy is not as simple as a one-off policy change, for two main reasons. First, it is a deeply rooted concept well-accepted by clinicians in Hong Kong that fasting has a protective effect against contrast-induced emesis and lowers the risk of aspiration pneumonia. It is also a convenient practice as an admission order for the majority of inpatients to avoid delay in investigations or potential procedures. However, this practice is not in the best interest of all patients, especially for the weak and fragile. In our experience, many inpatients underwent repeated episodes of prolonged fasting while waiting for urgent contrast-enhanced CT examinations. Due to rising demand despite limited resources, this would be seen more frequently if the policy had not been changed. Second, it is a general statement that fasting is no longer required prior to contrast administration. There are no specific exclusion criteria stated by ESUR guidelines, whereas the ACR manual on contrast media touched upon that 'for patients receiving conscious sedation, anaesthesia guidelines should be consulted'.[13,14] Despite the lack of specific instructions, it is imaginable that there are specific scenarios where fasting may be necessary or have added benefits. We devised our set of exclusion criteria locally based on the consensus opinion of our institutes' specialists (Table 1). Each institution may consider a variation of the exclusion criteria tailored to the demographics of their patients. Our exclusion criteria have two main bases: (1) There are patients at higher risk of aspiration; and (2) There are specific needs for fasting for image optimisation and interpretation.

Specific to certain risk groups, fasting may still be required. Adding to the ACR manual's note on patients undergoing conscious sedation, we expanded the exclusion to all patients receiving sedation/anaesthesia in accordance with anaesthesia guidelines for preoperative fasting, and for those expecting or potentially requiring sedation/anaesthesia in order to avoid potential delay in management. A similar rationale was used for patients expecting to undergo intervention or surgery. On the other hand, there is a group of patients who are inherently at higher risk of aspiration, e.g., those with bulbar palsy with impaired gag reflexes, and those with impaired consciousness levels. In these groups, the preparatory fasting aims mainly to reduce the volume of aspirate should the rare event of vomiting occur, as they are more vulnerable to the aftermath of vomiting. Another group of patients requiring special consideration is the paediatric population. ESUR guidelines[13] and the ACR contrast manual[14] did not specify a need for special consideration for the paediatric population. Compared with the adult population, there are, however, fewer published data evaluating the risk of vomiting with contrast media use. A small study by Ha et al[16] involving 864 patients aged from 1 day to 19 years (mean age = 8.4 ± 5.7 years) found

the incidence of vomiting was 2.1% in the study group with no occurrence of aspiration pneumonia. In Prince of Wales Hospital, we used the age of 6 years as a cut-off for the need for fasting in the paediatric population, based on the need for sedation prior to CT for patients under this age as suggested by our paediatric radiologist.

Specific to the potential impact on image interpretation, there has not been any specific dedicated study to evaluate the effect of a non-fasting policy on image quality. The gallbladder is known to distend with fasting, which may allow for better evaluation of subtle gallbladder pathology, e.g., small polyps. Gross changes in the gallbladder, e.g., acute cholecystitis, do not require fasting preparation for assessment. In addition, the duration of fasting may not necessarily correlate with the degree of gallbladder distension. We therefore only limited exclusion to indications to look for subtle gallbladder pathology. CT enterography and colonography require bowel preparation for optimal image quality and accurate image interpretation and were therefore excluded from the non-fasting policy. So far, with these exclusion criteria in place, we did not encounter any case where the interpretation has been hindered by the non-fasting state.

Combining international guidelines and local consensus opinion, we have implemented the non-fasting policy to all patients undergoing iodinated contrast-enhanced CT examinations in the radiology department with a set of limited exclusion criteria. Through a stepwise approach, we allowed time for adaptation and familiarisation by the clinical departments, and the policy has been met with a positive response with smooth transition. To our knowledge, preparatory fasting is still practised in many local institutions. We hope to advocate the implementation of a non-fasting policy for eligible patients across centres in order to provide patient-centred and evidence-based care, adhering to international standards.

CONCLUSION

Non-fasting contrast-enhanced CT is a safe and internationally recognised practice supported by evidence and international guidelines. Our experience showed a comparable safety profile with that of published studies in terms of low incidence of vomiting and aspiration pneumonia. Policy implementation is achievable through a stepwise approach with need for consideration of pre-set exclusion criteria.

REFERENCES

1. Schulz RA, Stein JA, Pelc NJ. How CT happened: the early development of medical computed tomography. J Med Imaging (Bellingham). 2021;8:052110.
2. Nyman U, Ekberg O, Aspelin P. Torsten Almén (1931–2016): the father of non-ionic iodine contrast media. Acta Radiol. 2016;57:1072-8.
3. Bush WH, Swanson DP. Acute reactions to intravascular contrast media: types, risk factors, recognition, and specific treatment. AJR Am J Roentgenol. 1991;157:1153-61.
4. Katayama H, Yamaguchi K, Kozuka T, Takashima T, Seez P, Matsuura K. Adverse reactions to ionic and nonionic contrast media. A report from the Japanese Committee on the Safety of Contrast Media. Radiology. 1990;175:621-8.
5. Hunt CH, Hartman RP, Hesley GK. Frequency and severity of adverse effects of iodinated and gadolinium contrast materials: retrospective review of 456,930 doses. AJR Am J Roentgenol. 2009;193:1124-7.
6. Kim YS, Yoon SH, Choi YH, Park CM, Lee W, Goo JM. Nausea and vomiting after exposure to non-ionic contrast media: incidence and risk factors focusing on preparatory fasting. Br J Radiol. 2018;91:20180107.
7. Liu H, Liu Y, Zhao L, Li X, Zhang W. Preprocedural fasting for contrast-enhanced CT: when experience meets evidence. Insights Imaging. 2021;12:180.
8. Lee BY, Ok JJ, Abdelaziz Elsayed AA, Kim Y, Han DH. Preparative fasting for contrast-enhanced CT: reconsideration. Radiology. 2012;263:444-50.
9. Li X, Liu H, Zhao L, Liu J, Cai L, Zhang L, et al. The effect of preparative solid food status on the occurrence of nausea, vomiting and aspiration symptoms in enhanced CT examination: prospective observational study. Br J Radiol. 2018;91:20180198.
10. Neeman Z, Abu Ata M, Touma E, Saliba W, Barnett-Griness O, Gralnek IM, et al. Is fasting still necessary prior to contrast-enhanced computed tomography? A randomized clinical study. Eur Radiol. 2020;31:1451-9.
11. Barbosa PN, Bitencourt AG, Tyng CJ, Cunha R, Travesso DJ, Almeida MF, et al. Journal club: preparative fasting for contrast-enhanced CT in a cancer center: a new approach. AJR Am J Roentgenol. 2018;210:941-7.
12. Tsushima Y, Seki Y, Nakajima T, Hirasawa H, Taketomi-Takahashi A, Tan S, et al. The effect of abolishing instructions to fast prior to contrast-enhanced CT on the incidence of acute adverse reactions. Insights Imaging. 2020;11:113.
13. European Society of Urogenital Radiology. Guidelines on Contrast Agents. 10th ed. Available from: https://adus-radiologie.ch/files/ESUR_Guidelines_10.0.pdf. Accessed 5 Jun 2023.
14. ACR Committee on Drugs and Contrast Media. American College of Radiology. ACR Manual on Contrast Media. 2023. Available from: https://www.acr.org/-/media/ACR/Files/Clinical-Resources/Contrast_Media.pdf. Accessed 16 Apr 2021.
15. Oowaki K, Saigusa H, Ojiri H, Ariizumi M, Yamagisi J, Fukuda K, et al. Relationship between oral food intake and nausea caused by intravenous injection of iodinated contrast material [in Japanese]. Nihon Igaku Hoshasen Gakkai Zasshi. 1994;54:476-9.
16. Ha JY, Choi YH, Cho YJ, Lee S, Lee SB, Choi G, et al. Incidence and risk factors of nausea and vomiting after exposure to low-osmolality iodinated contrast media in children: a focus on preparative fasting. Korean J Radiol. 2020;21:1178-86.

Hong Kong J Radiol. 2023;26:133-7. Epub 10 May 2023 | https://doi.org/10.12809/hkjr2317634

CASE REPORT

An Occult Androgen-Secreting Ovarian Tumour Revealed by NP-59 Scintigraphy: A Case Report

SH Kwok, WT Ngai

Department of Nuclear Medicine, Pamela Youde Nethersole Eastern Hospital, Hong Kong SAR, China

INTRODUCTION

Androgen-secreting tumours constitute a rare but important cause of hyperandrogenism, the possibility of which needs to be considered and excluded in patients with postmenopausal, severe, or rapidly progressive hyperandrogenism. Conventional anatomical imaging may help localise the source of androgen hypersecretion but is occasionally inconclusive. We describe a postmenopausal Chinese female with severe hyperandrogenism whose initial investigations were unrevealing. Iodine-131 6-beta-iodomethyl-19-norcholesterol (NP-59) scintigraphy successfully localised an occult, small androgen-secreting ovarian steroid cell tumour that was resected with subsequent resolution of hyperandrogenism.

CASE REPORT

A 49-year-old Chinese female presented with a 2-year history of hirsutism. She had early menopause at the age of 41 years but medical history was otherwise unremarkable. Clinical examination revealed hirsutism, male-pattern alopecia and facial acnes, while breasts and external genitalia were normal. She was also found to be hypertensive with blood pressure measuring around 170/110 mmHg. Hormonal profile revealed markedly elevated testosterone level of up to 33.9 nmol/L, more than 13 times the upper limit of normal level (<2.6 nmol/L). The rest of the hormonal profile and tumour marker panel were unremarkable. Imaging investigations to localise any androgen-secreting tumour were performed.

Transvaginal ultrasonography visualised a uterus of 6-week size, but the ovaries were not clearly seen. Contrast-enhanced computed tomography of the abdomen and pelvis did not reveal any adrenal or adnexal lesions, but several enhancing uterine nodules up to 1.6 cm, thought to be fibroids, were seen. Further ^{18}F-fluorodeoxyglucose positron emission tomography was also negative.

A dexamethasone-suppressed NP-59 scintigraphy was subsequently performed with intravenous administration of 37 MBq of NP-59. To suppress physiological adrenal uptake, oral dexamethasone 1 mg was prescribed 4 times daily for 13 days, starting 7 days before NP-59 injection.

Correspondence: *Dr SH Kwok, Department of Nuclear Medicine, Pamela Youde Nethersole Eastern Hospital, Hong Kong SAR, China*
Email: ksh727@ha.org.hk

Submitted: 4 Sep 2022; Accepted: 15 Nov 2022.

Contributors: Both authors designed the study. SHK acquired the data. Both authors analysed the data. SHK drafted the manuscript. WTN critically revised the manuscript for important intellectual content. Both authors had full access to the data, contributed to the study, approved the final version for publication, and take responsibility for its accuracy and integrity.

Conflicts of Interest: Both authors have disclosed no conflicts of interest.

Funding/Support: This study received no specific grant from any funding agency in the public, commercial, or not-for-profit sectors.

Data Availability: All data generated or analysed during the present study are available from the corresponding author on reasonable request.

Ethics Approval: Ethics approval has been obtained from the Hong Kong East Cluster Research Ethics Committee of Hospital Authority, Hong Kong (Ref No.: HKECREC-2022-038). Patient consent was waived by the Committee.

Planar scintigraphic images of the abdomen and pelvis were acquired from day 3 to 7 post-injection. Additional single-photon emission computed tomography–computed tomography (SPECT-CT) images were acquired on days 4 and 7. A positive finding was indicated by early visualisation of focal NP-59 uptake before day 5. Planar scintigraphic images from day 3 showed suspicious focal pelvic NP-59 uptake which persisted until day 7 (Figure 1), and a right adnexal lesion with NP-59 uptake was confirmed on SPECT-CT (Figure 2).

The patient underwent bilateral salpingo-oophorectomy. During the operation, the right ovary was found to be enlarged with a 2-cm unilocular cyst containing chocolate material. Histological findings of the right ovary were consistent with the presence of a small steroid cell tumour with no malignant features. Following removal of the tumour, her serum testosterone level normalised with resolution of virilising features. She also became normotensive.

DISCUSSION

Hyperandrogenism may manifest clinically as hirsutism and virilisation. Hirsutism is defined as excessive terminal hair that appears in a male pattern in women such as on the chin, upper lip or abdomen. Virilisation includes clinical features of more significant androgen excess such as clitoromegaly, deepening of the voice or increasing muscularity.[1] Causes of hyperandrogenism can be non-tumourous, such as polycystic ovarian syndrome, congenital adrenal hyperplasia, ovarian hyperthecosis, obesity, endocrinopathies, or iatrogenic; such causes can also be tumourous, such as adrenal or ovarian tumours.[2] Androgen-secreting tumours constitute a rare (5.8%) cause of hyperandrogenism although they are relatively more prevalent in postmenopausal (21.4%) than premenopausal women (2.0%).[3]

A clinical diagnostic algorithm for investigation of hyperandrogenism commonly includes adrenal and/or ovarian imaging to exclude an androgen-secreting tumour, especially in case of onset after menopause, severe clinical and/or biochemical hyperandrogenism, rapid progression, or presence of virilisation. In particular, very high serum testosterone (>150-200 ng/dL) and dehydroepiandrosterone sulphate (>6000 ng/mL) levels favour an androgen-secreting tumour of ovarian or adrenal origin, respectively.[2]

Ultrasonography and/or magnetic resonance imaging (MRI) are recommended imaging modalities to identify ovarian tumours.[2] Nonetheless androgen-secreting ovarian tumours may be difficult to detect if they are small in size. A recent study reported that ultrasonography and MRI failed to detect four of 31 androgen-secreting ovarian tumours (12.9%), ranging from 0.7 to 1.5 cm.[4] Although CT and MRI are recommended for detection of adrenal tumours,[2] incidental adrenal masses are common and may occur in 3% to 7% of adults, most of which are benign non-functioning adenoma.[5] Combined ovarian and adrenal vein sampling may be considered if ultrasonography, CT and MRI have failed to localise the androgen-secreting tumours, although its application has not been proven to reliably alter management. The success rate for catheterisation of all four veins, i.e., bilateral adrenal and ovarian veins, has been reported to be only 27%; hence, this technically difficult procedure may be considered only in centres with expertise.[6] Successful identification of androgen-secreting tumours with ^{18}F-fluorodeoxyglucose positron emission tomography has been reported in only a few isolated cases.[7]

The application of NP-59 in functional imaging commenced in the mid-1970s.[8] Steroid hormone synthesis initiates with arrival of cholesterol in adrenocortical cells by low-density lipoprotein. Twenty percent of NP-59 is incorporated in low-density lipoprotein and deposited in adrenocortical cells by a specific receptor, which does not follow the metabolic process and thus concentrates in the adrenocortical cells. This allows scintigraphic localisation of the hypersecreting adrenal and ovarian tumours in primary hyperaldosteronism, Cushing's syndrome, and hyperandrogenism. Previous case studies demonstrated the usefulness of NP-59 scintigraphy in localising both tumourous and non-tumourous ovarian and adrenal sources of androgen excess.[9-11] Among the reported cases, unilateral uptake was seen in androgen-secreting ovarian and adrenal tumours, and bilateral ovarian or adrenal uptake was seen in ovarian hyperthecosis and congenital adrenal hyperplasia. Normal scintigraphy was seen in peripheral conversion and increased end-organ sensitivity, while absent uptake (i.e., loss of normal physiological uptake) was seen in adrenocortical carcinoma. The unique role of NP-59 scintigraphy in localising the site of androgen hypersecretion was highlighted in two of the reported cases of adrenal hyperandrogenism, where the incidental abnormalities show absence of uptake. One patient had an adrenal lipoid cell tumour detected on CT. The other had congenital adrenal hyperplasia with adrenal glands

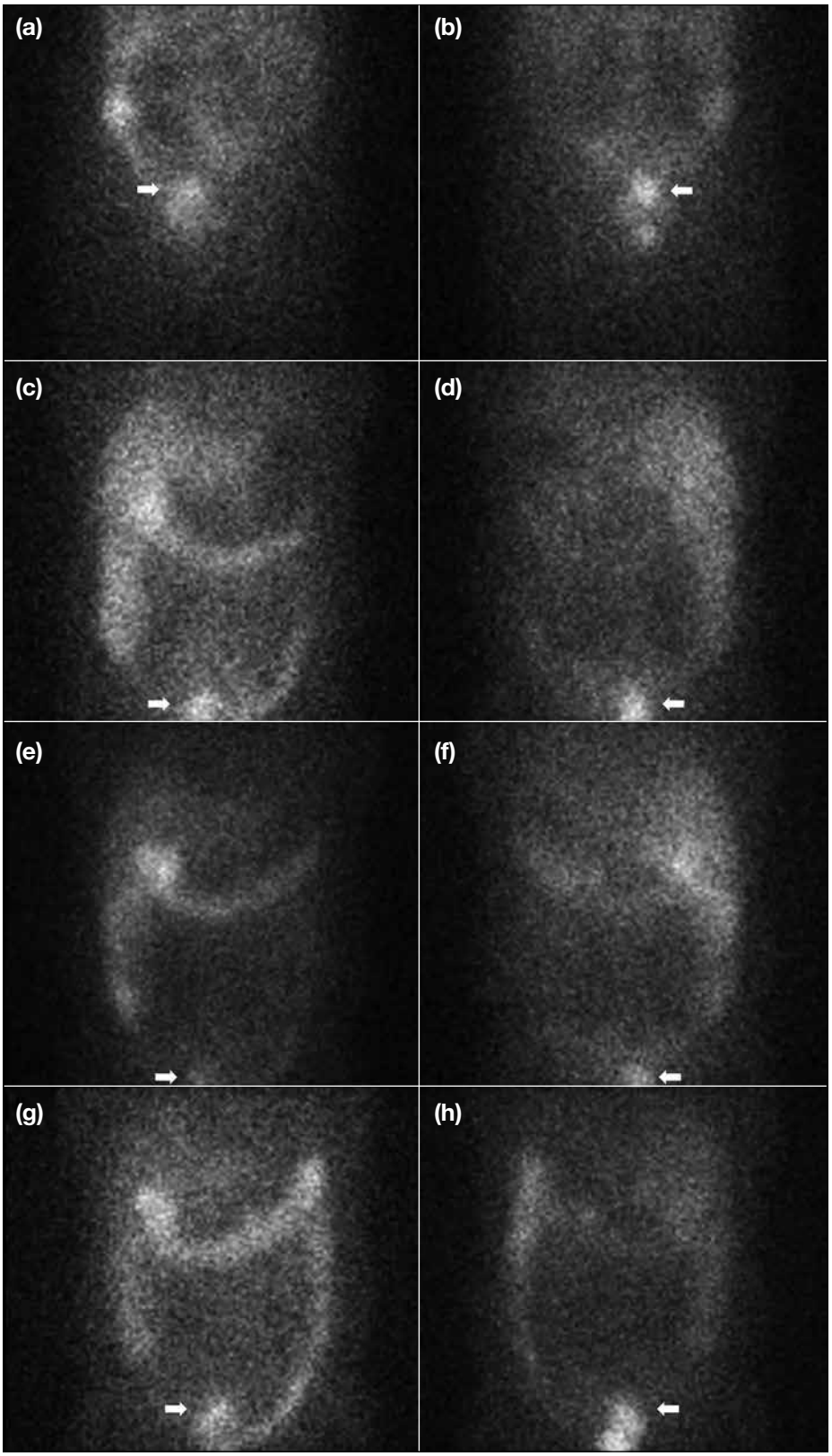

Figure 1. Iodine-131 6-beta-iodomethyl-19-norcholesterol (NP-59) scintigraphy with (a and b) day 3, (c and d) day 4, (e and f) day 5, and (g and h) day 7 anterior and posterior planar images of abdomen and pelvis. There was suboptimal coverage of the pelvis on day 5 images owing to initial assumption of pelvic activity (arrows) as physiological bowel activity. Day 3, 4 and 7 images raised the suspicion of possible abnormal focal increase in right adnexal NP-59 uptake (arrows), requiring additional single-photon emission computed tomography–computed tomography images for confirmation.

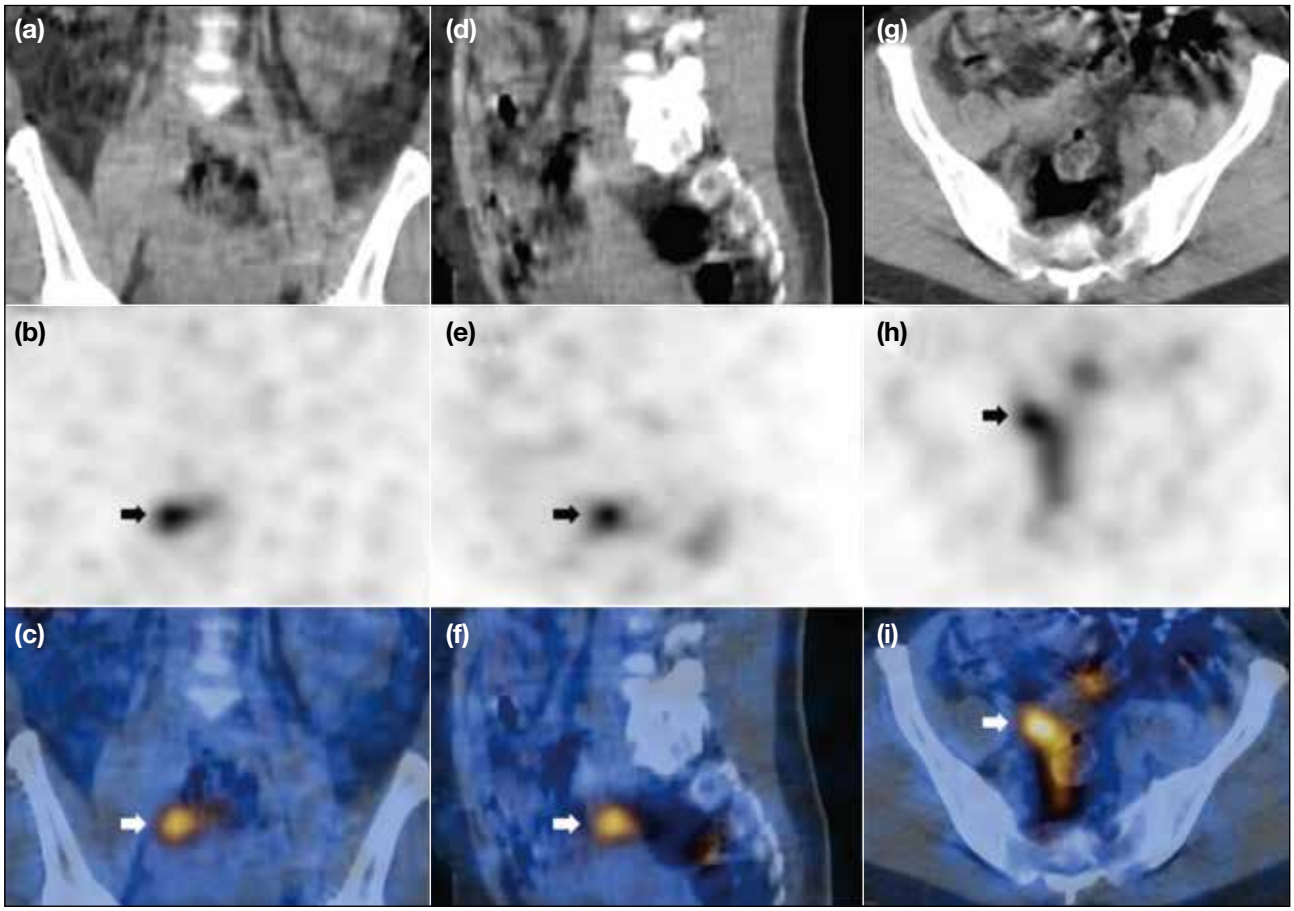

Figure 2. Iodine-131 6-beta-iodomethyl-19-norcholesterol (NP-59) scintigraphy with day 4 (a-c) coronal computed tomography (CT), single-photon emission computed tomography (SPECT) and fused SPECT-CT images, (d-f) sagittal CT, SPECT and fused SPECT-CT images, and (g-i) axial CT, SPECT and fused SPECT-CT images of pelvis. SPECT and fused images show an abnormal focal increase in NP-59 uptake at the right adnexal region (arrows) that could be distinguished from adjacent physiological large bowel activity.

appearing normal on CT. Both had incidental findings of ovarian masses, subsequently confirmed to be polycystic ovaries that were not contributory to the degree of hyperandrogenism. No false-positive NP-59 scintigraphic findings for hyperandrogenism have been reported in the English literature to date. Due to the rarity of this clinical condition, data on the diagnostic accuracy of NP-59 scintigraphy in hyperandrogenism are scarce.

As presence of intense physiological activity along the large bowel and its close proximity to androgen-secreting ovarian tumours hampers evaluation by NP-59 scintigraphy, preprocedural oral laxatives for bowel preparation have been recommended.[12] The availability of hybrid SPECT-CT technology, in addition to planar imaging, allows accurate delineation of any focal abnormal adnexal uptake from adjacent large bowel activity. The usefulness of SPECT-CT is well illustrated in this case where the focal abnormal adnexal uptake was difficult to appreciate on serial planar images but could be confirmed on SPECT-CT images.

There are several drawbacks to the widespread use of NP-59 scintigraphy in evaluation of hyperandrogenism. These include suboptimal image quality with iodine-131, relatively high radiation, prolonged imaging time, relatively high radiopharmaceutical cost, and potential adverse effects associated with use of high-dose dexamethasone as a pre-medication. Thus, NP-59 scintigraphy is often reserved for patients with clinical and biochemical evidence of ovarian or adrenal hypersecretion where conventional anatomical imaging has been unrevealing. A ^{18}F version of NP-59 is being developed for positron emission tomography imaging with promising initial data in imaging cholesterol trafficking and, specifically, uptake in adrenocortical

tissue.[13] It is expected that this ^{18}F version of NP-59 will become available for clinical use in the near future and provide higher image quality with lower radiation dose to help localise the site of hormone hypersecretion.

CONCLUSION

Accurate localisation of the source of androgen hypersecretion is critical to appropriate management in patients with suspected androgen-secreting tumours. This case report highlights the unique role of NP-59 scintigraphy in providing functional information and localising the site of androgen hypersecretion, which may not have been achievable by other non-invasive investigations. It is an indispensable and time-honoured nuclear medicine procedure that produces the most significant and conclusive results in such situations. Nevertheless the limitations of NP-59 scintigraphy limit its use to problem-solving rather than screening purposes. It is especially helpful in selected patients where there is a high suspicion of ovarian or adrenal hypersecretion but inconclusive conventional anatomical imaging.

REFERENCES

1. Martin KA, Anderson RR, Chang RJ, Ehrmann DA, Lobo RA, Murad MH, et al. Evaluation and treatment of hirsutism in premenopausal women: an Endocrine Society clinical practice guideline. J Clin Endocrinol Metab. 2018;103:1233-57.
2. Markopoulos MC, Kassi E, Alexandraki KI, Mastorakos G, Kaltsas G. Hyperandrogenism after menopause. Eur J Endocrinol. 2015;172:R79-91.
3. Elhassan YS, Idkowiak J, Smith K, Asia M, Gleeson H, Webster R, et al. Causes, patterns, and severity of androgen excess in 1205 consecutively recruited women. J Clin Endocrinol Metab. 2018;103:1214-23.
4. Zou M, Chen R, Wang Y, He Y, Wang Y, Dong Y, et al. Clinical and ultrasound characteristics of virilizing ovarian tumors in pre- and postmenopausal patients: a single tertiary center experience. Orphanet J Rare Dis. 2021;16:426.
5. Mayo-Smith WW, Song JH, Boland GL, Francis IR, Israel GM, Mazzaglia PJ, et al. Management of incidental adrenal masses: a white paper of the ACR Incidental Findings Committee. J Am Coll Radiol. 2017;14:1038-44.
6. Zaman A, Rothman MS. Postmenopausal hyperandrogenism: evaluation and treatment strategies. Endocrinol Metab Clin North Am. 2021;50:97-111.
7. Wong FC, Chan AZ, Wong WS, Kwan AH, Law TS, Chung JP, et al. Hyperandrogenism, elevated 17-hydroxyprogesterone and its urinary metabolites in a young woman with ovarian steroid cell tumor, not otherwise specified: case report and review of the literature. Case Rep Endocrinol. 2019;2019:9237459.
8. Prado-Wohlwend S; Grupo de Trabajo de Endocrinología de la SEMNIM. Functional imaging studies of the adrenal cortex. Rev Esp Med Nucl Imagen Mol (Engl Ed). 2020;39:393-404.
9. Taylor L, Ayers JW, Gross MD, Peterson EP, Menon KM. Diagnostic considerations in virilization: iodomethyl-norcholesterol scanning in the localization of androgen secreting tumors. Fertil Steril. 1986;46:1005-10.
10. Mountz JM, Gross MD, Shapiro B, Barkan AL, Woodbury MC, Schteingart DE, et al. Scintigraphic localization of ovarian dysfunction. J Nucl Med. 1988;29:1644-50.
11. Kazerooni EA, Sisson JC, Shapiro B, Gross MD, Driedger A, Hurwitz GA, et al. Diagnostic accuracy and pitfalls of [iodine-131]6-beta-iodomethyl-19-norcholesterol (NP-59) imaging. J Nucl Med. 1990;31:526-34.
12. Shapiro B, Nakajo M, Gross MD, Freitas JE, Copp J, Beierwaltes WH. Value of bowel preparation in adrenocortical scintigraphy with NP-59. J Nucl Med. 1983;24:732-4.
13. Brooks AF, Winton WP, Stauff J, Arteaga J, Henderson B, Niedbala J, et al. Development of fluorinated NP-59: a revival of cholesterol use imaging with PET. J Nucl Med. 2022;63:1949-55.

Hong Kong J Radiol. 2023;26:138-41. Epub 15 May 2023 | https://doi.org/10.12809/hkjr2317487

CASE REPORT

Successful Endovascular Management of Iatrogenic Aortic Coarctation Following Total Aortic Arch Repair in Type B Dissection: A Case Report

PP Ng[1], SCW Cheung[2], CKL Ho[3], KKY Man[2], KKH Choi[2]

[1]Department of Radiology and Imaging, Queen Elizabeth Hospital, Hong Kong SAR, China
[2]Department of Radiology, Queen Mary Hospital, Hong Kong SAR, China
[3]Department of Cardiothoracic Surgery, Queen Mary Hospital, Hong Kong SAR, China

INTRODUCTION

Frozen elephant trunk (FET) technique has been commonly used in the management of a wide variety of thoracic aortic pathology. Postoperative kinking of an FET stent graft resulting in clinically significant aortic coarctation is rare. We report a challenging case of a patient with chronic type B aortic dissection who underwent FET repair that was complicated by clinically significant FET graft kinking but successfully treated with endovascular stenting.

CASE REPORT

A 47-year-old man with a history of chronic type B aortic dissection had a dissection flap starting just distal to the origin of the aberrant right subclavian artery (SCA) and extending down to the aortic bifurcation. Sequential computed tomography angiography (CTA) showed progressive dilatation of an aortic arch dissecting aneurysm (5.8 cm) and narrowing of the true lumen. In May 2021, he underwent ascending and total aortic arch replacement with FET graft (Thoraflex Hybrid; Terumo Aortic, Renfrewshire, United Kingdom), aorto-right axillary artery bypass and embolisation of the aberrant right SCA with Amplatzer vascular plug (Abbott Medical, Plymouth [MN], US).

Following the surgery, he developed persistent hypertension despite multiple antihypertensive medications and progressive respiratory distress. There was significant upper and lower limb blood pressure (BP) discrepancy up to 40 mmHg. Echocardiogram demonstrated preserved left ventricular ejection fraction (60%). CTA on postoperative day 5 revealed kinking of the FET stent graft at the distal aortic arch with marked luminal stenosis (Figure 1a and b). Another finding was an endoleak from the aberrant right SCA, later managed by surgical ligation of the right SCA origin. Aortic angiogram confirmed high-grade stenosis of the FET graft at the distal aortic arch (Figure 1c). Intra-arterial BP measurement revealed a 53-mmHg pressure gradient across the stenosis.

Endovascular stenting of the iatrogenic aortic coarctation was performed with a bare-metal stent (BMS)

Correspondence: *Dr PP Ng, Department of Radiology and Imaging, Queen Elizabeth Hospital, Hong Kong SAR, China*
Email: npp782@ha.org.hk

Submitted: 6 Oct 2021; Accepted: 26 Jan 2022.

Contributors: All authors designed the study. PPN and KKHC acquired the data. All authors analysed the data. PPN, SCWC, CKLH and KKHC drafted the manuscript. All authors critically revised the manuscript for important intellectual content. All authors had full access to the data, contributed to the study, approved the final version for publication, and take responsibility for its accuracy and integrity.

Conflicts of Interest: The authors have no conflicts of interest to declare.

Funding/Support: This study received no specific grant from any funding agency in the public, commercial, or not-for-profit sectors.

Data Availability: All data generated or analysed during the present study are available from the corresponding author on reasonable request.

Ethics Approval: The patients were treated in accordance with the Declaration of Helsinki and provided written informed consent for all treatments and procedures and consent for publication.

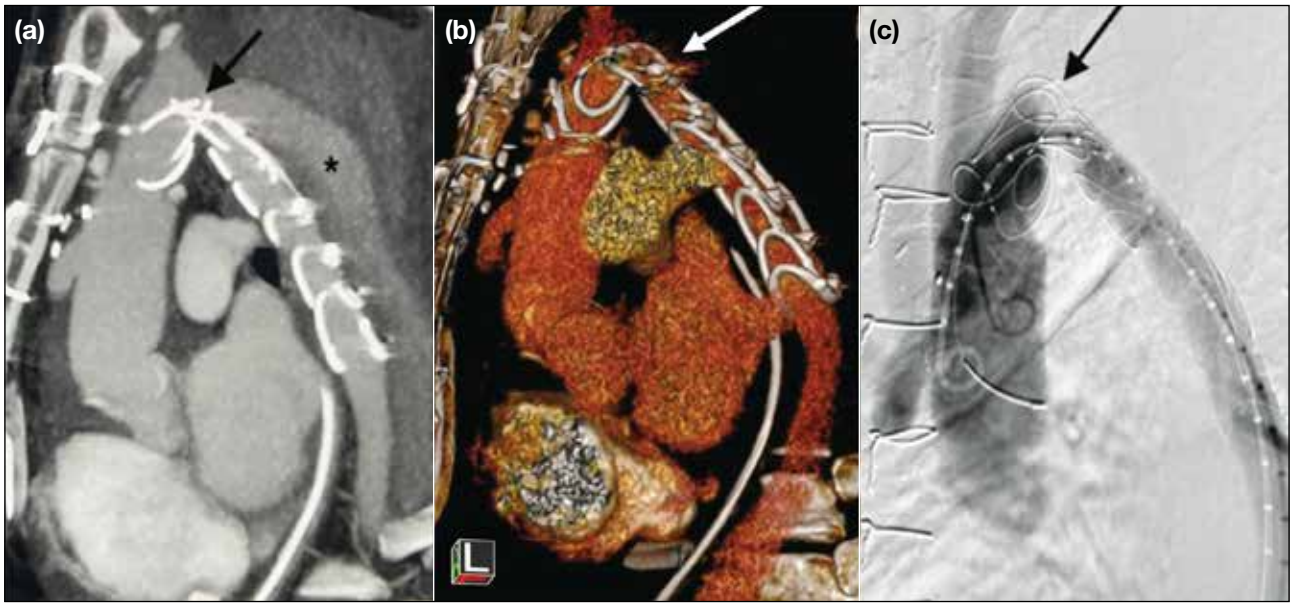

Figure 1. (a) Double oblique sagittal view of contrast-enhanced computed tomography angiography maximal intensity projection image and (b) three-dimensional reconstruction showing ascending and total aortic arch replacement with frozen elephant trunk (FET). There was kinking and severe stenosis at the distal aortic arch (arrows in [a] and [b]), as well as presence of endoleak in false lumen along the aortic arch and descending thoracic aorta (asterisk in [a]). (c) Digital subtraction angiogram in left anterior oblique view showing kinking of FET trunk with high-grade stenosis at the distal aortic arch.

[Sinus-XL 34 × 100 mm; OptiMed, Ettlingen, Germany] under local anaesthesia. Due to the acute angulation at the aortic arch and tight stenosis, an attempt to deploy across the stenosis within the FET was particularly challenging. Difficulties were encountered during passage of the delivery system across the stenosis as well as retraction of the outer sheath for stent deployment. To overcome these difficulties, balloon dilatation of the stenosis was first performed. This was followed by partial deployment of two-thirds of the stent within a 12-F sheath (Cook Medical, Bloomington [IN], US) with the sheath tip rested at the non-kinked portion of the FET. The entire complex was then advanced proximally to the desirable zone. The partially opened stent was deployed across the stenosis by unsheathing the 12-F sheath with constant forward pressure on the delivery system to avoid distal migration. Post-stenting dilatation with a 32-mm Coda balloon catheter (Cook Medical, Bloomington [IN], US) achieved satisfactory luminal expansion (Figure 2). Post-stenting BP gradient improved to 20 mmHg.

On day 3 post-stenting, the patient developed haemolytic anaemia and syncope. Urgent CTA revealed no source of bleeding. The BMS across the coarctation was partially collapsed but there was interval luminal gain when compared with preprocedural CTA (Figure 3). The haemolytic anaemia was suspected to be stent-related; a repeat aortic angiogram was performed on postoperative day 14 and demonstrated a small residual pressure gradient (8 mmHg) across the kinking. Since the stent remained partially collapsed, repeat balloon angioplasty was performed with 32-mm Coda balloon (Cook Medical, Bloomington [IN], US) and 26-mm Atlas balloon (Bard Medical, New Providence [NJ], US). Despite the lack of significant stent expansion on fluoroscopy, the pressure gradient disappeared by the end of procedure. The patient made an uneventful recovery and was subsequently discharged.

Follow-up CTA performed 1 month post-stenting revealed no interval collapse of the stent or luminal re-stenosis. The patient was asymptomatic with no upper and lower limb BP discrepancy or haemoglobin drop.

DISCUSSION

Although the FET technique is now widely used to manage thoracic aortic dissection, postoperative kinking of the stent graft that necessitates secondary intervention has rarely been reported in the literature. FET kinking often occurs at the junction of the distal aortic arch and descending aorta.[1] Risk factors for graft kinking include acute aortic arch angulation, marked true

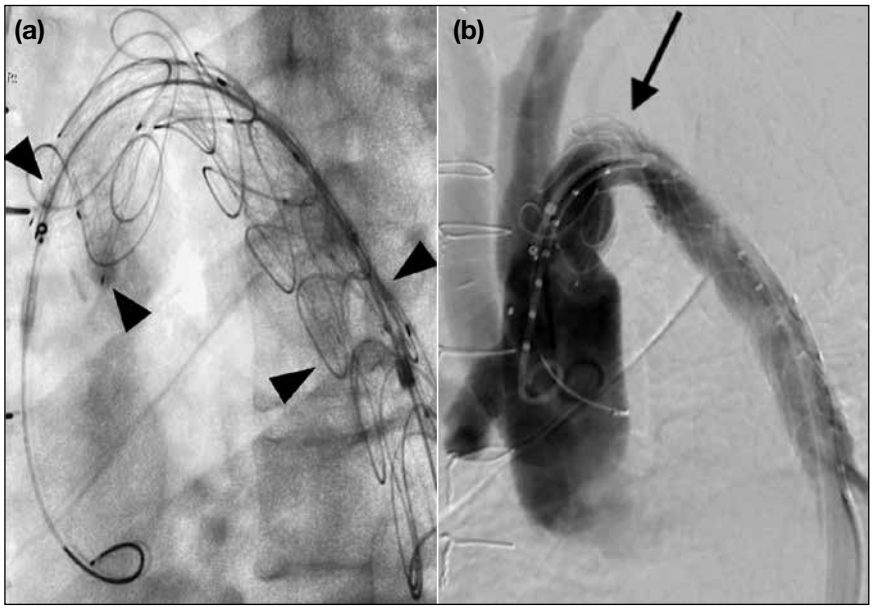

Figure 2. (a) Post-stenting and balloon angioplasty radiograph showing successful bare-metal stent deployment (arrowheads) within the frozen elephant trunk. Note the struts of the bare-metal stent are more densely packed than that of the stent graft. (b) Post-stenting and balloon angioplasty digital subtraction angiogram showing satisfactory luminal expansion (arrow).

Figure 3. Double oblique sagittal contrast-enhanced computed tomography angiography image showing partial collapse of the bare-metal stent (white arrow) within the frozen elephant trunk (black arrow) at the site of kinking. Note the interval expansion of aortic lumen.

lumen narrowing, a rigid chronic dissection membrane, reperfusion of false lumen, use of a low radial force device or presence of a non-stent part in the FET graft.[2-4] Although rare, kinking can result in coarctation, graft thrombosis, haemolytic anaemia, and heart failure.

Secondary surgery to rectify the kinked graft can be complex and necessitate cardiopulmonary bypass. Endovascular repair offers a minimally invasive option that can be performed under local anaesthesia. Realigning a stent within the kinked graft may provide adequate scaffolding to maintain graft patency. Complications include stent fracture, migration, and collapse.

Graft kinking in this patient was both clinically and radiologically significant, as evidenced by the presence of heart failure, haemolytic anaemia, marked luminal narrowing on imaging, and significant pressure gradient. Possible contributing factors in this case included acute aortic arch angulation, rigid chronic dissection flap, and stenotic true lumen. As angioplasty alone would not have provided adequate scaffolding, alignment of the FET with stent was chosen.

An ideal stent in this scenario would have high radial force without compromised flexibility. Stent grafts are often preferred since they are available in a wide range of sizes, up to 46 mm in diameter, and with tapering property; they also provide additional safety in case of

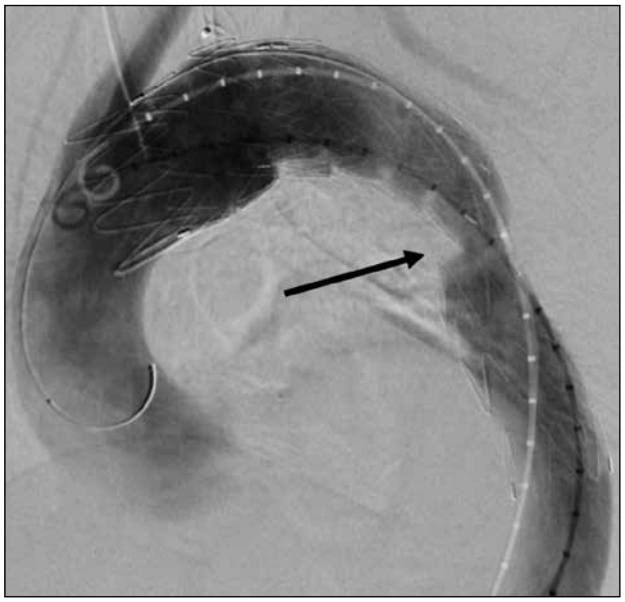

Figure 4. Digital subtraction angiogram from a different patient with post–thoracic endovascular aortic repair stent graft–induced new entry (SINE) tear at the distal end of the stent, resulting in significant true lumen narrowing and need for subsequent distal stent graft extension. Post–stent graft extension showed persistent narrowing (arrow) at the site of SINE due to insufficient mechanical support from the fabric between the nitinol rings.

inadvertent aortic rupture during the procedure. In our experience, better support can be achieved by positioning the stent struts at the most stenotic point to maximise mechanical support (Figure 4). This is more achievable with BMS because their stent struts are more densely packed compared with stent grafts where the nitinol rings are typically separated by 10 to 15 mm of fabric.

Sinus-XL is a self-expanding uncovered nitinol stent with a closed-cell design that has been proven to be safe and durable in treating adult aortic coarctation.[5] Despite its low profile and the ability to deliver up to 36 mm stent within a 10-F introducer, we experienced difficulties in traversing the kink and stent deployment because the acute angle prevented outer-sheath retraction by the coaxial pull-back system. This would have been even more challenging if a similarly sized stent graft had been chosen since it would have required 20-F access.

Most stent manufacturers discourage operators from deploying stents across an acute angle due to potential entrapment of the delivery system. Nonetheless stent deployment can be facilitated by methods that straighten the target coverage, as in our patient. Other methods include use of buddy wires or the body flossing technique. These techniques were less appropriate for our patient given the recent surgical anastomosis; overcorrecting the existing anatomy might have increased the risk of anastomosis-related complications. Moreover, degree of stent apposition does not necessarily correlate with the pressure gradient across the kinking, as illustrated in this case. Thus, in cases of tight stenosis, aggressive balloon dilatation to pursue a 'perfectly' expanded stent may not be necessary and should be avoided.

In conclusion, FET stent graft kinking is rarely encountered but can result in significant haemodynamic consequences. Endovascular stenting is a safe and effective alternative to surgery. In our patient, we illustrate the advantages of a BMS over a stent graft in offering more focal support to the kinked portion in a low-profile setting. Stenting across the severely kinked graft can be technically challenging and require additional manoeuvres, as demonstrated by our case.

To date, no study has compared BMS with covered stents for treatment of aortic coarctation; head-to-head bench comparison with reference to radial forces is also lacking. Although we believe that endovascular repair can be considered for patients with FET graft kinking to avoid a second major operation, the decision to use a BMS or covered stent should be tailored to the individual and take account of the underlying pathology and anatomy.

REFERENCES

1. Roselli EE, Bakaeen FG, Johnston DR, Soltesz EG, Tong MZ. Role of the frozen elephant trunk procedure for chronic aortic dissection. Eur J Cardiothorac Surg. 2017;51(suppl 1):i35-9.
2. Shrestha M, Bachet J, Bavaria J, Carrel TP, De Paulis R, Di Bartolomeo R, et al. Current status and recommendations for use of the frozen elephant trunk technique: a position paper by the Vascular Domain of EACTS. Eur J Cardiothorac Surg. 2015;47:759-69.
3. Morisaki A, Isomura T, Fukada Y, Yoshida M. Kinking of an open stent graft after total arch replacement with the frozen elephant technique for acute type A aortic dissection. Interact Cardiovasc Thorac Surg. 2018;26:875-7.
4. Ouzounian M, Hage A, Chung J, Stevens LM, El-Hamamsy I, Chauvette V, et al. Hybrid arch frozen elephant trunk repair: evidence from the Canadian Thoracic Aortic Collaborative. Ann Cardiothorac Surg. 2020;9:189-96.
5. Kische S, D'Ancona G, Stoeckicht Y, Ortak J, Elsässer A, Ince H. Percutaneous treatment of adult isthmic aortic coarctation: acute and long-term clinical and imaging outcome with a self-expandable uncovered nitinol stent. Circ Cardiovasc Interv. 2015;8:e001799.

Hong Kong J Radiol. 2023;26:142-52. Epub 31 May 2023 | https://doi.org/10.12809/hkjr2317507

PICTORIAL ESSAY

Multidisciplinary Management of Ovarian, Fallopian Tube and Peritoneal Cancers with Emphasis on the Role of Cross-Sectional Imaging

OL Chan[1], SC Young[2], WWL Yip[3], WH Chong[1], KY Kwok[1]

[1]Department of Radiology, Tuen Mun Hospital, Hong Kong SAR, China
[2]Department of Obstetrics and Gynaecology, Tuen Mun Hospital, Hong Kong SAR, China
[3]Department of Clinical Oncology, Tuen Mun Hospital, Hong Kong SAR, China

INTRODUCTION

Ovarian cancer is the eighth most common cancer among women worldwide and the second most common gynaecological cancer mortality after cervical cancer.[1] In Hong Kong, ovarian cancer ranks as the sixth most common cancer in female and the most common cause of gynaecological cancer mortality in 2020.[2] Approximately two-thirds of patients with ovarian cancer are reported to present with stage III-IV disease.[3,4] High-grade serous carcinoma accounts for about 70% of malignant ovarian tumours.[5]

There is recent evidence that ovarian or peritoneal cancer may have a common origin from the fimbrial end of the fallopian tubes. The ovarian cancer staging system was updated in 2014 to include cancer of the fallopian tubes and peritoneum.[3]

One of the most important prognostic factors in ovarian cancer is the volume of residual disease after surgery. Cytoreductive surgery is the mainstay of treatment and is considered optimal if there is no or ≤1 cm of gross residual tumour and suboptimal if the residual tumour is >1 cm.[6,7]

In patients who present with advanced-stage disease, preoperative imaging to assess the abdominopelvic disease burden can help identify those at risk of having >1 cm gross residual disease and help avoid futile laparotomy. These patients may be first treated with neoadjuvant chemotherapy followed by reassessment imaging and interval debulking surgery if optimal tumour debulking is deemed possible.[3]

At our institution, management of patients with ovarian, fallopian tube and peritoneal cancers is discussed by a multidisciplinary team consisting of gynaecologists, radiologists, and oncologists. A multidisciplinary approach to cancer management has been shown to improve a patient's quality of life and prognosis.[8,9]

Correspondence: *Dr OL Chan, Department of Radiology, Tuen Mun Hospital, Hong Kong SAR, China*
Email: col950@ha.org.hk

Submitted: 23 Nov 2021; Accepted: 7 Apr 2022.

Contributors: All authors designed the study. OLC acquired and analysed the data, and drafted the manuscript. SCY, WWLY, WHC and KYK critically revised the manuscript for important intellectual content. All authors had full access to the data, contributed to the study, approved the final version for publication, and take responsibility for its accuracy and integrity.

Conflicts of Interest: All authors have disclosed no conflicts of interest.

Funding/Support: This study received no specific grant from any funding agency in the public, commercial, or not-for-profit sectors.

Data Availability: All data generated or analysed during the present study are available from the corresponding author on reasonable request.

Ethics Approval: The study was approved by the New Territories West Cluster Research Ethics Committee of Hospital Authority, Hong Kong (Ref No.: NTWC/REC/21066). A waiver for written informed consent of patients was granted by the Committee as this manuscript is for pictorial review only and does not involve patient treatment/procedures.

This article describes the role of imaging in the management of patients with ovarian cancer. The anatomy of common sites of peritoneal lesions is reviewed and features that may preclude optimal debulking surgery are highlighted.

ROLE OF IMAGING

The role of imaging in the management of ovarian cancer is to delineate the disease extent so that primary treatment can be planned and indicate possible sites for image-guided core biopsy for histological confirmation when necessary.[4]

Previous studies compared the diagnostic accuracy of different imaging modalities for detection of peritoneal carcinomatosis in ovarian cancer. Computed tomography (CT), magnetic resonance imaging, and positron emission tomography/computed tomography (PET/CT) all demonstrated >90% accuracy when compared with diagnostic laparoscopy.[10] Magnetic resonance imaging has the advantage of providing better soft tissue differentiation but is less readily available and motion artefacts may affect image quality. PET/CT is useful for whole-body assessment but is likewise not readily available. CT remains the most commonly performed pretreatment imaging since it has high accuracy and accessibility.

Compared with diagnostic laparoscopy, CT has a high accuracy of >90% for detection of peritoneal deposits. It is also more accurate in detecting peritoneal disease in upper abdominal regions when compared with laparoscopy. Limitations of CT are nonetheless its reported decreased sensitivity of <80% in depicting implants <1 cm in size, and inferior accuracy compared with laparoscopy in detecting disease in pelvic and small intestinal mesenteric regions.[11]

At our institution, CT of the abdomen and pelvis is performed for pretreatment staging, with the lung bases included in the scan range. The latter enables a search for suspicious cardiophrenic lymph nodes and pleural effusion that will require further investigations such as pleural tapping to look for stage IV disease.[4] Looking for stage IV disease is essential because this group of patients may not be candidates for surgical debulking.

In patients with inoperable disease, interval debulking is considered after two to three cycles of systemic chemotherapy.[3] As well as monitoring cancer antigen 125 level, CT should be used to assess treatment response and the feasibility of interval debulking surgery. PET/CT is often supplementary when CT findings are inconclusive.[4] Arrangement of timely follow-up imaging and planning for interval debulking surgery following neoadjuvant chemotherapy can be facilitated by a multidisciplinary meeting.

PERITONEAL ANATOMY AND FLOW OF PERITONEAL FLUID

Knowledge of the anatomy of the peritoneum and flow of peritoneal fluid is important when assessing peritoneal spread of disease. The internal surfaces of the abdominopelvic cavity are lined with parietal peritoneum. The visceral peritoneum lines the organs that are intraperitoneal. The potential space between these two layers of peritoneum is the peritoneal cavity and generally contains a small amount of fluid to allow frictionless movement of visceral organs within the abdominal cavity. Ascites is often detected in a disease state and may be due to increased capillary permeability or obstructed lymphatics resulting in overall increased peritoneal fluid.[12]

There are multiple peritoneal folds and reflections that compartmentalise the abdominopelvic cavity. The transverse mesocolon divides the peritoneal cavity into the supracolic and infracolic spaces. The supracolic space is separated by the falciform ligament into the left and right. The right supracolic space contains the right subphrenic space, subhepatic space, and the lesser sac. The left supracolic space includes the perihepatic and left subphrenic space. The infracolic space is further divided by the small bowel mesentery into the larger left and smaller right spaces. The small bowel mesentery attaches from the ligament of Treitz at the left upper quadrant to the ileocaecal junction at the right iliac fossa.

Initially, peritoneal fluid collects at a gravity-dependent site, the pouch of Douglas in woman and the rectovesical space in men. It travels in a cephalad direction, entering the paracolic gutters and then the supracolic spaces. On the left side, fluid passage is superiorly limited by the phrenicocolic ligament, hence more peritoneal fluid flows into the right paracolic gutter (Figure 1). The flow of peritoneal fluid is slow or arrested at dependent regions due to gravity, and fluid stasis allows tumour cells to be deposited. The four dependent areas include the rectouterine pouch, right lower quadrant, sigmoid colon, and right paracolic gutters.

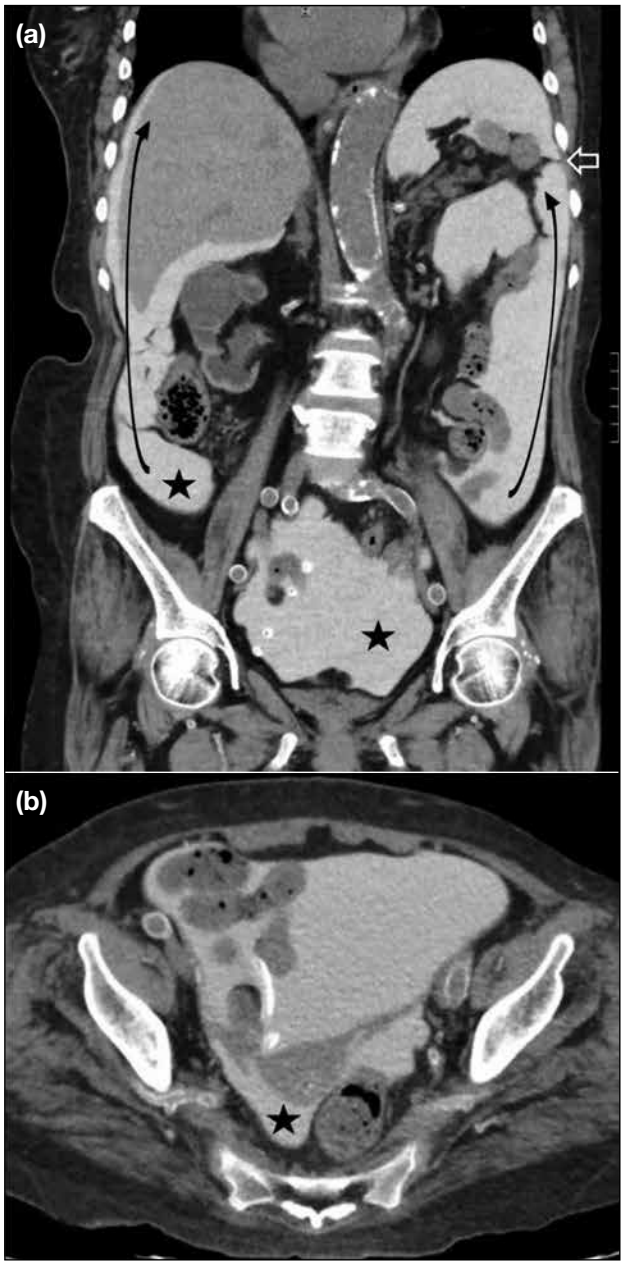

Figure 1. (a) Coronal and (b) axial images of computed tomography peritoneogram with intraperitoneal contrast to demonstrate peritoneal cavity anatomy. Peritoneal fluid initially collects at the pelvis, then travels cephalad due to pressure gradients produced by inspirations (curved arrows in [a]). Fluid passage on the left side is superiorly limited by the phrenicocolic ligament (open arrow in [a]). The rectouterine pouch, right lower quadrant, sigmoid colon, and right paracolic gutters (asterisks in [a] and [b]) are dependent regions in which there is stasis of peritoneal fluid.

ASSESSMENT OF ABDOMINOPELVIC DISEASE BURDEN

The most frequent routes for dissemination of ovarian cancer are by direct pelvic invasion and via transcoelomic peritoneal spread.[13] Less frequently, it may also spread along the lymphatics via the utero-ovarian, infundibulopelvic and round ligament pathways.[3] The most common lymphatic spread is along the utero-ovarian pathway to the para-aortic and paracaval nodes at the level of the kidney.[7] Haematogenous spread is rare and seldom present at initial diagnosis.

Primary Tumour

The size and location of the primary ovarian tumour should be described. Pelvic sidewall invasion is suspected when the distance between the tumour and the muscular pelvic sidewall is <3 mm, or when there is encasement of >90% of the circumference of iliac vessels.[13] Any invasion to the adjacent organs such as the urinary bladder or rectum should be noted since it may require additional surgical input from other subspecialties to achieve optimal debulking (Figure 2).

Peritoneal Carcinomatosis

Assessment of peritoneal carcinomatosis is crucial since it affects staging and subsequent management. The presence of ascites raises a suspicion of peritoneal involvement and loculated ascites usually indicates peritoneal metastasis. Signs of early peritoneal disease are subtle and can be easily missed. Multiplanar reformatted CT images are helpful in the assessment of peritoneal lesions. Coronal and sagittal reformatted

Figure 2. Contrast computed tomography demonstrating large heterogenous pelvic tumour blended with the uterus, with extension to the pouch of Douglas and the rectum. Optimal debulking of this tumour will likely require pelvic exenteration and requires input from a colorectal surgeon.

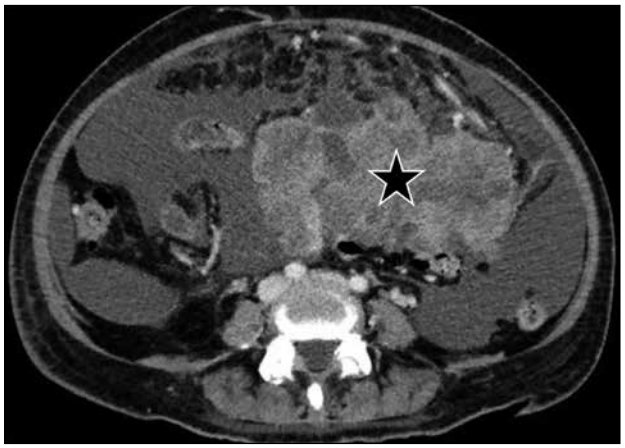

Figure 3. Contrast computed tomography image demonstrating large left ovarian tumour (asterisk), loculated ascites and omental stranding, suggestive of peritoneal metastases.

Figure 4. Contrast computed tomography images demonstrating right subphrenic deposits (arrows in [a] and [b]) that are best appreciated on coronal image. (b) Larger subphrenic deposits can cause scalloping of liver contour.

images improve detection of lesions on curved surfaces such as the diaphragm, paracolic gutters, and pelvis (Figure 3).[7]

The operability of peritoneal lesions is related to multiple factors such as the location of peritoneal deposits, their morphology and multiplicity, and their size and relationship with adjacent organs. Peritoneal carcinomatosis can present with a wide range of morphological appearance on CT. Subtle soft tissue infiltration, mild thickening or nodularity of the peritoneum may be the only findings in early peritoneal disease. Soft tissue peritoneal implants are usually observed in advanced peritoneal disease. These can present as solitary or multiple nodules, or coalesce to form plaque-like lesions and larger masses. They may show contrast enhancement; metastases from serous cystadenocarcinoma may be calcified.[12]

Upper Abdomen

The right subphrenic region is frequently involved since there is preferential flow of peritoneal fluid along the right side of the abdomen. Coronal and sagittal images enable better assessment of peritoneal deposits at the hemidiaphragm. Nodular- or plaque-like thickening may be observed. Larger deposits at the subphrenic region may cause scalloping of the liver or splenic contour. On post-contrast phase, these implants are hypoenhancing relative to the liver or splenic parenchyma (Figure 4).

In the upper abdomen, it is also essential to look for any involvement of the peritoneal ligaments, including the gastrohepatic and gastrosplenic ligaments (Figure 5). Increased soft tissue stranding, thickening or nodular deposits at these ligaments usually suggest involvement.

Any tumour deposits at the perihepatic spaces should be specified, including the fissure for falciform ligament, gallbladder fossa, porta hepatism, and lesser sac (Figure 6). Peritoneal lesions at these sites, particularly when >2 cm in size, are probably non-resectable.[14] Any subcapsular implants at the Morison's pouch extending to the inferior vena cava must be described because they pose a surgical challenge due to increased bleeding risk.[7]

Since haematogenous metastases are extremely rare at presentation, apparent parenchymal involvement of the liver and spleen are more commonly caused by invasive serosal surface implants rather than haematogenous metastases (Figure 7). Differentiation of a surface lesion versus parenchymal invasion lesion is particularly important for the liver because partial hepatectomy may

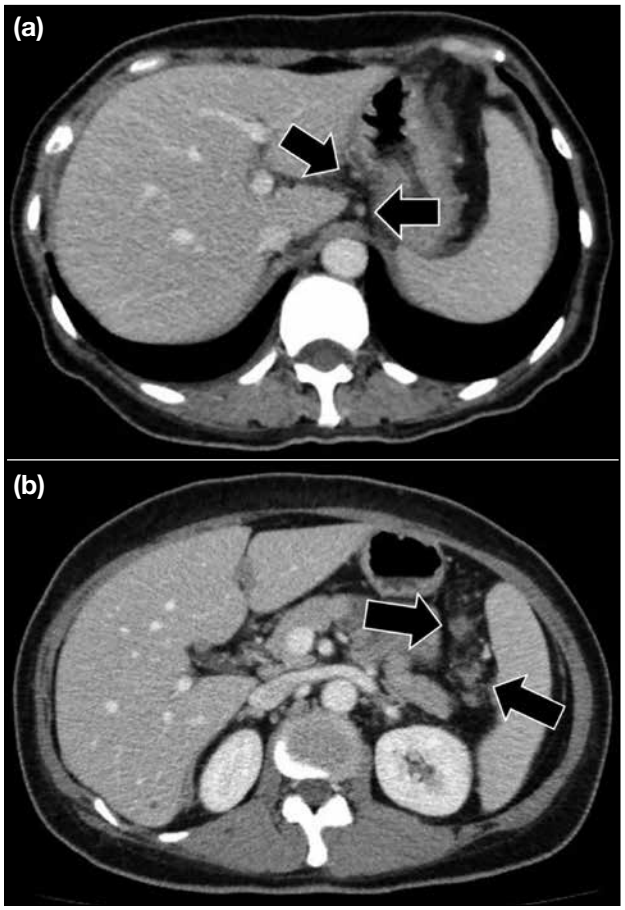

Figure 5. Contrast computed tomography images demonstrating peritoneal deposits at the upper abdominal ligaments, where (a) shows nodular deposits at the gastrohepatic ligament (arrows) and (b) shows nodular deposits at the gastrosplenic ligament (arrows).

be required in the latter with assistance of a hepatobiliary surgeon. Distinguishing between a surface lesion and invasive parenchymal lesion at the spleen is less important because splenectomy is more easily performed (Figure 8).[13]

Paracolic Gutters, Omentum, and Mesentery

The bilateral paracolic gutters are also common sites of peritoneal deposits because of peritoneal fluid stasis. It is helpful to assess with both axial and coronal images. Tumour deposits present as irregular thickening and nodularity (Figure 9).

Infiltration of the omental fat can present as increased soft tissue stranding and omental nodules of various sizes. When these small nodules coalesce, they give rise to larger omental plaques or mass-like lesions that are commonly referred to as omental cakes. Greater omental involvement usually does not preclude surgery since omentectomy is routinely performed in debulking surgery. Nonetheless extension of omental metastases to the anterior abdominal wall or umbilicus may preclude surgery (Figure 10).[4,12]

Infiltration of the mesentery can present as misty mesentery or clustered soft-tissue nodules (Figure 11). Peritoneal deposits at the mesentery can cause tethering of the bowel loops and intestinal obstruction. Intestinal obstruction is a common morbidity associated with metastatic ovarian cancer, reported to occur in about

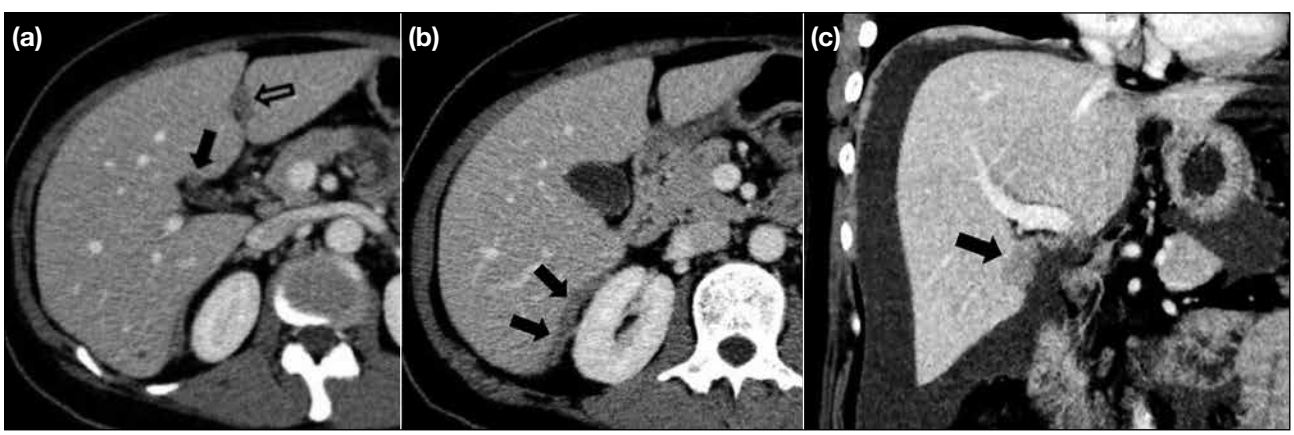

Figure 6. Contrast computed tomography images demonstrating peritoneal deposits at the perihepatic spaces, where (a) shows deposits at the falciform ligament (open arrow) and gallbladder fossa (block arrow), (b) shows deposits at the Morison's pouch (arrows), and (c) shows deposits at the hepatic hilum (arrow). It is important to identify these peritoneal deposits on pretreatment imaging since they are difficult to visualise on laparoscopy.

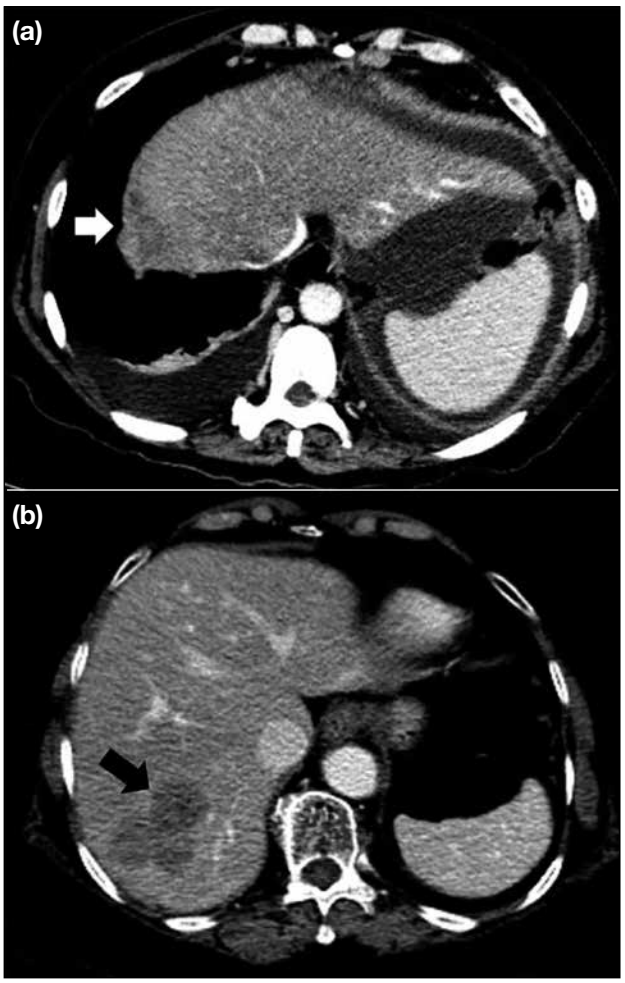

Figure 7. (a) A subphrenic deposit with hepatic parenchymal invasion (arrow) and (b) a haematogenous hepatic metastasis (arrow). Presence of these lesions might require assistance from a hepatobiliary surgeon for optimal bulking.

50% of cases.[12] Detection of segmental small bowel obstruction and extensive tumour deposits on the small bowel surface or at the mesenteric root is important because these features may preclude surgery.[14] Serosal implants at the bowel loops are difficult to detect, particularly in the absence of complications such as intestinal obstruction. Involvement of the small bowel may present as segmental mural thickening and soft-tissue mass involving the serosa and adjacent mesentery. Depending on the extent of involvement, these bowel serosal implants may be resected with the assistance of a gastrointestinal surgeon.

In the pelvis, common sites of deposits include the surface of the urinary bladder, sigmoid mesocolon, pelvic sidewall, pouch of Douglas, and surface of the sigmoid and rectum. Lesions at the bilateral uterosacral ligament and pelvic sidewall are better seen on axial and coronal images. Lesions at the peritoneal surface of the bladder, pouch of Douglas, and rectosigmoid regions are better observed on sagittal images. Again, these deposits can present as soft tissue thickening or a mass (Figure 12).

Lymphadenopathy

Lymphatic spread commonly involves the para-aortic lymph nodes. An enlarged node with >1 cm short axis suggests malignant lymphadenopathy.[13] Apart from increased nodal size, necrosis or clustering of lymph nodes are also suspicious features of metastatic involvement. Any enlarged lymph node at the suprarenal

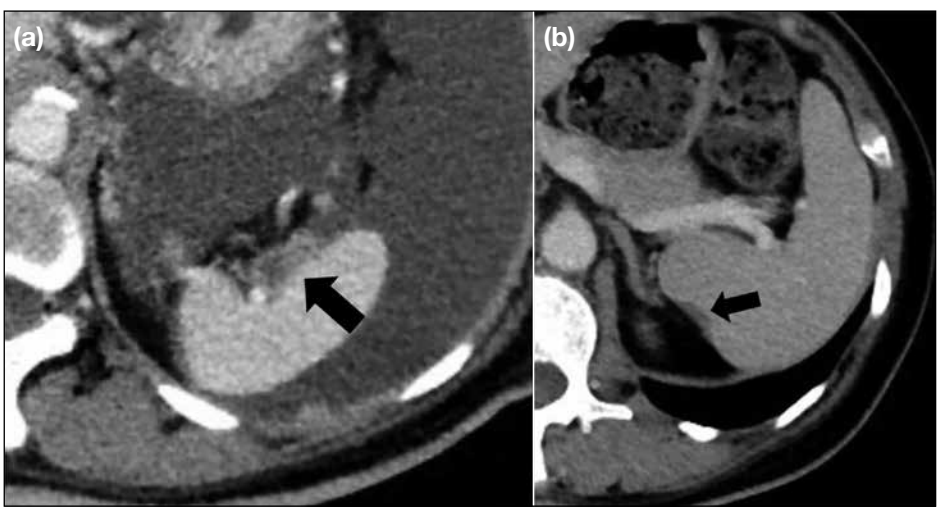

Figure 8. Contrast computed tomography images demonstrating deposit on the splenic surface, with (a) showing deposit at the splenic hilum (arrow) and (b) showing deposit at the posteromedial surface of the spleen (arrow). As these sites are difficult to assess on laparoscopy, pretreatment imaging is essential.

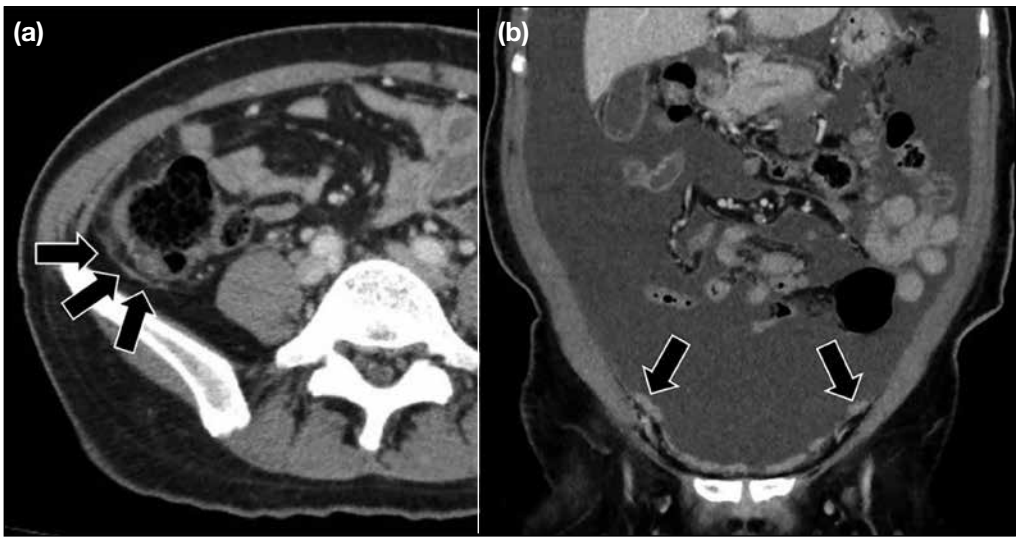

Figure 9. (a) Axial and (b) coronal images from contrast computed tomography demonstrating deposits at the paracolic gutters (arrows).

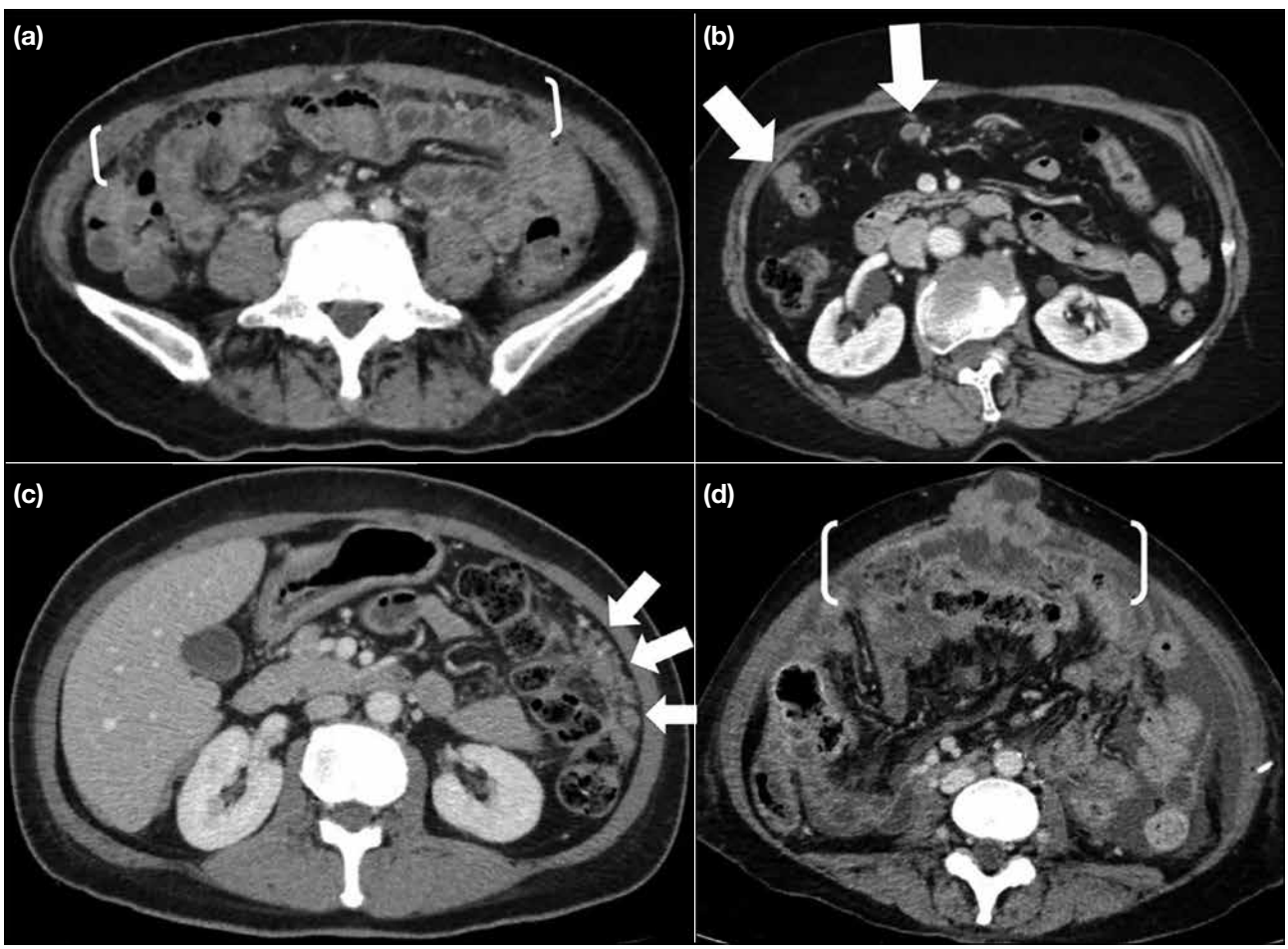

Figure 10. Contrast computed tomography images demonstrating the different morphologies of omental deposits, from mild increased stranding at the omentum (brackets in [a]), small omental nodules (arrows in [b]), confluent nodules and plaque-like deposits (arrows in [c]), to omental cake appearance with extension to the umbilicus (brackets in [d]).

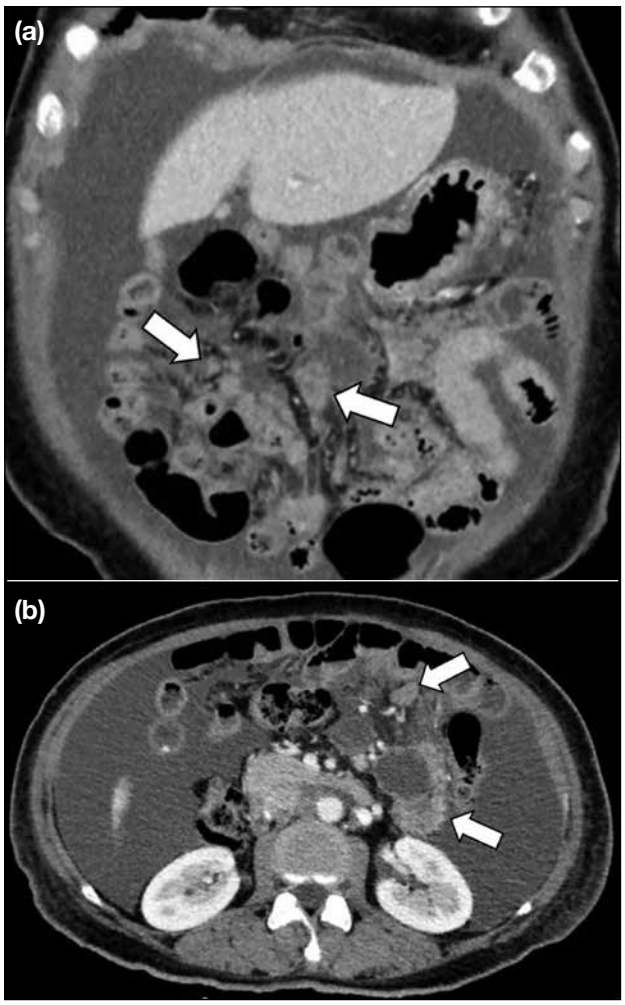

Figure 11. (a) Coronal and (b) axial images from contrast computed tomography demonstrating nodular deposits at the mesentery (arrows).

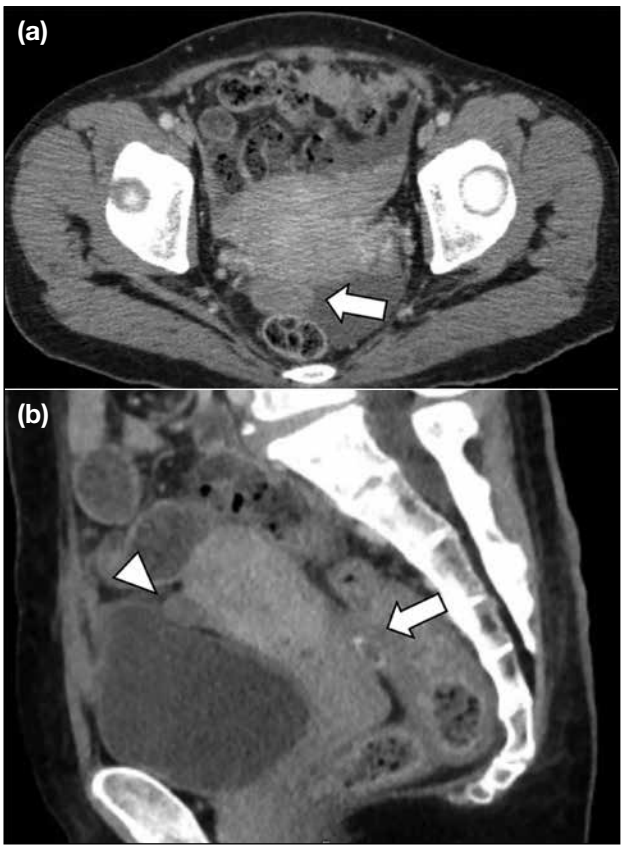

Figure 12. Contrast computed tomography images demonstrating peritoneal disease at the pelvis, with (a) showing deposits at the pouch of Douglas (arrow). (b) This image allows better appreciation of deposits at the peritoneal surface of the urinary bladder (arrowhead) and pouch of Douglas (arrow).

para-aortic, portacaval, porta hepatis or celiac axis should be specified because these sites may preclude surgery (Figures 13 and 14).

Lung Base

Assessment of the lung bases on preoperative CT is crucial since these extraperitoneal sites are not accessible by laparoscopy. The cardiophrenic lymph node is considered enlarged when the short axis is >5 mm[7,15] and may suggest stage IV disease. This precludes surgery. Any pleural effusion should be further investigated to look for stage IV disease that is deemed inoperable (Figures 15 and 16).

Assessment for Interval Debulking Surgery

At our institution, follow-up imaging is performed after three cycles of neoadjuvant chemotherapy in patients with inoperable disease. Images are reviewed at the multidisciplinary meeting for consideration of interval debulking surgery (Figures 17 and 18).

Cancer of the ovaries, fallopian tubes and peritoneum share similar morphological and clinical features. In patients with advanced disease, a tubal or ovarian origin can be difficult to delineate because tumour growth may obscure the primary site.[6] Preoperative assessment for these patients should be similar.

Figure 19 summarises CT assessment of peritoneal lesions and the Table lists potentially non-resectable disease.

CONCLUSION

Pretreatment imaging is helpful to evaluate

Figure 13. Malignant para-aortic lymphadenopathy above the level of the renal vein (circle in [a]) and enlarged paracaval lymph node (arrow in [b]). These are considered surgically difficult sites.

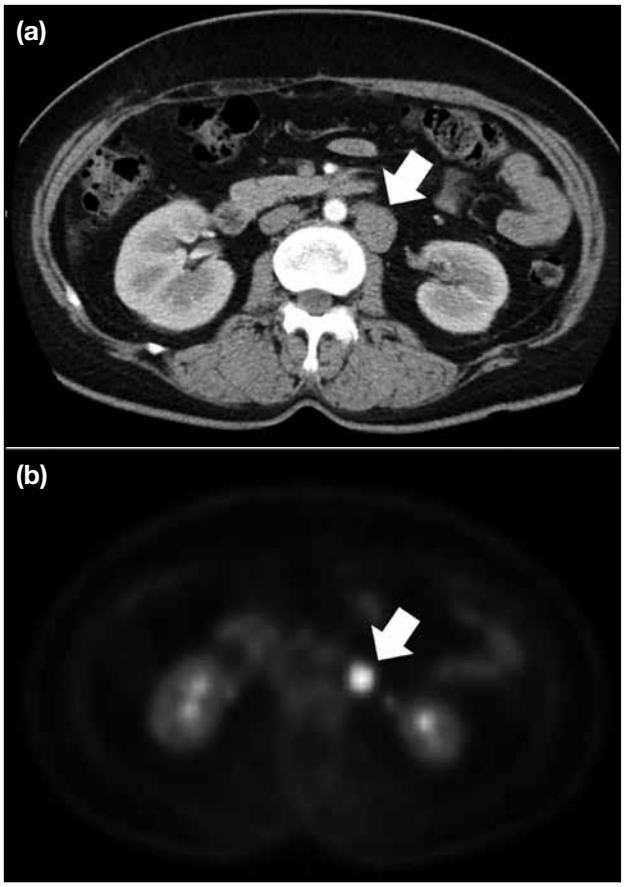

Figure 14. (a) Contrast enhanced computed tomography image demonstrating a solitary enlarged left para-aortic lymph node (arrow). (b) Further evaluation with positron emission tomography shows that this lymph node is hypermetabolic with standardised uptake value of 11 (arrow), suggestive of metastatic lymphadenopathy.

abdominopelvic disease burden in patients with ovarian, fallopian tube and peritoneal cancers, and to identify patients at risk of having suboptimal debulking surgery in whom laparotomy would be futile. It has been shown that CT has high accuracy in detecting peritoneal lesions. Assessment of peritoneal involvement can be improved by understanding the peritoneal anatomy, route of tumour dissemination, as well as common sites of peritoneal deposits. The role of radiologists in the multidisciplinary team is to alert clinicians to the presence of lesions that may complicate surgery or preclude optimal debulking. Patient-centred management should be discussed at the multidisciplinary meeting to decide which of cytoreductive surgery or neoadjuvant chemotherapy is most appropriate.

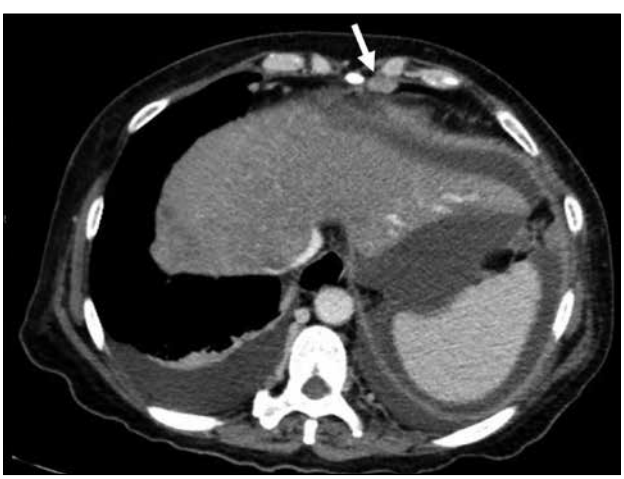

Figure 15. Contrast computed tomography image demonstrating bilateral pleural effusion and an enlarged cardiophrenic lymph node (arrow), worrisome of stage IV disease.

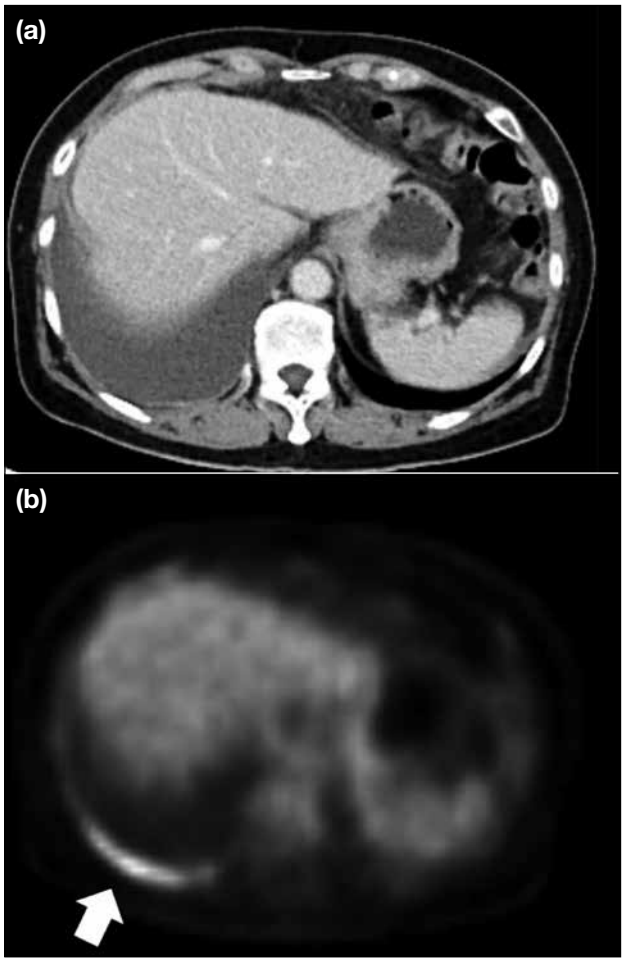

Figure 16. (a) Contrast enhanced computed tomography image showing right pleural effusion. (b) Positron emission tomography shows increased fluorodeoxyglucose uptake along the pleura (arrow), suggestive of metastatic deposits and stage IV disease.

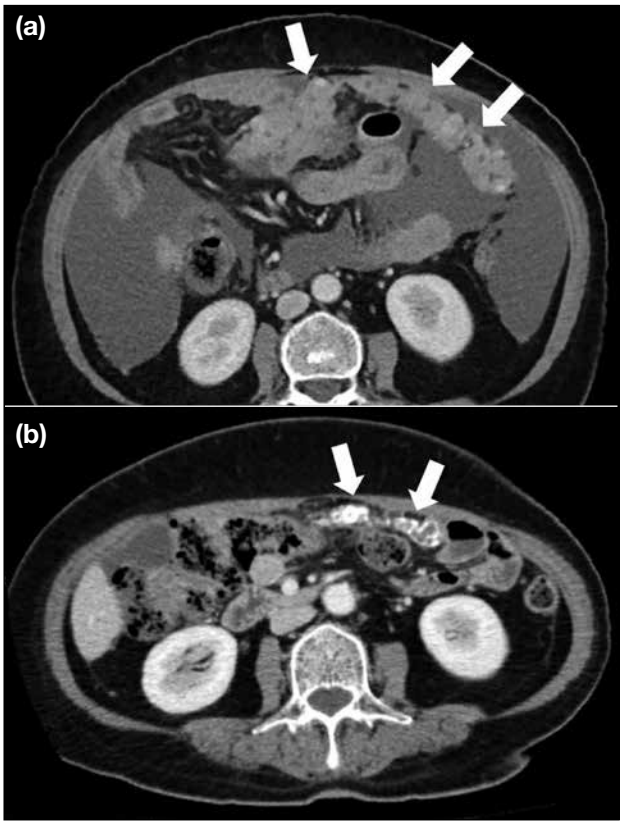

Figure 18. (a) Staging computed tomography (CT) image showing extensive omental deposits (arrows). (b) Follow-up CT after neoadjuvant chemotherapy showing interval shrinkage of omental deposits (arrows). Development of calcifications at the omental deposits is suggestive of post-treatment changes.

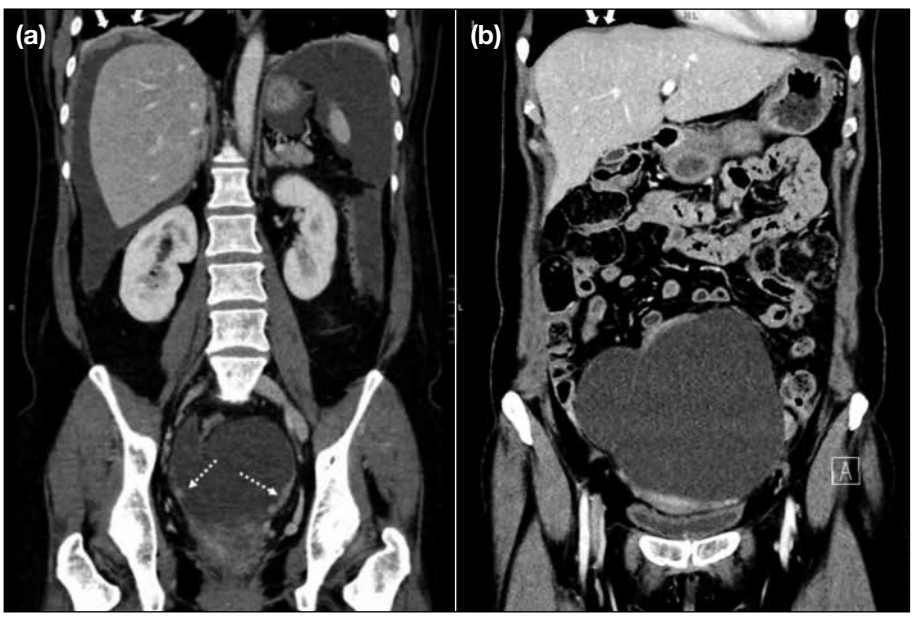

Figure 17. (a) Staging computed tomography (CT) image showing extensive peritoneal deposits at the right subphrenic region (arrows), which are surgically challenging. The primary ovarian tumour with solid components (dashed arrows) is also detected. (b) Follow-up CT after neoadjuvant chemotherapy showing interval shrinkage of the concerned right subphrenic deposits (arrows). The primary tumour also shows a decreased solid component. Images were reviewed at the multidisciplinary meeting and the patient subsequently underwent interval debulking surgery.

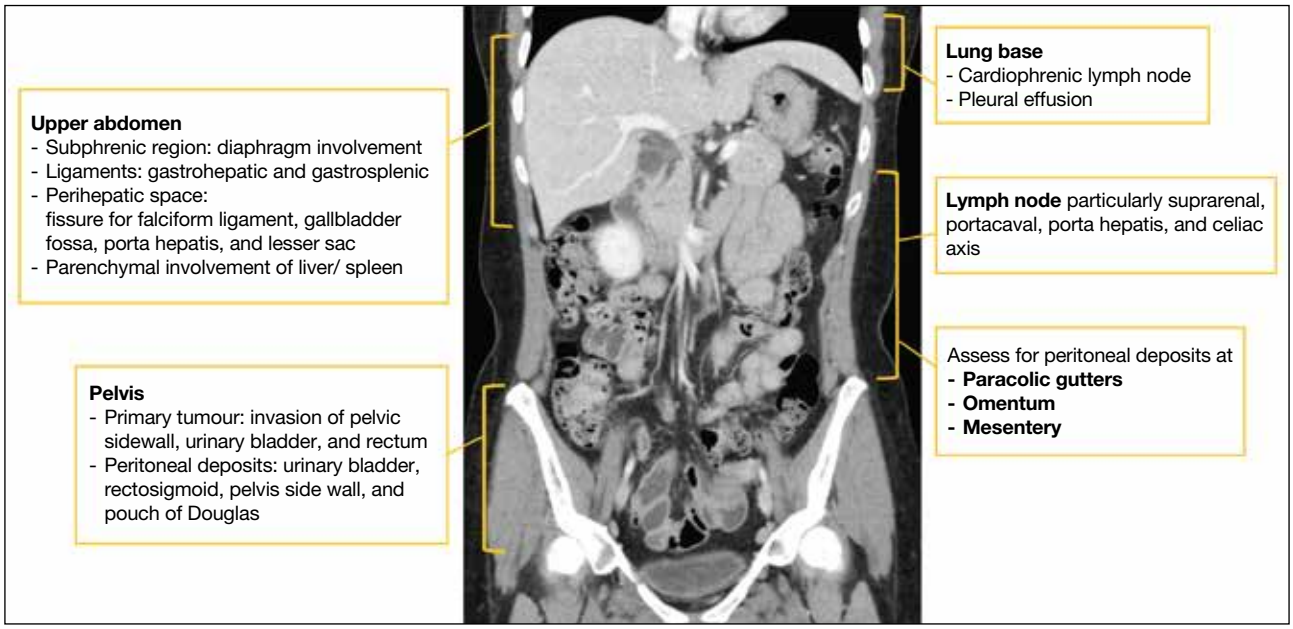

Figure 19. Summary of computed tomography assessment of peritoneal lesions.

Table. Summary of potentially non-resectable diseases.

• Implants >2 cm at the diaphragm, lesser sac, porta hepatis, fissure for falciform ligament, gallbladder fossa, gastrohepatic or gastrosplenic ligament
• Haematogenous hepatic parenchymal metastases
• Extensive involvement of the mesenteric root
• Pelvic sidewall invasion
• Involved lymph nodes superior to the level of renal vein (including suprarenal para-aortic, portacaval, porta hepatis, and celiac axis)
• Pleural infiltration and cardiophrenic lymph nodes

REFERENCES

1. Sung H, Ferlay J, Siegel RL, Laversanne M, Soerjomataram I, Jemal A, et al. Global Cancer Statistics 2020: GLOBOCAN estimates of incidence and mortality worldwide for 36 cancers in 185 countries. CA Cancer J Clin. 2021;71:209-49.
2. Hong Kong Cancer Registry. Overview of Hong Kong Cancer Statistics of 2020. Hong Kong Hospital Authority; Oct 2021. Available from: https://www3.ha.org.hk/cancereg/pdf/overview/Overview%20of%20HK%20Cancer%20Stat%202020.pdf. Assessed 26 Apr 2023.
3. Berek J, Kehoe ST, Kumar L, Friedlander M. Cancer of the ovary, fallopian tube, and peritoneum. Int J Gynecol Obstet. 2018;143 Suppl 2:59-78.
4. Forstner R, Sala E, Kinkel K, Spencer J; European Society of Urogenital Radiology. ESUR guidelines: ovarian cancer staging and follow-up. Eur Radiol. 2010;20:2773-80.
5. Saida T, Tanaka YO, Matsumoto K, Satoh T, Yoshikawa H, Minami M. Revised FIGO staging system for cancer of the ovary, fallopian tube, and peritoneum: important implications for radiologists. Jpn J Radiol. 2015;34:117-24.
6. Javadi S, Ganeshan DM, Qayyum A, Iyer RB, Bhosale P. Ovarian cancer, the revised FIGO staging system, and the role of imaging. AJR Am J Roentgenol. 2016;206:1351-60.
7. Nougaret S, Addley HC, Colombo PE, Fujii S, Al Sharif SS, Tirumani SH, et al. Ovarian carcinomatosis: how the radiologist can help plan the surgical approach. Radiographics. 2012;32:1775-800.
8. Falzone L, Scandurra G, Lombardo V, Gattuso G, Lavoro A, Distefano AB, et al. A multidisciplinary approach remains the best strategy to improve and strengthen the management of ovarian cancer (Review). Int J Oncol. 2021;59:53.
9. Spencer JA. A multidisciplinary approach to ovarian cancer at diagnosis. Br J Radiol. 2005;78 Spec No 2:S94-102.
10. Schmidt S, Meuli RA, Achtari C, Prior JO. Peritoneal carcinomatosis in primary ovarian cancer staging: comparison between MDCT, MRI, and 18F-FDG PET/CT. Clin Nucl Med. 2015;40:371-7.
11. Ahmed SA, Abou-Taleb H, Yehia A, El Malek NA, Siefeldein GS, Badary DM, et al. The accuracy of multi-detector computed tomography and laparoscopy in the prediction of peritoneal carcinomatosis index score in primary ovarian cancer. Acad Radiol. 2019;26:1650-8.
12. Pannu HK, Bristow RE, Montz FJ, Fishman EK. Multidetector CT of peritoneal carcinomatosis from ovarian cancer. Radiographics. 2003;23:687-701.
13. Sahdev A. CT in ovarian cancer staging: how to review and report with emphasis on abdominal and pelvic disease for surgical planning. Cancer Imaging. 2016;16:19.
14. Sugarbaker PH. Surgical responsibilities in the management of peritoneal carcinomatosis. J Surg Oncol. 2010;101:713-24.
15. Kolev V, Mironov S, Mironov O, Ishill N, Moskowitz CS, Gardner GJ, et al. Prognostic significance of supradiaphragmatic lymphadenopathy identified on preoperative computed tomography scan in patients undergoing primary cytoreduction for advanced epithelial ovarian cancer. Int J Gynecol Cancer. 2010;20:979-84.

Hong Kong J Radiol. 2023;26:153-60. Epub 8 May 2023 | https://doi.org/10.12809/hkjr2317410

PICTORIAL ESSAY

Hysterosalpingographic Findings from Uterus to Peritoneal Cavity: A Pictorial Essay

SC Wong, KS Yung, RLS Chan, WH Luk

Department of Radiology, Princess Margaret Hospital, Hong Kong SAR, China

BACKGROUND

With social trends of late marriage and increasing maternal age, there is ongoing demand for assisted reproduction and subfertility investigations. Since tubal occlusion is an important cause of female subfertility,[1] assessment of tubal patency is a crucial part of investigations to identify the cause of subfertility.

Hysterosalpingography (HSG) is a fluoroscopic examination of the uterus and fallopian tubes with contrast instillation through the cervical canal. It has remained a popular investigation of tubal patency in modern reproductive medicine despite being invented more than 100 years ago.[2] It is considered a standard first-line test for assessment of tubal patency[3,4] in view of its reliability, less invasiveness than laparoscopy, and more efficient use of medical resources.[4]

With age-related fertility decline,[4] expeditious management is essential. Severity of tubal disease identified on HSG guides the management decision for intervention.[5] A finding of bilateral tubal occlusion prompts early referral for consideration of in vitro fertilisation. Detection of uterine cavity or contour abnormalities on HSG can guide further imaging, endoscopic investigations, and intervention. A radiologist's familiarity with HSG interpretation and awareness of the spectrum of pathology is advantageous to overall patient care and outcome.

This article presents a pictorial review of HSG cases with emphasis on a spectrum of pathologies including tubal occlusion, tuboperitoneal pathologies, uterine contour anomalies, and intracavity filling defects.

PERFORMING HYSTEROSALPINGOGRAPHY

Prior to instrumentation of the uterine cavity, exclusion of pregnancy and active pelvic infection are of utmost importance.

The optimal time to perform HSG is between day 7 and 12 of the menstrual cycle.[6] This helps avoid pregnancy and improve image interpretation with the thinner endometrium of the early proliferative phase. Conducting the examination during active menstruation may impair assessment of the endometrial cavity configuration. Contrast injection into an already distended uterine cavity during active heavy menstruation may also cause unnecessary patient discomfort.

Correspondence: *Dr SC Wong, Department of Radiology, Princess Margaret Hospital, Hong Kong SAR, China*
Email: wsc696@ha.org.hk

Submitted: 7 Jun 2021; Accepted: 3 Aug 2021.

Contributors: All authors designed the study, acquired the data, and analysed the data. SCW drafted the manuscript. All authors critically revised the manuscript for important intellectual content. All authors had full access to the data, contributed to the study, approved the final version for publication, and take responsibility for its accuracy and integrity.

Conflicts of Interest: All authors have disclosed no conflicts of interest.

Funding/Support: This study received no specific grant from any funding agency in the public, commercial, or not-for-profit sectors.

Data Availability: All data generated or analysed during the present study are available from the corresponding author on reasonable request.

Ethics approval: This study was approved by the Kowloon West Cluster Research Ethics Committee of Hospital Authority, Hong Kong [Ref No.: KW/EX-21-108(161-08)]. Patient consent was waived by the Committee.

The patient should be positioned in a lithotomy position for pelvic examination. Aseptic technique with cleansing and draping of the perineum, speculum examination to expose the cervical os, followed by cleansing of the ectocervix and vagina are mandatory before catheter insertion to minimise the risk of ascending infection.

Different catheters can be used for an HSG, including infant Foley catheter (8 Fr) or commercially available HSG 5F catheters (CooperSurgical, Trumbull [CT], United States). In our institution, an 8-Fr infant Foley catheter and water-soluble contrast (such as iohexol or iodixanol) are used.

Flushing of the Foley catheter and all extension tubes to eliminate dead space before catheterisation will help reduce introduction of air bubbles into the uterus. Catheter insertion followed by slow gentle inflation of the balloon (around 1-3 mL of water) to secure the catheter is required. Nulliparous patients generally tolerate a lower volume of balloon distension than patients with prior pregnancy.

With successful catheterisation, the patient is repositioned supine for fluoroscopic examination. The standard views in HSG are based on the recommendations of the American College of Radiology's Practice Parameter for the Performance of Hysterosalpingography.[6,7] Chapman & Nakielny's Guide to Radiological Procedures[8] is also in consensus with the above references.

Based on the above recommendations, the standard set in each HSG study should contain four images: (1) early uterine filling (to assess small uterine filling defects); (2) late uterine filling and tubal filling (to assess uterine contour and tubal abnormalities); (3) peritoneal spillage (to document tubal patency), and (4) an image taken after Foley balloon deflation and catheter removal (to assess the lower uterine segment and endocervical canal).

If tubal occlusion is suspected, manoeuvres such as delayed screening, decubitus position, and use of spasmolytic agents (glucagon or hyoscine butylbromide) should be performed in an attempt to determine if it is genuine.

HYSTEROSALPINGOGRAPHIC FINDINGS

Normal Anatomy

The uterine cavity has a well-defined smooth border with inverted triangular shape and no persistent filling defect

Figure 1. (a) A 27-year-old woman with normal triangular uterine cavity without filling defect on hysterosalpingography. (b) A 30-year-old woman with normal fallopian tube appearance. Note the mucosal folds (arrows) in the ampullary portions of both tubes.

(Figure 1a). The fallopian tubes are evident as thin, elongated smooth lines with a widening at the ampullary portion and variable pelvic location.[6] Opacification of the ampullary portion of the fallopian tube can be confirmed by visualisation of mucosal folding (Figure 1b).[6] Free peritoneal contrast spillage from the fimbrial end indicates tubal patency.

Tubal Pathology

Non-opacification of the fallopian tube or absence of peritoneal contrast spillage can be due to cornual smooth muscle spasm or genuine tubal pathology. The sensitivity and specificity of assessing bilateral tubal patency or occlusion on HSG has been reported to be 92.1% and 85.7%, respectively.[9] There is no published consensus on the most effective manoeuvre to relieve cornual spasm.

Laparoscopy is considered as the traditional clinical reference standard for diagnosis of tubal disease.[5,9] Chromotubation of the fallopian tubes with contrast dye injection and visualisation of peritoneal dye spillage provides assessment of tubal patency.

Tubal Occlusion

Tubal occlusion manifests as abrupt transition from the contrast-filled proximal fallopian tube to a non-opacified distal portion and absent peritoneal contrast spillage (Figure 2). Tubal occlusion can be due to pelvic adhesions from prior pelvic inflammatory disease, endometriosis, or less commonly to congenital Müllerian duct malformation.[6,10]

Tuboperitoneal Pathologies

Hydrosalpinx

Hydrosalpinx represents a distended fallopian tube with serous fluid accumulation secondary to tubal blockage (Figure 3).[11] It is associated with pelvic inflammatory disease, endometriosis, or prior tubal surgery (e.g., ligation), tubal pregnancy or rarely tubal malignancy. On HSG, hydrosalpinx manifests as contrast-filled dilated fallopian tubes without distal contrast spillage into the peritoneal cavity.[6]

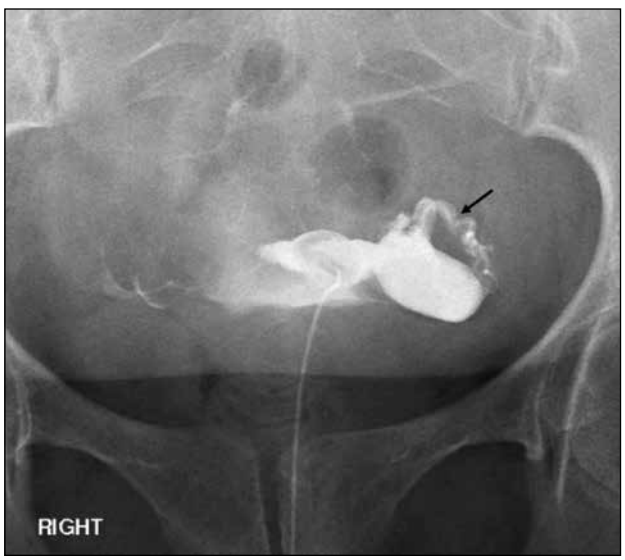

Figure 2. A 32-year-old woman with distal left fallopian tube blockage without hydrosalpinx. Delayed hysterosalpingography images show persistent round contrast collection closely related to the distal left fallopian tube. Normal mucosal fold pattern at the non-distended ampullary portion is still visible (arrow) and would not be present in hydrosalpinx. Peritoneal contrast spillage originated from the patent right tube. Subsequent laparoscopic chromotubation confirmed distal left fimbrial end blockage without hydrosalpinx formation. Right tube was patent.

Figure 3. A 33-year-old woman with left hydrosalpinx. Delayed hysterosalpingography film demonstrated persistent absence of peritoneal contrast spillage compatible with bilateral tubal blockage. Distended contrast fills the left fallopian tube with horizontal folds (arrows) resembling a cogwheel pattern, suggestive of hydrosalpinx formation. Subsequent laparoscopic surgery confirmed left 5 × 3 cm hydrosalpinx.

Peritubal adhesion and pelvic peritoneal loculated collections

Pelvic inflammatory disease can result in pelvic and peritoneal scarring and consequent adhesion bands around the pelvic organs.[11] Adhesions around the fallopian tubes can result in tubal blockage with loculated contrast collections.[6] A loculated pelvic collection can manifest as a persistent localised contrast-filled region in delayed screening on HSG (Figure 4).

Salpingitis isthmica nodosa

Salpingitis isthmica nodosa (SIN) is a fallopian tube disease of unknown aetiology that is characterised by proximal tubal (isthmic portion) nodular thickening, associated diverticulosis of isthmic tubal epithelium invading into the muscular layer with secondary smooth muscle hypertrophy, and preserved smooth serosal surface (Figure 5).[12] Features are more often bilateral than unilateral. The reported incidence of SIN is 0.6% to 11% in healthy fertile females with a strong association with infertility and ectopic pregnancy.[13] Although SIN can be diagnosed on HSG from its distinctive appearance, histological proof is the gold standard.[12] The presence of nodular outpouchings along the cornual isthmic portions of fallopian tubes on HSG represents contrast-filled tubal diverticula.[6,10] The tubal outpouchings may measure up to 2 cm.[12]

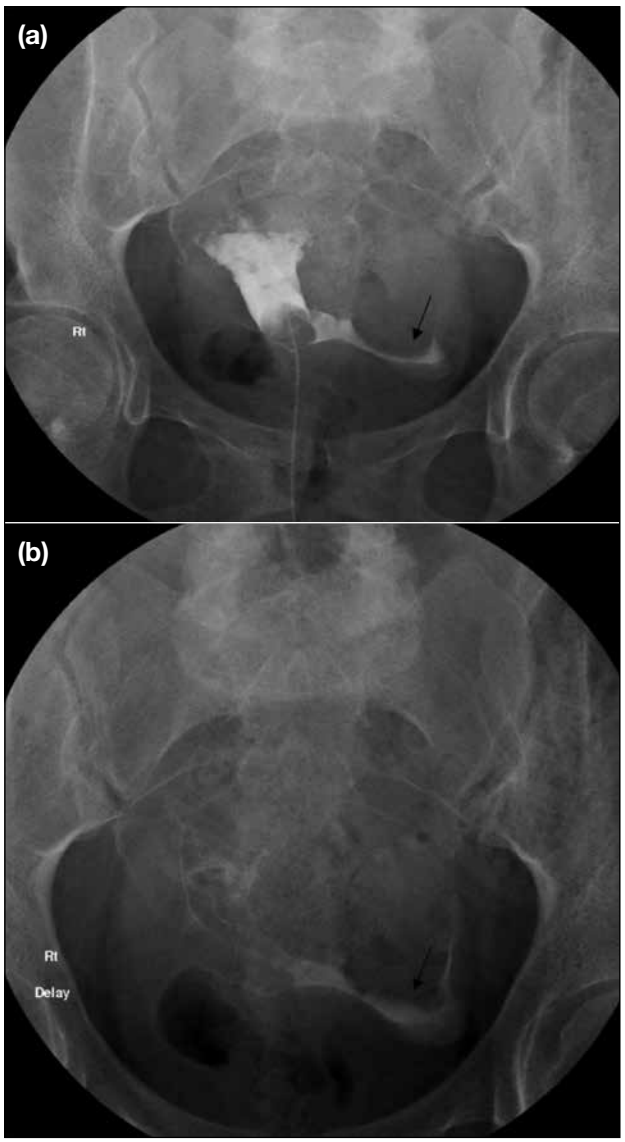

Figure 4. A 28-year-old woman with a history of pelvic inflammatory disease. (a) Hysterosalpingography showing loculated fluid collection (arrow). (b) Delayed film after ambulation showing persistent localised contrast pooling at the left pelvic region (arrow) suggests the presence of a loculated fluid collection.

Uterine Cavity Contour Abnormalities

Uterine cavity contour abnormalities can be categorised as uterine cavity outpouching or extrinsic indentation or irregular outline (that can be associated with prior surgery, infection or inflammation).

Contour outpouching

Adenomyosis is the extension of endometrial glandular tissue into the myometrium and can be diffuse or focal in extent (Figure 6). When regions of endometrial glands are connected to the uterine cavity, they can become opacified on HSG study and show as diverticula or outpouchings in the uterine cavity.[6] Further imaging with ultrasound or magnetic resonance imaging (MRI) allows confirmation of the diagnosis and visualisation of the extent of adenomyotic changes. Differentiation with irregular cavity outline may be encountered if HSG is performed during menstruation (Figure 7).

Uterine contour indentation

Leiomyoma is a benign tumour composed of uterine smooth muscle (Figure 8). Sizable leiomyoma, especially at a submucosal location, may be evidenced by smooth indentation of the uterine cavity with cavity distortion on HSG.[6,10] Distorted endometrial cavity contour may contribute to subfertility owing to changes in endometrial receptivity, development, and hormone environment.[10]

Intracavity Filling Defects

Sensitivity of HSG in detecting intrauterine abnormalities has been reported to be about 58.2%, compared with 82% for ultrasonography.[10] Intracavity filling defects can be artefactual and due to air bubbles or intracavity pathology such as endometrial polyps, intracavity leiomyoma, or synechiae. Persistent and stationery filling defects are more suspicious of intracavity pathology. Preprocedural flushing of the catheter helps minimise the chance of air bubble contamination.

Endometrial polyps

Endometrial polyps are benign focal proliferations of endometrial tissue, usually seen as smooth oval to roundish filling defects on HSG (Figure 9). Saline infusion sonohysterography with ultrasound assessment after saline instillation into the uterine cavity can help distinguish the causes of an intracavity filling defect with superior accuracy for endometrial polyps than transvaginal ultrasound or HSG.[14] Hysteroscopy is the gold standard for diagnosis[14] and can be applied to provide therapeutic treatment with polypectomy or adhesiolysis.

Synechiae

Intrauterine adhesions or synechiae result from insult to the basal endometrial lining, such as prior surgery (especially dilatation and curettage) or endometritis (Figure 10). Asherman's syndrome is the presence of intrauterine adhesions with clinical manifestations of abnormal menstruation (e.g., amenorrhoea/hypomenorrhoea) and subfertility.[6] On HSG, adhesions are more often linear, irregular or angulated.

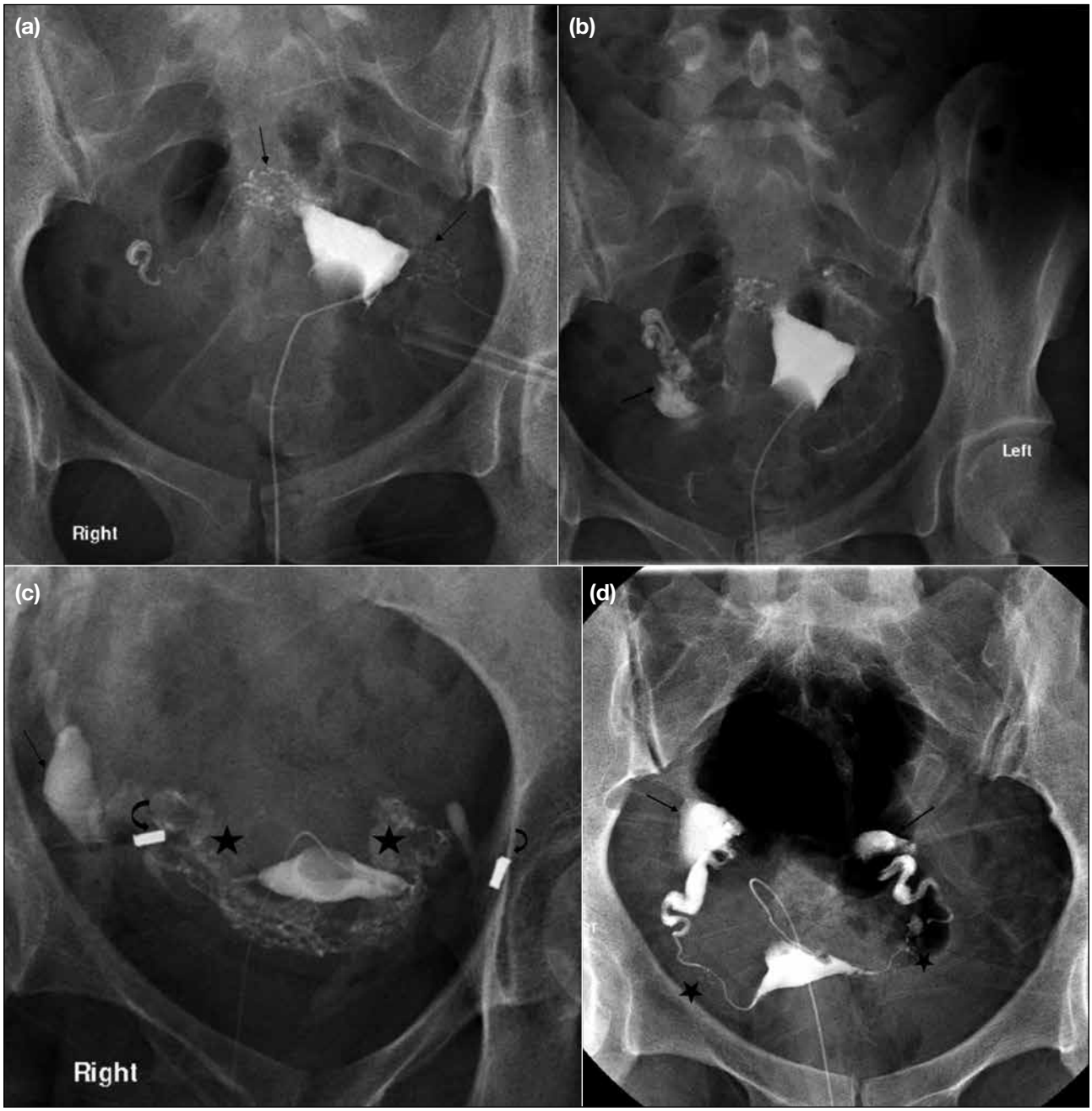

Figure 5. Three cases of salpingitis isthmica nodosa (SIN). (a and b) A 29-year-old woman with SIN, patent right tube and blocked left tube. (a) Tiny nodular contrast-filled outpouching at bilateral isthmic fallopian tubes (arrows). (b) Further imaging showing peritoneal contrast spillage (arrow), from patent right tube. (c) A 42-year-old woman with SIN with prior bilateral tubal ligation and right hydrosalpinx (ordinary arrow). The patient requested reversal of tubal ligation. Hysterosalpingography shows bilateral tubal ligation clips (curved arrows). Nodular outpouchings from bilateral proximal tubes (stars) were compatible with SIN. Bullous dilatation of right distal fallopian tube suggests hydrosalpinx. (d) A 38-year-old woman with bilateral SIN and blocked distal tubes. Typical SIN features in bilateral isthmic portions (stars) were more conspicuous on the left. Nondilated bilateral ampullary portions with normal mucosal fold pattern. Roundish contrast collections adjacent to distal fallopian tube (arrows) with lack of peritoneal spillage suggest bilateral distal blocked tubes.

Variant Anatomy or Congenital Malformation

Arcuate uterus

Arcuate uterus is classified as class VI Müllerian duct abnormality according to the American Fertility Society scheme.[15] Arcuate uterus arises from incomplete septal resorption at the level of the uterine fundus resulting in mild focal bulging. On HSG it manifests as broad mild concavity of the fundal cavity contour (Figure 11). Further imaging with three-dimensional ultrasound

Figure 6. A 32-year-old woman with adenomyoma. Known fundal adenomyoma was found on prior transvaginal ultrasound. Hysterosalpingography demonstrates irregular uterine cavity contour with small outpouchings at fundal aspects (arrows), in keeping with deep extension of endometrial glandular tissues within the myometrium.

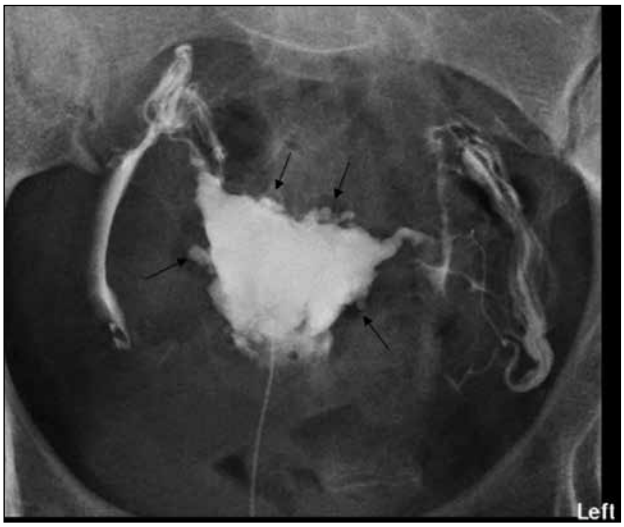

Figure 7. A 32-year-old woman with menstruation-related cavity changes mimicking diffuse adenomyosis. Hysterosalpingography (HSG) was performed at day 6 of menstruation. Irregular uterine cavity with multiple small contrast-filled outpouchings (arrows) are evident. Subsequent pelvic ultrasound showed unremarkable uterus without features of adenomyosis. No history of dysmenorrhoea was reported. Performing HSG during menstruation may result in diagnostic errors as cavity changes during menstruation may mimic diffuse adenomyosis.

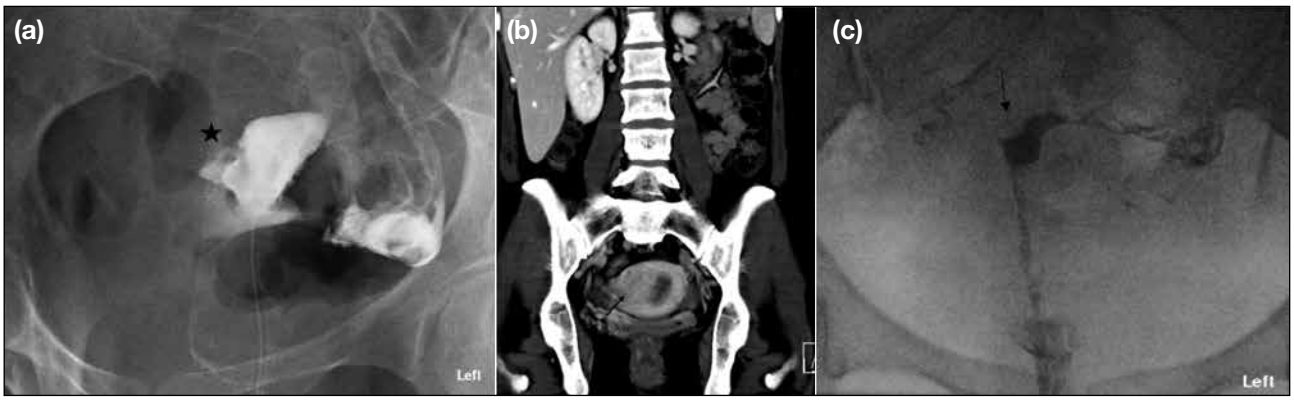

Figure 8. (a and b) A 29-year-old woman with leiomyoma indenting the uterine cavity. (a) Hysterosalpingography showed indentation (star) of the right uterine cavity. (b) Follow-up computed tomography scan of the abdomen and pelvis showed a hypoenhancing uterine mass (arrow) suggestive of leiomyoma with displacement and indentation of the right fundal uterine cavity. (c) A 36-year-old woman with submucosal leiomyoma. Hysterosalpingography showed a filling defect at right cornual region (arrow) with smooth border. Hysteroscopy showed a fundal polypoid lesion and polypectomy was performed. Pathology revealed submucosal leiomyoma.

or MRI to visualise the normal outer uterine contour is helpful. It has been regarded as a normal uterine variant without significant adverse impact on fertility.[15,16]

Congenital uterine anomalies

The wide spectrum and complex pathogenesis of congenital uterine anomalies are beyond the scope of this pictorial review. The developmental stages of the uterus include organogenesis of paired Müllerian ducts, fusion, and septal resorption. Disorders in these developmental stages result in congenital uterine anomalies with varying severity and implications for fertility.[10] HSG offers valuable information regarding uterine cavity morphology and can suggest the presence of a congenital uterine anomaly. Further evaluation with three-dimensional pelvic ultrasound or MRI is warranted

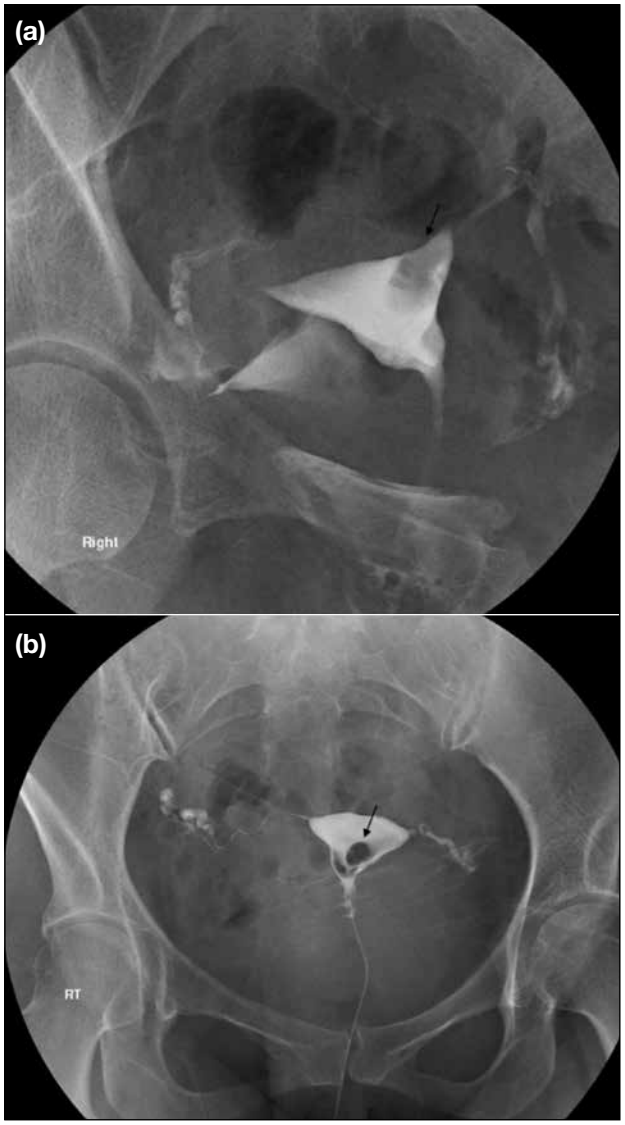

Figure 9. Two cases of benign endometrial polyps. (a). A 33-year-old woman with left cornual endometrial polyp. Hysterosalpingography revealed a filling defect with smooth border at the left cornua (arrow), suspicious of endometrial polyp. Follow-up hysteroscopy with polypectomy confirmed presence of a 1-cm endometrial polyp with benign histology. (b) A 33-year-old woman with intracavity endometrial polyp. Hysterosalpingography shows a roundish intracavity filling defect with smooth border (arrow). Hysteroscopy revealed endometrial polyp with polypectomy performed and subsequent benign histology.

Figure 10. A 38-year-old woman with uterine synechiae with Asherman's syndrome. Intracavity irregular angulated filling defect was observed on hysterosalpingography (arrow), confirmed by subsequent hysteroscopy with adhesiolysis performed.

Figure 11. A 37-year-old woman with arcuate uterus. Hysterosalpingography shows broad concavity at fundal cavity contour (arrow). Prior computed tomography of pelvis and follow-up transvaginal ultrasound showed smooth convex outer fundal contour. Overall features were consistent with arcuate uterus.

for assessment of outer or fundal uterine contour for accurate diagnosis.

CONCLUSION

HSG is vital in reproductive medicine given its reliability in diagnosing tubal occlusion with relatively low invasiveness. Systematic interpretation of HSG findings and understanding of the spectrum of pathologies, including uterine contour changes, intracavity filling defects, tubal patency, and tuboperitoneal pathology will facilitate identification of the cause of female subfertility and expedite management to improve reproductive outcome.

REFERENCES

1. Dun EC, Nezhat CH. Tubal factor infertility: diagnosis and management in the era of assisted reproductive technology. Obstet Gynecol Clin North Am. 2012;39:551-66.
2. Omidiji OA, Toyobo OO, Adegbola O, Fatade A, Olowoyeye OA. Hysterosalpingographic findings in infertility—what has changed over the years? Afr Health Sci. 2019;19:1866-74.
3. Infertility workup for the women's health specialist: ACOG Committee Opinion, Number 781. Obstet Gynaecol. 2019;133:e377-84.
4. Fertility problems: assessment and treatment. London: National Institute for Health and Care Excellence (NICE); Sep 2017.
5. Practice Committee of the American Society for Reproductive Medicine. Role of tubal surgery in the era of assisted reproductive technology: a committee opinion. Fertil Steril. 2021;115:1143-50.
6. Simpson WL Jr, Beitia LG, Mester J. Hysterosalpingography: a reemerging study. Radiographics. 2006;26:419-31.
7. American College of Radiology. ACR Practice Parameter for the Performance of Hysterosalpingography. Available from: https://www.acr.org/-/media/ACR/Files/Practice-Parameters/HSG.pdf. Accessed 1 Apr 2021.
8. Watson N. Reproductive system. In: Watson N, Jones H, editors. Chapman & Nakielny's Guide to Radiological Procedures. 6th ed. Edinburgh, UK: Saunders; 2014. p 159-62.
9. Foroozanfard F, Sadat Z. Diagnostic value of hysterosalpingography and laparoscopy for tubal patency in infertile women. Nurs Midwifery Stud. 2013;2:188-92.
10. Vickramarajah S, Stewart V, van Ree K, Hemingway AP, Crofton ME, Bharwani N. Subfertility: what the radiologist needs to know. Radiographics. 2017;37:1587-602.
11. Revzin MV, Mathur M, Dave HB, Macer ML, Spektor M. Pelvic inflammatory disease: multimodality imaging approach with clinical-pathologic correlation. Radiographics. 2016;36:1579-96.
12. Jenkins CS, Williams SR, Schmidt GE. Salpingitis isthmica nodosa: a review of the literature, discussion of clinical significance, and consideration of patient management. Fertil Steril. 1993;60:599-607.
13. Majmudar B, Henderson PH 3rd, Semple E. Salpingitis isthmica nodosa: a high-risk factor for tubal pregnancy. Obstet Gynecol. 1983;62:73-8.
14. Soares SR, Barbosa dos Reis MM, Camargos AF. Diagnostic accuracy of sonohysterography, transvaginal sonography, and hysterosalpingography in patients with uterine cavity diseases. Fertil Steril. 2000;73:406-11.
15. The American Fertility Society classifications of adnexal adhesions, distal tubal occlusion, tubal occlusion secondary to tubal ligation, tubal pregnancies, Müllerian anomalies and intrauterine adhesions. Fertil Steril. 1988;49:944-55.
16. Ubeda B, Paraira M, Alert E, Abuin RA. Hysterosalpingography: spectrum of normal variants and nonpathologic findings. AJR Am J Roentgenol. 2001;177:131-5.

CATEGORIES OF PAPERS

Hong Kong Journal of Radiology publishes various categories of articles. Each category serves a distinct purpose and is judged by different criteria.

EDITORIAL

Commissioned article presenting the author's opinion on a topical subject or an article published in the current issue. Unsolicited Editorials are not accepted.

Format: An abstract is not required. The text is limited to 1000 words, with a maximum of 1 table or figure, and up to 10 references.

REVIEW ARTICLE

Systematic reviews or meta-analyses of recent developments in a specific topic. Scoping reviews of the literature that identify area(s) for future research will also be considered. No new information is described, and no subjective opinion or personal experiences are expressed.

Format: A structured abstract of ≤ 250 words; headings should include: Objective(s), Methods, Results, Conclusion. The text is limited to 5000 words, with a maximum of 20 tables and figures (total), and up to 60 references.

ORIGINAL ARTICLE

Provides new information based on original research. Includes prospective studies with in-depth statistical analysis, unique retrospective observations of a disease or disorder, and studies of novel applications of an interventional procedure or treatment method.

Format: A structured abstract of ≤ 250 words; headings should include: Objective(s), Methods, Results, Conclusion. The text is limited to 3500 words, with a maximum of 20 tables and figures (total), and up to 50 references.

PERSPECTIVE

Narrative review articles discussing recent developments in a specific topic. No new information is described; may include subjective opinion or personal experiences.

Format: An unstructured abstract of ≤ 250 words. The text is limited to 2500 words, with a maximum of 20 tables and figures (total), and up to 60 references.

PICTORIAL ESSAY

Teaching exercise with message in the figures and legends. Emphasis is on quality of the illustrations and clinical relevance of the message.

Format: An abstract is not required. The text is limited to 2500 words, with a maximum of 20 tables and figures (total), and up to 15 references.

CASE REPORT

Brief discussion of a case with unique features not previously described. Additional cases (case series) may be added to augment the discussion. The discussion should be succinct and focus on a specific message.

Format: An abstract is not required. The text is limited to 1500 words, with a maximum of 8 tables and figures (total), and up to 15 references.

BRIEF COMMUNICATION

This includes post-meeting commentary, update on new imaging or therapeutic advances, brief description of a specific technique or procedure or new equipment. Teaching exercise aimed at describing a certain radiological or radiotherapeutic technique for trainees and practising radiologists is also welcome.

Format: An abstract is not required. The text is limited to 1500 words, with a maximum of 8 tables and figures (total), and up to 15 references.

LETTER TO THE EDITOR

Short letter on any matter of interest to journal readers, including comments on an article that has previously appeared in the journal. The authors of the article commented on would be invited to reply.

Format: An abstract is not required. The text is limited to 500 words, with up to 5 references. Figures and tables are permitted only exceptionally.

INFORMATION FOR AUTHORS

Aims and Scope

Hong Kong Journal of Radiology is the official peer-reviewed academic journal of the Hong Kong College of Radiologists. It is a multidisciplinary journal covering research work pertaining to the science and practice of the component specialties of the College. The journal publishes various categories of papers, including Reviews, Original Articles, Perspectives, Pictorial Essays, Case Reports, Brief Communications, and Letters to the Editor. Manuscripts will be subject to rigorous peer review. *HKJR* adheres to the Recommendations for the Conduct, Reporting, Editing, and Publication of Scholarly Work in Medical Journals of the International Committee of Medical Journal Editors (ICMJE; www.icmje.org), and the Core Practices of the Committee on Publication Ethics (COPE; publicationethics.org/).

Journal Policies

Reporting Guidelines: *HKJR* recommends the use of reporting guidelines in the preparation of manuscripts, such as those advocated by the EQUATOR Network (eg, CONSORT for randomised trials).

Funding: Any sponsor(s) of the research involved, along with grant number(s) should be provided.

Conflicts of interest: All authors must provide a statement reporting any conflicts of interest. Where none exist, please state 'The authors have no conflicts of interest to declare.'

Ethics: All studies must be conducted in accordance with the Declaration of Helsinki. For studies involving humans, a statement must be included in the manuscript that provides the name of the review board and approval number (or waiver). A statement on patient/guardian consent must also be included. For studies involving animals, appropriate ethics approval is required, and this should be stated in the manuscript.

Submission: Manuscripts should be submitted online via HKAMedTrack (www.hkamedtrack.org/hkjr). Manuscripts must be unpublished works that are not under consideration by another publication.

Copyright: On acceptance of an article by the journal, the corresponding author will be asked to transfer copyright of the article to the College.

Editing: Accepted manuscripts will be copyedited according to journal style. Authors are responsible for all statements made in their work, including changes made by the copy editor.

Proofs and Reprints: The corresponding author will receive page proofs, which should be proofread and returned promptly. Corrections are limited to printer's errors — no substantial author's changes will be made without charge. Quotes for extra copies of reprints are available at the Editorial Office.

Manuscript Preparation

In general, manuscripts should be prepared following the 'IMRaD' structure as recommended by the ICMJE. Please provide a **blinded** manuscript and separate title page in Word format (.doc or .docx). Manuscripts must be written in English. For accepted manuscripts, an abstract in Traditional Chinese will also be required.

Authors: Provide the full name, qualifications (maximum of two), and affiliation (where the study was conducted) for all authors. The authors' names in Chinese characters, if available, should also be provided. **The corresponding author**, on behalf of the authors, is responsible for all contact with the journal. Provide the full name, postal address, telephone and fax numbers, and email address of the corresponding author.

Title: Concisely convey the main topic of the study. Avoid obvious terms such as "a study of" or "novel". If appropriate, please include the study design in the title (eg, 'randomised controlled trial', 'systematic review', 'case report'). An abbreviated title of <45 characters is also required.

Abstract: For article types requiring an abstract, this should provide a complete summary of the article, including the aims/purpose, main methods, key results, and conclusions. Abbreviations and clinical or technical jargon should be avoided. Please refer to the Categories of Papers for details.

Key Words: Five relevant index terms should be provided, selected from the Medical Subject Headings (MeSH; www.ncbi.nlm.nih.gov/mesh).

Tables: Submit tables on separate pages in as simple a format as possible. They should be numbered and concisely titled. Abbreviations should be defined in footnotes.

Figures: Restricted to the minimum necessary to support the textual material. Illustrations should be submitted as separate files (.jpg format, ≥350-dpi resolution). All figures should be numbered with a legend to indicate the anatomical area and pathological condition shown. All symbols and abbreviations should be defined in the legend. Please ensure that legends and illustrations correspond.

References: Should be numbered in the order in which they are first cited in the text. Each reference citation should be in superscript Arabic numerals after full-stops and commas. In the reference list, include the complete title, and names and initials of all authors.

Acknowledgement(s): Any individuals who contributed substantially to the study but does not qualify for inclusion as an author should be acknowledged. Written permission from acknowledged individuals is required.

Please refer to the *HKJR* website for further guidance:
http://www.hkjr.org/page/information-authors

TAXOTERE®
(docetaxel)

GENERAL DRUG STATUS

Taxotere has been approved as "General Drug Status" as of April 2023 in the Hospital Authority of Hong Kong

Indicated for the following:

- Prostate Cancer
- Breast Cancer
- Non-small Cell Lung Cancer (NSCLC)
- Head and Neck Cancer
- Gastric Adenocarcinoma

Presentation: Docetaxel concentrate and solvent for solution for infusion. Indications and dosage: Breast Cancer: In combination with doxorubicin and cyclophosphamide for adjuvant treatment of operable node-positive and node-negative breast cancer (docetaxel 75 mg/m² 1-hour after doxorubicin 50 mg/m² and cyclophosphamide 500 mg/m² every 3 weeks for 6 cycles); in combination with doxorubicin for treatment of locally advanced or metastatic breast cancer with no previous cytotoxic therapy (docetaxel 75 mg/m² and doxorubicin 50 mg/m2 every three weeks); monotherapy for the treatment of locally advanced or metastatic breast cancer after failure of cytotoxic therapy containing an anthracycline or an alkylating agent (docetaxel 100 mg/m² every three weeks); in combination with trastuzumab for treatment of metastatic breast cancer whose tumors overexpress HER2 and with no previous chemotherapy for metastatic disease (docetaxel 100 mg/m² every three weeks with trastuzumab administered weekly); in combination with capecitabine for treatment of locally advanced or metastatic breast cancer after failure of cytotoxic chemotherapy containing an anthracycline (docetaxel 75 mg/m² every three weeks combined with capecitabine at 1250 mg/m² twice daily [within 30 minutes after a meal] for 2 weeks followed by 1-week rest period). Non-small cell lung cancer (NSCLC): Treatment of locally advanced or metastatic NSCLC after failure of prior platinum-based chemotherapy (docetaxel 75 mg/m² every three weeks); in combination with cisplatin for treatment of unresectable, locally advanced or metastatic NSCLC with no previous chemotherapy for this condition (docetaxel 75 mg/m² immediately followed by cisplatin 75 mg/m² over 30-60 minutes every three weeks). Prostate cancer: In combination with prednisone or prednisolone for treatment of metastatic castration-resistant prostate cancer (docetaxel 75mg/m² every three weeks and prednisone or prednisolone 5mg orally twice daily administered continuously); in combination with androgen-deprivation therapy (ADT), with or without prednisone or prednisolone for treatment of metastatic hormone-sensitive prostate cancer (docetaxel 75 mg/m² every three weeks for 6 cycles and prednisone or prednisolone 5 mg orally twice daily may be administered continuously). Head and Neck cancer: In combination with cisplatin and 5-fluorouracil for induction treatment of locally advanced squamous cell carcinoma of the head and neck (followed by radiotherapy: docetaxel 75mg/m² as a 1 hour infusion, followed by cisplatin 75mg/m² over 1 hour, on day one, followed by 5-fluorouracil 750mg/m² per day as a continuous infusion for 5 days, repeated every 3 weeks for 4 cycles) (followed by chemoradiotherapy: docetaxel 75mg/m² as a 1 hour infusion on day 1, followed by cisplatin 100mg/m² as a 30-minute to 3-hour infusion, followed by 5-fluorouracil 1000mg/m²/day as a continuous infusion from day 1 to day 4, repeated every 3 weeks for 3 cycles). Gastric Adenocarcinoma: In combination with cisplatin and 5-fluorouracil for treatment of metastatic gastric adenocarcinoma, including adenocarcinoma of the gastroesophageal junction, with no prior chemotherapy for metastatic disease (docetaxel 75mg/m² as a 1-hour infusion, followed by cisplatin 75mg/m², as a 1- to 3-hour infusion (both on day 1 only), followed by 5-fluorouracil 750mg/m² per day given as a 24-hour continuous infusion for 5 days, starting at the end of the cisplatin infusion, repeated every 3 weeks). Further Dosage Information: Docetaxel is administered as a 1-hour infusion every three weeks. (Breast, NSCLC, gastric & head and neck cancers) Premedication consisting of an oral corticosteroid, such as dexamethasone 16 mg per day (e.g. 8 mg BID) for 3 days starting 1 day prior to docetaxel administration, unless contraindicated, can be used. Prophylactic G-CSF may be used to mitigate the risk of hematological toxicities. (Metastatic castration-resistant prostate cancer) Given the concurrent use of prednisone or prednisolone the recommended premedication regimen is oral dexamethasone 8 mg, 12 hours, 3 hours and 1 hour before the docetaxel infusion. (Metastatic hormone-sensitive prostate cancer) Irrespective of the concurrent use of prednisone or prednisolone, the recommended premedication regimen is oral dexamethasone 8 mg 12 hours, 3 hours, and 1 hour before docetaxel infusion. For dosage adjustments during treatment, please refer to detailed prescribing information. Contraindications: Hypersensitivity to docetaxel or any excipients, patients with baseline neutrophil count of <1,500 cells/mm³, pregnancy and lactation, severe liver impairment. Precautions: Premedication consisting of an oral corticosteroid is needed. Frequent monitoring of complete blood counts (retreat with docetaxel if ANC ≥1,500 cells/mm³ before next cycle, and dose reduction recommended if severe neutropenia, i.e. <500 cells/mm³ for seven days or more). Patients treated with docetaxel in combination with cisplatin and 5-fluorouracil should receive prophylactic G-CSF to mitigate the risk of complicated neutropenia (febrile neutropenia, prolonged neutropenia or neutropenic infection) and should be closely monitored. Closely monitor patients for early manifestations of serious gastrointestinal toxicity. Enterocolitis could develop at any time and could lead to death as early as on the first day of onset. Observe closely for hypersensitivity reactions especially during the first and second infusions. Hypersensitivity reactions may occur within a few minutes following the initiation of the infusion of docetaxel, thus facilities for the treatment of hypotension and bronchospasm should be available. Severe reactions, such as severe hypotension, bronchospasm or generalised rash/erythema require immediate discontinuation of docetaxel and appropriate therapy and should not be re-challenged. Monitor closely patients who have previously experienced a hypersensitivity reaction to paclitaxel, they may be at risk to develop more severe hypersensitivity reaction. Inform patients about signs and symptoms of serious skin manifestations and closely monitor these patients. If signs and symptoms suggestive of these reactions appear, consider discontinuation of docetaxel. Monitor closely for severe fluid retention. If new or worsening pulmonary symptoms develop, patients should be closely monitored, promptly investigated, and appropriately treated. Interruption of docetaxel therapy is recommended until diagnosis is available. For patients with elevated liver function test (LFTs), recommend dose is 75 mg/m² and LFTs should be measured at baseline and before each cycle. For patients with serum bilirubin levels >ULN and/or ALT and AST >1.5 times the ULN concurrent with serum alkaline phosphatase levels >6 times the ULN, docetaxel should not be used unless strictly indicated. The development of severe peripheral neurotoxicity requires a reduction of dose. When patients are candidates for treatment with docetaxel in combination with trastuzumab, they should undergo baseline cardiac assessment and further monitored during treatment (e.g. every three months). Patients with impaired vision should undergo a prompt and complete ophthalmologic examination. In case cystoid macular oedema is diagnosed, docetaxel treatment should be discontinued and appropriate treatment initiated. Patients should be monitored for second primary malignancies. Closely monitor patients at risk of tumour lysis syndrome. Contraceptive measures must be taken during and for at least three months after cessation of therapy. Concomitant use of docetaxel with strong CYP3A4 inhibitors should be avoided. Amount of alcohol in this product and the side effects may impair ability to drive or use machines. Patients should be warned of this potential impact and be advised not to drive or use machines if they experience these side effects. Additional precautions in adjuvant treatment of breast cancer: G-CSF and dose reduction should be considered in complicated neutropenia. Evaluate and treat promptly on symptoms such as abdominal pain and tenderness, fever, diarrhea, with or without neutropenia. Monitor for symptoms of congestive heart failure during therapy and during the follow up period. Interactions: Metabolism of docetaxel may be modified by the concomitant administration of compounds which induce, inhibit or are metabolised by cytochrome P450-3A. Docetaxel may increase the clearance of carboplatin. CYP3A4 inhibitors. Undesirable effects: Neutropenia, anaemia, alopecia, nausea, vomiting, stomatitis, diarrhoea, asthenia, hypersensitivity reactions (flushing, rash with or without pruritis, chest tightness, back pain, dyspnoea, fever or chills etc.). Parasesthesia, dysesthesia, pain, infusion site reactions, infections, thrombocytopenia, anorexia, peripheral sensory neuropathy, peripheral motor neuropathy, arrhythmia, hypertension, haemorrhage, nail disorders, myalgia, arthralgia, fluid retention, increase in blood bilirubin, alkaline phosphatase, AST, ALT. For uncommon, rare and very rare undesirable effects, please refer to the full prescribing information. Preparations: 20mg x 1 vial, 80mg x 1 vial. Legal Classification: Part 1, First & Third Schedules Poison Full prescribing information is available upon request. API-HK-DOC-20-11

MAT-HK-2300364 (1/2023) 4IC_2779

sanofi

Sanofi Hong Kong Limited
1/F & SECTION 212 on 2/F, AXA SOUTHSIDE, 38 WONG CHUK HANG ROAD,
WONG CHUK HANG, HONG KONG
Tel: (852) 2506 8333 Fax: (852) 2506 2537

The Hong Kong Society of Diagnostic Radiologists Trust Fund

Hong Kong Society of Diagnostic Radiologists Research Grant

The Hong Kong Society of Diagnostic Radiologists (HKSDR) was founded in 1977 to promote interflow of professional knowledge in diagnostic radiology and to foster close contact among doctors working in the field of diagnostic radiology. The HKSDR Trust Fund was established in 1985.

Taking into account the rapid progress in imaging technology and thus the need to promote research to advance our knowledge and to serve our patients better, the Trust Fund offers three awards of up to HK$17,000 each and is open to application.

The application should be made by the principal investigator of the research project related to the scientific or clinical aspects of diagnostic radiology to be conducted in Hong Kong. The principal investigator should be a trainee/specialist in the field of diagnostic radiology. He/she has to be a registered medical practitioner in Hong Kong.

Application and enquiry can be directed to:

Dr. Lam Chiu Ying Flora, Hon Secretary of Trust Fund Working Group
c/o Ms. HY Ng, Department of Diagnostic & Interventional Radiology
Kwong Wah Hospital
25 Waterloo Road, Yaumatei, Kowloon, Hong Kong.
Tel: (852) 3517 5189

AOSPR 2023

21st Annual Scientific Meeting of
Asian and Oceanic Society for
Paediatric Radiology

2nd-3rd SEPTEMBER

HONG KONG 香港

@ Hong Kong Academy of Medicine
Jockey Club Building

www.aospr2023.org

Organised by

Supported by